

THE SPATIAL MODELING OF THE VEGETATIVE PROPAGATION OF THALASSIA
TESTUDINUM

by

MELISSA LEE PIRCHIO

(Under the Direction of Adrian Burd)

ABSTRACT

I developed a spatially explicit model of *Thalassia testudinum* growth and vegetative propagation in Florida Bay. *Thalassia* is an ecologically important species in terms of primary production and habitat complexity; however, losses occur on many spatial scales, ranging from several meters to hundreds of kilometers. Recovery of disturbed meadows is primarily through vegetative elongation of the rhizomes. After 5-year simulations, the model produced annual maximum and minimum above-ground biomass values similar to those measured at monitoring locations within Florida Bay. Additionally, the model illustrated seagrass re-growth into bare patches and propagation away from vegetated patches into bare areas. The results suggest that considering the spatial dimension of seagrass growth can give modelers and those using the models more insight into the dynamics of vegetative propagation. Through sensitivity analysis of model output, I determined further research is needed on two important components of the plants: phosphorus uptake kinetics and resource allocation.

INDEX WORDS: *Thalassia*, Florida Bay, seagrass, modeling, spatial dynamics, production, vegetative growth

THE SPATIAL MODELING OF THE VEGETATIVE PROPAGATION OF THALASSIA
TESTUDINUM

by

MELISSA LEE PIRCHIO
B.A.E., University of North Florida, 2003

A Thesis Submitted to the Graduate Faculty of The University of Georgia in Partial Fulfillment
of the Requirements for the Degree

MASTER OF SCIENCE

ATHENS, GEORGIA

2007

© 2007

Melissa Lee Pirchio

All Rights Reserved

THE SPATIAL MODELING OF THE VEGETATIVE PROPAGATION OF THALASSIA
TESTUDINUM

by

MELISSA LEE PIRCHIO

Major Professor: Adrian Burd

Committee: Merryl Alber
Christof Meile

Electronic Version Approved:

Maureen Grasso
Dean of the Graduate School
The University of Georgia
December 2007

DEDICATION

This work is dedicated to my loving family. My husband, Anthony, has provided me endless support in the pursuit of my dreams. My son, Vincent, is my inspiration to follow through.

ACKNOWLEDGEMENTS

First and most importantly, I would like to thank Dr. Adrian Burd for providing me with wonderful opportunities throughout my master's work, for his dedication to helping me along the course my studies, from the research to the writing, and most of all, for being caring and patient throughout my master's career and the life changes that have accompanied it. Thanks also go to Drs. Merryl Alber and Christof Meile, whom this study could not have been completed without, and Dr. Harlan Miller my fearless lab-mate. I would also like to thank the Departments of Biology and Marine Sciences for giving me Graduate Teaching Assistantships.

TABLE OF CONTENTS

	Page
ACKNOWLEDGEMENTS	v
LIST OF TABLES.....	viii
LIST OF FIGURES	x
CHAPTER	
1 INTRODUCTION.....	1
Seagrass Ecology	1
Seagrass Below Ground Biomass and Vegetative Propagation.....	5
Seagrasses in Florida Bay.....	6
Current Modeling Efforts	8
This Study.....	9
2 MODEL	14
Introduction to Cellular Automata	14
Data Used.....	16
Model Description.....	17
3 SENSITIVITY ANALYSIS.....	41
Introduction.....	41
Half-Saturation Constant for Phosphorus Uptake.....	43
Production Allocation.....	47
Conclusions.....	50

4	CASE STUDIES	65
	Introduction.....	65
	Random Spatial Distribution	66
	Idealized Patterns	70
	Motor Vessel Injuries	74
	Conclusion	78
5	DISCUSSION	115
	Summary.....	115
	Future Research.....	119
	Conclusions.....	121
	REFERENCES	123
	Appendix	131

LIST OF TABLES

	Page
Table 2.1: Plant associated parameters, symbols, units and values used in the model.....	29
Table 2.2: Parameters, symbols, units and values used in the model.....	30
Table 3.1: Summary of results from the quantitative sensitivity analysis of the model to variations in the phosphorus half-saturation constant, K_m	54
Table 3.2: Summary of results from the quantitative sensitivity analysis of the model to variations in the proportion of production allocated to above and below-ground biomass.....	55
Table 4.1: Simulation results for model runs examining the influence of the perimeter-to-area ratio on gap fill-in rates	84
Table 4.2: Simulation results for model runs examining the effect of shape on the gap fill-in rate.	85
Table 4.3: Simulation results for model runs examining the spread of rhizome and leaf biomass radiating from a central square patch of seagrass in the center of the grid	86
Table 4.4: Simulation results for model runs examining the spread of rhizome and leaf biomass radiating from various shapes of seagrass placed at the center of the grid	87
Table 4.5: Simulation results from model runs examining the effect of varying phosphorus concentrations (μM) on the recovery of <i>Thalassia</i> into a large-scale boat propeller blowout.....	88

Table 4.6: Simulation results for model runs examining the effect of varying phosphorus concentrations (μM) and sediment sulfide concentrations (μM) on the recovery into a gap in a seagrass bed 89

LIST OF FIGURES

	Page
Figure 1.1: Diagram of the anatomy of the seagrass (a) <i>Thalassia testudinum</i> , (b) <i>Syringodium filiforme</i> , and (c) <i>Halodule wrightii</i>	12
Figure 1.2: Florida Bay, the Florida Keys and the Everglades	13
Figure 2.1: Two-dimensional cellular automata models through time.	31
Figure 2.2: Examples of data available from long-term monitoring	32
Figure 2.3: Conceptual diagram of model development.....	33
Figure 2.4: Diagrammatic representation of H_{sat}	34
Figure 2.5: The effect of temperature on P_{max} as a function in this model	35
Figure 2.6: The relative effect of Phosphorus concentration on photosynthesis.....	36
Figure 2.7: The calculated hourly flux of Oxygen and DOC from the seagrass belowground components into the surrounding sediments.	37
Figure 2.8: The imposed effect of Sulfide Concentration on the Oxygen Flux into the sediments from overlying bottom-water.....	38
Figure 2.9: Relative Effect of Sulfide Concentration on the Maximum Rate of Photosynthesis of <i>Thalassia testudinum</i>	39
Figure 2.10: A diagram representing the spread of seagrass rhizomes into surrounding cells	40
Figure 3.1: Variation of phosphorus uptake limitation on photosynthesis with phosphorus concentration and half-saturation constant (K_m).....	56
Figure 3.2: The ratio of below: above ground biomass over time from model output.	57

Figure 3.3: Above- and Below-ground biomass over 5 years with K_m values of 0.1 (A.), 0.5 (B.) and 0.75 (C.) μM	58
Figure 3.4: Above- and Below-ground biomass over 5 years with K_m values of 0.1 (A.) and 0.5 (B.) μM	59
Figure 3.5: Above- and Below-ground biomass over 5 years with K_m values of 0.5 (A.) and 0.75 (B.) μM	60
Figure 3.6: A conceptual diagram showing the flow of photosynthetically derived product through the seagrass.	61
Figure 3.7: Biomass over time varying the allocation of production to above and below compartments (70/30(A.) and 67.5/32.5(B.)).....	62
Figure 3.8: Biomass over time varying the allocation of production to above and below compartments (62.5/37.5(A.) and 60/40(B.)).....	63
Figure 3.9: Seasonal variation in total production as seen in <i>Thalassia testudinum</i> in Lower Laguna Madre Texas.....	64
Figure 4.1: Model results of above-ground biomass over a five year period using two different initial conditions:	90
Figure 4.2: Graph showing the median sediment sulfide concentration (μM) reaching steady state after 3 years	91
Figure 4.3: The relationship between the leaf biomass at the end of three years and at the end of five years	92
Figure 4.4: Frequency distribution of leaf biomass in each cell within the grid. The initial distribution (blues bars) was imposed and was a normal distribution with biomass of $150 \pm 15 \text{ g DW m}^{-2}$	93

Figure 4.5: Frequency distribution of leaf biomass in each cell within the grid. The initial distribution (blues bars) was imposed and was a normal distribution with biomass of 150 ± 30 g DW m ⁻²	94
Figure 4.6: Frequency distribution of leaf biomass in each cell within the grid. The initial distribution (blues bars) was imposed and was a normal distribution with biomass of 150 ± 45 g DW m ⁻²	95
Figure 4.7: Frequency distribution of leaf biomass in each cell within the grid. The initial distribution (blues bars) was imposed and was a normal distribution with biomass of 200 ± 60 g DW m ⁻²	96
Figure 4.8: The relationship between initial and final leaf biomass and after a five year simulation with an initial above-ground biomass of 200 ± 40 g DW m ²	97
Figure 4.9: The two sites that were selected for model comparison [TS/Ph 9-Duck Key- and TS/Ph 11-Sprigger Bank] located within Florida Bay.....	98
Figure 4.10: Comparison of the model leaf biomass (blue) with field measurements from Sprigger Bank (green) and Duck Key (red).....	99
Figure 4.11: Initial Spatial Distribution of seagrass biomass within the model domain.	100
Figure 4.12: Initial Spatial Distribution of seagrass biomass within the model domain.....	101
Figure 4.13: The effect of the perimeter to area ratio of the seagrass gap to the rate of fill into the gap after five years.	102
Figure 4.14: Final spatial distribution of seagrass biomass, leaf (left hand frames) and rhizomes (right hand frame) after 5 years for initial conditions A (top row) and B (bottom row) from Table 4.2.....	103

Figure 4.15: Final spatial distribution of seagrass leaf (left hand frames) and rhizome (right hand frames) biomass after 5 years for initial conditions C (top row) and D (bottom row) from Table 4.2.....	104
Figure 4.16: Final spatial distribution of seagrass leaf (left hand panels) and rhizome (right hand panels) biomass after 5 years of simulation for patch evolution cases A and B (Table 4.4)	105
Figure 4.17: Final spatial distribution of seagrass leaf (left hand panels) and rhizome (right hand panels) biomass after 5 years of simulation for patch evolution cases C and D (Table 4.4)	106
Figure 4.18: Two perimeters mapped from the large-scale study shortly after the boat grounding occurred in May 1993 (area ~7300 m ²) and 4.8 yr later, when the site was sampled for presence of <i>Thalassia testudinum</i> seedlings in January 1998 (area ~1560 m ²)	107
Figure 4.19: Initial spatial distribution of seagrass biomass showing the gap created by the boat grounding documented in Whitfield et al. (2004).....	108
Figure 4.20: Final biomass distribution of rhizome after various simulations.....	109
Figure 4.21: Initial spatial distribution of seagrass biomass in the model grid showing a simulated prop scar (10m x 4m)	113
Figure 4.22: Scatter plot of initial leaf biomass of an individual cell against total leaf biomass in surrounding cells.....	114

CHAPTER 1

INTRODUCTION

Seagrass Ecology

Seagrass beds are some of the most productive ecosystems in the world (Zieman and Wetzel 1980) with an average production of $1012 \text{ g DW m}^{-2} \text{ y}^{-1}$ (Duarte and Chiscano 1999) compared to average production of $292 \text{ g DW m}^{-2} \text{ y}^{-1}$ in coral reefs and $1095 \text{ g DW m}^{-2} \text{ y}^{-1}$ in marsh plants (Hemminga and Duarte 2000). In addition to their high productivity, seagrass meadows provide habitat for sessile organisms such as epiphytes, sponges and soft corals, as well as breeding grounds for invertebrates such as scallops and snails. Seagrass beds, with their innate structural complexity, also serve as a protected nursery habitat for many juvenile fish (Heck et al. 2003). The biodiversity found in seagrass beds is critical to the sustainability of many surrounding ecosystems such as coral reefs (Goecker et al. 2005) and mangrove forests (Connolly et al. 2005). Many commercially important species, including grouper, shrimp, and lobster, inhabit seagrass beds and surrounding regions (Larkum et al. 1989 and Phillips and McRoy 1980). Seagrasses, and their attached epiphytes, provide a food source to fisheries species not only within their habitat but also transferred to surrounding habitats (Connolly et al. 2005). For example, coral reef fishes such as the parrotfish use the seagrass beds as a food source (Larkum et al. 1989).

The ecological importance of seagrass-based ecosystems is also recognized by many regulatory organizations. For example, the South Atlantic Fishery Management Council designates seagrass beds as essential fish habitat (www.safmc.net). The high

biodiversity maintained within seagrass meadows makes seagrasses useful indicator species of ecosystem health (Dennison and Orth 1993) and they are used as such by organizations such as the Environmental Protection Agency (EPA) through their Environmental Monitoring and Assessment Program (<http://www.epa.gov/emap/index.html>) and the Indian River Lagoon National Estuary Program (<http://www.sjrwmd.com/programs/outreach/irlnep/index.html>).

Light and temperature are primary influences on both the distribution and primary production of seagrasses (Zieman and Wetzel 1980). Seagrass meadows only persist in regions with low light attenuation. Increased concentrations of epiphytes, phytoplankton, particulates, tannins, and dissolved inorganic carbon increase light attenuation in the water column. Seagrasses can reduce epiphyte growth by continuously growing (Larkum et al. 1989) and physical environmental conditions, such as the hydrology, can also affect light attenuation. For example, riverine inputs with high sediment loads can dramatically decrease light availability such that certain regions, such as the Georgia coast, do not support any submerged aquatic vegetation. Seagrass meadows are known to increase sedimentation of small particulates if sediment loads are not too high, thereby helping maintain water clarity (Gacia et al. 1999). *Thalassia testudinum* prefers areas with a mean water velocity of 5-100 cm s⁻¹ (Koch 2001); this value allows for the accumulation of sediments through interaction with the seagrass blades, while not increasing turbidity drastically enough to decrease light penetration.

Seagrass species are found in water temperatures between approximately 19 and 36°C (Zieman 1975). More specifically, *Thalassia testudinum* demonstrates optimum

growth at 30°C (Zieman 1975). High temperatures result in increased photosynthetic and respiration rates as well as decreased oxygen solubility.

Other key factors affecting seagrass distribution and production include water column features, such as salinity and nutrient availability, and sediment composition (Koch 2001). Different species of seagrass have different tolerances for salinity fluctuations and Zieman (1975) demonstrated that variations in salinity can have a negative effect on seagrass growth and productivity. For example, the tropical species *Thalassia testudinum* exhibits optimal growth at a salinity range between 20 and 40 PSU (Berns 2001), while the sub-tropical species *Ruppia maritima* exhibits optimal growth at a salinity range between 0 and 40 PSU (Berns 2001). Seagrass salinity tolerance is a result of physiological adaptations such as the presence of protective leaf sheaths and ion pumps (Larkum et al. 1989).

Seagrasses are commonly found in anoxic sediments where sulfide toxicity is a common problem. *Thalassia testudinum* die-off was observed at sulfide concentrations between 1000 and 3000 µM at a sediment depth of 8 to 10 cm (Carlson et al. 1998), whereas mortality of the temperate seagrass *Zostera marina* increases at sulfide levels near 400 µM and above measured at between 5 to 15 cm depth (Goodman et al. 1995, Koch 2001). Experimental studies have shown that the combined effects of high sulfide levels (greater than 6 mM), high temperatures (greater than 35°C), and high salinities (greater than 55-60 PSU) lead to complete mortality in *Thalassia testudinum* (Koch and Erksine 2001). Seagrasses prefer a sediment composition of clay and silt of less than 20% and organic content less than 5%, as coarser sediments are often more oxygenated and have lower sulfide concentrations (Koch 2001).

The two main nutrients required for seagrass growth are nitrogen and phosphorus. In general, nitrogen has been shown to be the nutrient limiting production in open ocean marine systems dominated by phytoplankton; whereas production in coastal marine ecosystems, such as long-residence time estuaries, is generally phosphorous limited (Smith 1984). Following the work of Smith, studies in Florida Bay have shown that seagrass productivity is often limited by phosphorus concentrations (Fourqurean and Zieman 1992). In order to fully exploit the nutrients surrounding the plants, seagrasses have developed mechanisms for absorption through both roots and leaves (Larkum et al. 1989 and Lee and Dunton 1999).

Declines and disturbances in seagrass meadows have been documented world wide (Short and Wyllie-Echeverria 1996). Seagrass disturbances can range in size from small scale disturbances ($\approx 10 \text{ m}^2$) to large scale (100 km^2) losses. Some losses can be attributed to natural causes such as hurricanes or biological interactions such as infection by the slime mold *Labyrinthula spp.* (Hemminga and Duarte 2000). However, in the majority of documented cases the declines can be attributed to human activity (Short and Wyllie-Echeverria 1996). Anthropogenic causes for loss include coastal eutrophication (Lapointe and Barile 2004) and motor-vessel groundings in which boat propellers cause an excavation of the seagrass bed and/or soil (Whitfield et al. 2004). In the coastal waters of Florida, aerial surveys indicate that approximately 70,000 ha of seagrass meadow have been damaged by motor-vessels (Sargent et al. 1995). ‘Prop scars’, which only damage the above ground biomass, typically recover over timescales of years (e.g., *Thalassia* can take anywhere from 5-10 years to recover from prop scar damage (Dawes et al. 1997)) while the larger and more devastating ‘blowhole’ injuries, in which the below-ground

biomass and soil are unearthed, have no documented long term recovery (Whitfield et al. 2004). Many times natural and anthropogenic causes combine to exaggerate the losses, such as hurricanes inhibiting the recovery of propeller scars (Whitfield et al. 2004). Recovery of seagrass into disturbed areas occurs mostly through the activity of the below-ground biomass (Williams 1990, Kenworthy et al. 2002).

Seagrass Below Ground Biomass and Vegetative Propagation

The seagrass plant is organized by a series of ramets with interconnected rhizome systems. An individual ramet includes a bundle of leaves, a short shoot, a rhizome (horizontal or vertical), and the surrounding root system. The short shoots are similar to stems in land plants. The details of the plant architecture vary from species to species. The tropical species *Thalassia testudinum* (Figure 1.1(a)) contains one or more roots per rhizome node, and each root possesses many root hairs, increasing the plant's ability to absorb nutrients (Larkum et al. 1989). The tropical species *Syringodium filiforme* and *Halodule wrightii* contain several branched roots per rhizome node and in contrast to *Thalassia*, few root hairs (Figures 1.1b and c). The area surrounding the roots and rhizome within the sediments is referred to as the rhizosphere. Seagrasses release oxygen and dissolved organic carbon into the rhizosphere which hosts a community of cyanobacteria, alpha proteobacteria, fungi and other unidentified microorganisms (Kuo et al. 1981, Larkum et al. 1989, Weidner et al. 1996); this release is accompanied by high metabolic costs to the plant.

Reproduction in seagrasses occurs in two forms. Seagrasses propagate mainly asexually through rhizome elongation, although there has been little research on factors affecting rhizome elongation rates. This rate varies by species from several meters to a

few centimeters per year (Hemminga and Duarte 2000), with measurements of *Thalassia testudinum* in Laguna Madre, Texas found to be approximately 60 cm y⁻¹ (Kaldy and Dunton 2000). Sexual reproduction occurs through flowering and hydrophilous pollination (Durako and Moffler 1987). During seedling establishment in *Thalassia*, rhizome elongation rates are significantly lower, and range from 6-27 cm y⁻¹ (Whitfield et al. 2004).

Models of the horizontal distribution of seagrasses require an understanding of the mechanisms of clonal growth. This is the vegetative propagation that produces new ramets that are genetically identical (clonal) to the plant they spread from. The mechanisms of clonal growth include the ability to translocate resources such as soluble carbohydrates and nutrients via the plant's rhizome system (Marba et al. 2002), possibly as a response to gradients in environmental conditions such as light availability (Tomasko and Dawes 1989), nutrient concentration, sulfide concentrations in the sediment, water temperature, and salinity. Aside from the spatial aspect of the translocation and its benefits for growth, it is important to examine the interactions between connected ramets, especially in response to stress from varying resource concentration gradients particularly if examining a region with spatial heterogeneity in resources.

Seagrasses in Florida Bay

Florida Bay is located to the south of the Florida peninsula. The Gulf of Mexico borders the western boundary and the Florida Keys, a combination of both natural and artificial islands, provide the borders to the south and east (Figure 1.2). The Keys protect the bay from the influence of the Florida Current, the Gulf Stream, and the Atlantic Ocean. The Bay is an inverse estuary, having few freshwater inputs. Evaporation is the

driving force in salinity changes, with increases seen due to warmer temperature in the summer. The salinity of the bay increases from the Northeastern portion Southwest, whereas the temperature of the bay does not demonstrate significant spatial variability. The nutrient regime of the bay varies spatially with the eastern portion of the bay having a carbon-to-phosphorus molar ratio of approximately 2,000 while the western basin has a ratio of 200 (Fourqurean and Zieman 1992).

Seagrass beds are a prominent feature of the ecosystem in Florida Bay with three main species of seagrasses found: *Thalassia testudinum* (turtle grass), *Halodule wrightii* (shoal grass), and *Syringodium filiforme* (manatee grass). *Halodule wrightii* is the early colonizing species, able to grow in shallower waters, while *Thalassia testudinum* is the later successional species that has more specific habitat requirements such as deeper sediments for the development of a more complex root system. The succession of species allows for increased sedimentation, thereby promoting favorable conditions for colonization and growth of *Thalassia*. Carbonate sediments present in the bay affect seagrass production because the phosphate binds to the carbonate particles (McGlathery et al. 1994) thereby exaggerating any phosphorus limitation. These seagrass beds support economically advantageous species such as pink shrimp, spiny lobster, and in the past queen conch.

This dynamic ecosystem has gone through many changes over the past century, many of them affecting the seagrass populations (Zieman 1999). The dramatic increase in human population experienced in South Florida during the last part of the 20th century affected the bay significantly as land development increased. The resulting management of the waterways of South Florida altered the hydrology, with water redirected from the

natural flow of the Everglades into the Bay causing drastic variations in salinity. Water is now redirected to urban areas with runoff channeled by canals creating additional inputs into the Bay. This bypassing of the natural filtering system of the Everglades is a direct human impact on Florida Bay.

Current Modeling Efforts

In the seagrass research community, there is currently a need for a connection between modeling efforts, monitoring programs, and field research (Bortone 2000). Current seagrass models focus on the development and growth of the above ground material. The H_{sat} model developed for *Zostera marina* (Zimmerman et al. 1994) calculates production based on maximum photosynthesis rate (P_{max}) and daily hours of saturating irradiance (H_{sat}). Herzka and Dunton (1998) used field data from *Thalassia testudinum* in Laguna Madre, Texas and attempted to use the H_{sat} method to model production; however, the model underestimated production values by 70% of the calculated integrated production values. In 2001, Burd and Dunton (2001) created a light-driven model of above and below-ground production and biomass for *Halodule wrightii* and verified the model using field data from Laguna Madre, Texas. Their whole plant approach demonstrated the need to further look at resource allocation. This was evident from the fact that recovery of below-ground biomass preceded that of the above-ground following a prolonged period of light reduction caused by a brown tide bloom (Burd and Dunton 2001).

Many problems are encountered in the development of such detailed models. Seagrass models are limited by the availability of data that can be used to estimate the parameters built into them, and data of above- and below-ground biomass that can be

used to validate the models. The models also do not consider spatial variations in plant biomass and density and in particular they consider only the vertical transport of carbon, not the translocation of material horizontally through the root/rhizome network (Burd and Dunton 2001). Lateral transport of materials is important for the expansion of the rhizome network as it feeds the production of the apical meristem where new growth occurs. Consequently, these existing models cannot accurately model the effects of spatial heterogeneity and disturbance in a seagrass bed.

Spatially explicit models have been developed for terrestrial vegetation and used to study spatial dynamics and interspecific competition (Silvertown 1992). A recent cellular automata model developed by Giusti and Marsili-Libelli (2005) examined the spatial propagation of widgeon grass, *Ruppia maritima*, through sexual reproduction via seed dispersal and asexual reproduction via rhizome expansion as a function of hydrology and nutrient availability. This model was successful in predicting the growth of submerged vegetation in the Orbetello Lagoon. Cellular automata models have also been developed to examine spatial dispersal of both terrestrial (Cain 1995) and aquatic vegetation (Chen et al 2002); however, there are no models available that examine marine submerged macrophytes that reproduce primarily through asexual vegetative propagation.

This Study

The importance of the Florida Bay ecosystem makes it a prime site for research using modeling techniques. One of the most pressing issues in this region is the cause of the major seagrass die-back in the late 1980s-early 1990s that has affected over 27,000 ha of seagrass beds and led to the loss of approximately 25% of above-ground biomass of the dominant species, *Thalassia testudinum* (Robblee 1991). Different stressors have

been hypothesized for this decline including salinity (Fourqurean et al. 1999), temperature (Fourqurean et al. 1999), sulfide toxicity (Goodman et al. 1995), hypoxia (Robblee et al. 1999, Lapointe and Barile 2004), eutrophication (Lapointe and Barile 2004) and infection by slime mold (Robblee et al. 1999). Because of growing concern for this area, there are many long term monitoring projects conducted by Florida Coastal Everglades Long Term Ecological Research (FCE-LTER), the Florida Keys National Marine Sanctuary (FKNMS), the South Florida Water Management District (SFWMD) and the Southeast Environmental Research Center (SERC). This data availability is one of the key factors supporting model development.

In this project, a model of growth and production for *Thalassia testudinum* was developed using the setting of Florida Bay. Most existing seagrass models use biomass per unit area as their main variable, with the option of varying the environmental parameters with time but not space. This model includes a spatial component which is particularly important in a region such as Florida Bay where physical, biological, and chemical conditions vary spatially. Spatial modeling takes into account the horizontal vegetative spread of seagrass and its relationship to changes in biomass density. Examining the vegetative propagation of seagrass bed dynamics through modeling can produce insights into the process by which seagrasses are able to colonize new patches. The aim was to use the model to increase the understanding of key factors in seagrass propagation, and to examine the community response to multiple stressor situations. To accomplish this, the model incorporated spatial variation using a cellular automaton model.

Cellular Automata provide an alternative to describing spatial variation using systems of partial differential equations. A Cellular Automaton (CA) is a rule-based, spatially-explicit model based on a unit area. Using rules based on the ecology and physiology of the seagrass plants, this model can provide a spatial representation of the system and its dynamic interactions. This type of model is useful in demonstrating important spatial behavior in seagrass beds. Also, by representing seagrass reproduction through cellular automata, the model can be used to investigate factors such as resource availability and interactions among varying resource regimes.

This project also aimed to examine the feasibility and validity of using cellular automata for studying the spatial variability of seagrass bed dynamics. The factors affecting seagrass growth and production in Florida Bay are well known from the long history of field and experimental research done in the system. In addition, the model was used to determine which of these factors must be included in the model. The results from this will give an indication of the variables and parameters important to developing such a model. This model can help scientists trying to understand this ecosystem and the managers who must make vital decisions in terms of the hydrology of the bay, and protection agencies who want to maintain the seagrass as a link for other endangered communities surrounding such as coral reefs.

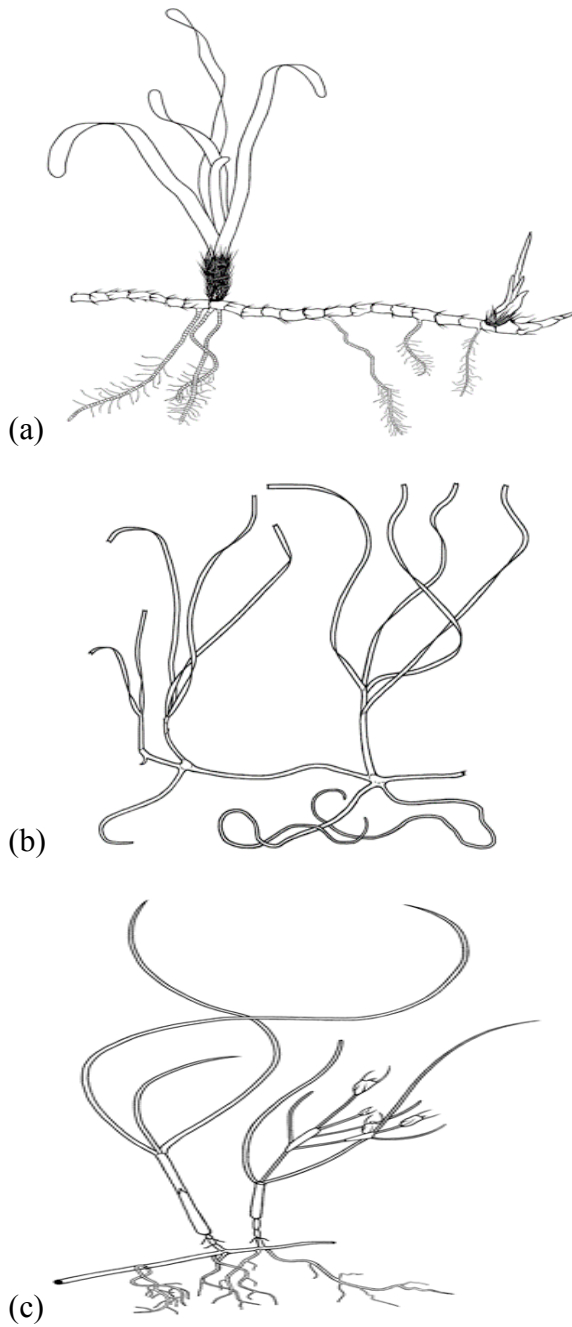


Figure 1.1 Diagram of the anatomy of the seagrass (a) *Thalassia testudinum*, (b) *Syringodium filiforme*, and (c) *Halodule wrightii*. (Florida Department of Environmental Protection [<http://www.dep.state.fl.us/coastal/habitats/seagrass/>])

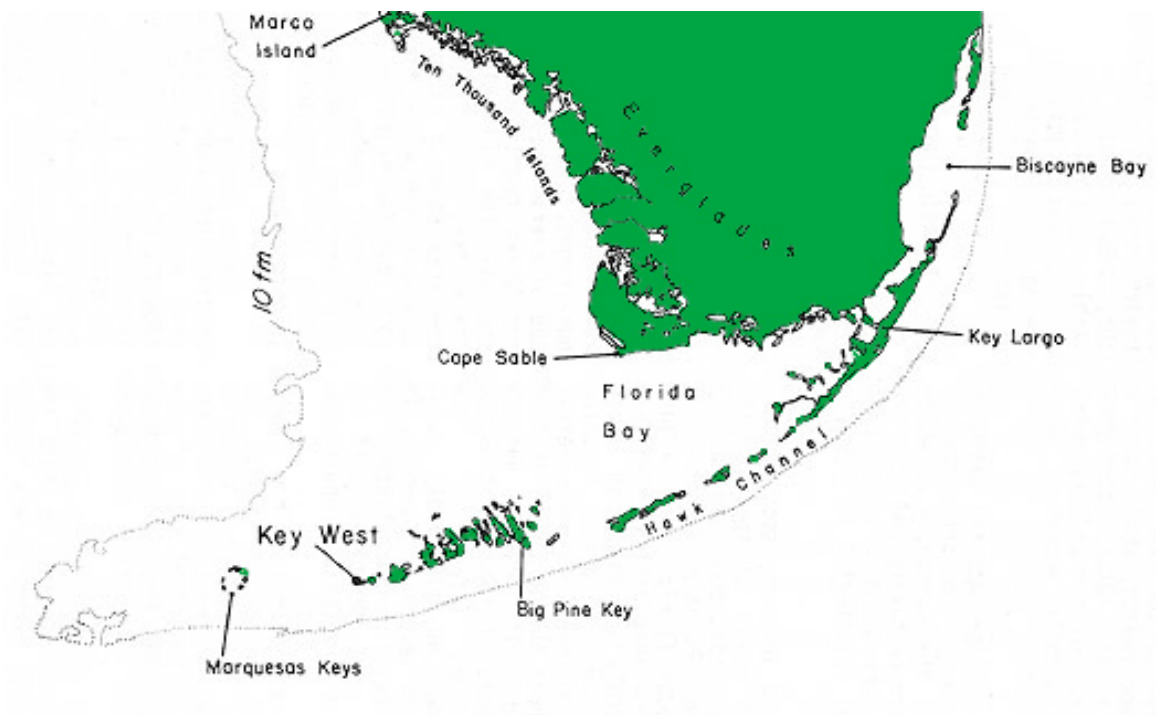


Figure 1.2 Florida Bay, the Florida Keys and the Everglades (U.S. Fish and Wildlife Service [<http://www.flmnh.ufl.edu/Fish/southflorida/images/floridakeys.jpg>])

CHAPTER 2

MODEL

Introduction to Cellular Automata

Models of spatial dynamics in ecology are often formulated using reaction-diffusion-advection equations (Murray 1989; Haefner 1996). In contrast, cellular automata (CA) use a discrete, rule based structure to represent spatial processes, rather than a system of dynamic equations, and can accurately represent the complex behavior of a system over time (Wolfram 1983). They thus provide an alternative structure for model behaviors that are often solved using continuous time models based on differential equations. CA were originally developed by John von Neumann and Stanislaw Ulam as a means of simulating biological, self-replicating systems (von Neumann 1963). John Conway developed von Neumann's ideas and produced a two-dimensional CA, *The Game of Life*, which was popularized by Martin Gardner in *Scientific American* and which stimulated research on these idealized systems (Dewdney 1989). Cellular automata have since been used to model dynamical systems in a wide array of fields from physics to ecology and biology. Examples include the modeling of fire spread (Sarkar and Abbasi 2006), forest dynamics (Schlicht and Iwasa 2006, Rammig et al. 2006), and soil erosion (D'Ambrosio et al. 2001).

Cellular Automata can be broken down into three main components:

1. The construction of a cellular automaton begins by establishing a discrete representation of the spatial domain, comprising an array (grid) of sites (cells). In its simplest form, this is a rectangular grid of square cells that

completely covers the domain being considered (Figure 2.1). The grid geometry may be more complicated, and, based on the scale relevant to the system being studied, can be in one, two, or three dimensions.

2. Each cell within the grid is assigned a value (state) from a finite number of possible states. A simple CA may have only two possible states, 0 and 1, depending on whether a cell is “dead” or “alive”, respectively (Figure 2.1). More complicated CA can have more possible states. For example, possible states may range from 0 to 10, with each value representing a range of coverage or biomass. Additionally, a cell may be assigned multiple values representing the biomass of several different plant species within the cell.
3. A set of rules is established to update the states of the cells at each discrete time step. The rules can be the most difficult component of the CA to develop and implement, and usually depend upon the states of cells in the defined local neighborhood. In addition, the rules can depend on variables that are defined on additional grids. For example, a CA of plant growth may have rules dependant upon the sediment nutrient concentration. This can be tracked by using an additional grid layer and equations representing inputs and outputs of nutrients from a cell. The rules can be applied simultaneously or in some specified order. Usually, all cells are updated simultaneously. However, there are significant differences produced in model output when the order of how cells are updated deviates from this (Ruxton and Saravia 1998).

A simple example of a CA follows and is represented in Figure 2.1. For each cell in a grid, the cellular neighborhood defines which adjacent cells affect the state of a given

cell. There are two common types of neighborhoods in two dimensions: the Moore neighborhood (Figure 2.1a) which consists of the eight cells surrounding the cell of interest, and the von Neumann neighborhood (Figure 2.1b) which consists of the cells directly above, below and to the sides of the cell of interest. This example uses two possible cell states, 0 (white) and 1 (blue). The rule for changing the state of cell at each time step in this example depends only on the sum of the states in the local neighborhood of the cell of interest. A cell with a state of 1 keeps that state if the neighborhood sum equals 2 or 3. If the sum is greater than 3 or less than 2, the cell state shifts to 0. A cell that has a state 0 can only shift to a state of 1 if the neighborhood sum equals 3. These rules are designed to mimic the spread of a population based on existing population density: empty cells can only become populated by immigration from surrounding cells if the neighborhood is heavily populated. This example shows the effect of using different neighborhoods. Using a Moore neighborhood, an oscillation is set up between two different patterns as there are more neighbors to consider with each evaluation of the rules. In the case of the von Neumann neighborhood there is insufficient population density to sustain a population as only four neighbor cells are evaluated.

Data Used

The Southeast Environmental Research Center (SERC) data includes temperature, salinity, turbidity, and both nitrogen and phosphorous concentrations (Figure 2.2 a, b). The South Florida Water Management District (SFWMD) data includes temperature, salinity, turbidity, photosynthetically active radiation (PAR) and various water column concentrations. Other data including irradiance and sediment sulfide concentrations was taken from published research in the field (Fourqurean and Zieman 1991 and Borum

2005). The Florida Coastal Everglades Long-term Ecological Research (FCE-LTER) and Florida Keys National Marine Sanctuary (FKNMS) examine seagrass density and health while also recording important environmental parameters such as salinity, temperature, secchi depth and turbidity. Seagrass density is measured quarterly in the Bay using standing crop biomass (Figure 2.2 c) in addition to the standard Braun Blanquet method (Fourqurean 2001).

Model Description

To simulate vegetative growth of *Thalassia testudinum* in Florida Bay, we used a CA with cells representing 1 m² as analogs of a meter square quadrat. In addition to the two-dimensional domain, it was assumed that the seagrass below-ground components and the biochemistry involved will be taking place in the top 40 cm of the sediment (Fourqurean et al. 1992). Additional “resource” layers were used to represent the spatial distributions of sediment nutrients and sulfide, which allowed the plants to respond to the spatial variability. A variety of initial conditions were chosen to represent different scenarios of biomass and resources being investigated. Each cell was assigned a state based on the biomass in that cell and the cell states were updated monthly, although biomass is updated daily. The CA will use a Moore neighborhood as this is more realistic for this natural system. The von Neumann neighborhood would be an unrealistic choice because the corner cells all come in contact with the center cell; therefore, their influence would undoubtedly be felt.

Representations of CA on a computer are finite, and so the boundaries can have a strong impact on the evolution of the system. Periodic boundary conditions are the most commonly used. Here, the computational domain wraps around itself so that the

neighborhood of a cell on the far right hand side of the domain contains the cells that are on the far left hand side of the domain. In the model developed, as well as in the simple example above, we have used periodic boundary conditions.

A conceptual diagram shows the development of the model framework (Figure 2.3). The model incorporates two timescales: a daily unit time step for production and a monthly time step for vegetative propagation. The reason for this is that production and resource allocation operate on much shorter timescales (hours to days) than rhizome elongation (weeks to months). The monthly time step incorporated the CA, while the daily time step responds only to conditions within the individual cell. Production is forced by light, with additional limiting factors of water temperature, sediment phosphorous and sulfide concentrations. The rules we have implemented for both production and propagation are updated in the order they are represented both in the text and through the flow of the conceptual diagram (Figure 2.3). Biomass for each cell is updated simultaneously. *Thalassia* biomass is initially divided into four compartments: leaves (20%), short shoots (25%), roots (8.5%) and rhizomes (36.5) (Fourqurean and Zieman 1992). These compartments each have their own respiratory rates (a function of temperature), and turnover (i.e. mortality) rates. The model runs for 5 years at an assigned location with specific latitude and longitude.

Light

The production model is based on the H_{sat} model developed by Zimmerman (1994). Photosynthetically active radiation (PAR) is calculated from the hourly irradiance at a given location (Iqbal 1983) assuming clear skies and a flat air-water interface. Daily production (P) is then calculated using the maximum rate of

photosynthesis (P_{max}) for the plant multiplied by the number of hours (H_{sat}) per day that the incident irradiance (I) was greater than the saturating irradiance (I_k) (Figure 2.4).

$$P = P_{max} \cdot H_{sat}$$

Values for P_{max} and I_k (Table 2.1) were obtained from P vs. I curves developed for *Thalassia testudinum* in Florida Bay (Fourqurean and Zieman 1991). This model assumes negligible photoinhibition, which has only been rarely observed in seagrasses (Hemminga and Duarte 2000).

Temperature

The effect of temperature on the physiological parameters of photosynthesis (Figure 2.5) and respiration were modeled following Burd and Dunton (1999): (terms are defined in Table 2.1)

$$\Gamma(T) = \Gamma_o \exp\left\{\xi[T(t) - T_o]\right\} = \Gamma_o \exp(\Gamma \Delta T)$$

Additionally, Herzka and Dunton (1997) described the seasonal effect temperature has on P_{max} specifically showing how increase in P_{max} correlated to higher temperatures while P_{max} decreased in the fall correlating it with cooler temperatures.

Phosphorous Limitation

A nutrient grid was created with phosphorous concentrations at each cell; the values can be the same throughout the grid or can be randomly assigned at each site based on the mean phosphorous concentrations found in the given area.

The effect of phosphorus limitation was calculated using a Michaelis-Menten factor and an appropriate half-saturation constant (K_m). Research conducted on *Thalassia* from Florida Bay determined K_m values ranging from 1-12 μM , however these values were calculated based on P_i concentrations from 0.5-25 μM (Gras et al. 2003).

Florida Bay seagrasses usually experience concentrations much lower, between 0.01-1.0 μM (Szmant and Forrester 1996 and Boyer et al. 1997).

In the model, this nutrient limitation (Figure 2.6) is expressed multiplicatively with the light limitation on production, such that the limiting factor, Q_p , for the root and leaf uptake rates are defined independently as

$$Q_p = P_i / (K_m + P_i)$$

This represents a modified Monod response based on the following assumptions: cell receptors on the surface are used by enzymes for uptake and no transport limitation occurs.

The total limitation is affected by both leaf and root uptake and is therefore shown by the following equation:

$$Q_p = (Q_{root} + Q_{leaf}) / 2$$

This formulation was selected because although both leaf and root uptake are important, very little data exist on the differentiation of the two uptakes. There is still considerable debate on which uptake dominates in a given seagrass system, especially when looking at tropical seagrass species in oligotrophic regions such as Florida Bay's carbonate sediments (Gras et al. 2003). Additionally, seagrasses are able to adapt to the better source of nutrients, whether water column or porewater (Touchette and Burkholder 2000). This equation will be easily used when better estimates of the different values for the uptake parameters of both roots and leaves are determined.

The resulting nutrient limited production is expressed as a proportion of the production up to this step:

$$Production = Q_p \cdot P$$

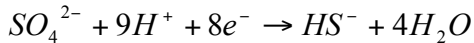
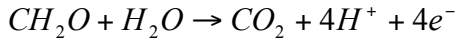
Sulfide Sedimentary Feedback

Thalassia plants have been shown to transport photosynthetically derived oxygen to their root and rhizome structure to counteract the anoxic sediments associated with their rhizosphere. Seagrasses also leak labile dissolved organic carbon (DOC) into the sediments thereby stimulating the microbial loop. Approximately 15-30% of gross primary production (Kaldy et al. 2006) is released from *Thalassia* below-ground biomass as DOC. The amount of oxygen released through below-ground parts can vary based on primary production and sediment chemistry. Bodensteiner (2006) measured 6% of net primary production is released as O₂.

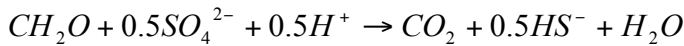
The DOC released by the plant feeds dissimilatory sulfate reduction, producing hydrogen sulfide and carbon dioxide. Additionally, sulfide is produced through bare sediment respiration. Ku et al. (1999) reported an areal sulfate reduction rate of 200 $\mu\text{mol cm}^{-2} \text{yr}^{-1}$ in terms of carbon in unvegetated regions of Florida Bay. Oxygen feeds sulfide oxidation resulting in the production of sulfate. In addition to the oxygen released by the plants into the sediments, there is also diffusion of oxygen into the sediments through the overlying water. Assuming the equivalent amount of respiration that takes place in unvegetated (bare) sediments still occurs within seagrass beds, the minimum amount of carbon equivalents required to balance the oxygen entering the sediment from the bottom water would be 200 $\mu\text{mol cm}^{-2} \text{yr}^{-1}$. The maximum amount of oxygen that can enter the sediments is driven by a strong concentration gradient between the bottom water and anoxic sediments based on diffusion. Using an average bottom water oxygen concentration, we calculated the rate of diffusion. Using this maximum and the bare sediment estimate as a minimum, we develop a linear relationship driven by the hydrogen

sulfide concentration in the sediments, based on the understanding that an increase in the hydrogen sulfide concentration in the sediments would drive more oxygen diffusion into the sediments. We set 2 mM as the value that draws the maximum oxygen diffusion into the sediments from the bottom water.

In our simplified system the half reactions are:



This is a simplification of the system's sulfur cycle, specifically focusing on dissimilatory sulfate reduction and excluding both the oxidative cycle and sulfide precipitation. Additionally, it also assumes that organic matter can be represented as CH₂O. Combining these 2 reactions gives:



In our model, the sulfide dynamics are driven by plant DOC leakage, plant O₂ leakage, sulfate reduction in the sediment and oxidation of sulfide by O₂. These can be represented by the following equation:

$$\frac{\partial HS}{\partial t} = R_{OC_plant} - R_{O_2_plant} + R_{OC_sed} - R_{O_2_sed}$$

The terms in the equation above are:

R_{OC_{plant}}: sulfide introduced via DOC leakage. This is set to a constant percentage of gross primary production (GPP) between 15-30% (Kaldy et al. 2006).

R_{O_{2plant}}: sulfide consumed from plant O₂ leakage. This is calculated based on the amount of DOC released from the plant and the GPP of the plant (Figure 2.7).

This parameter was established using relationships observed from simulations of the model developed by Miller et al. (2007).

R_OC_sed: sulfide produced through (bare) sediment respiration. Using the rate found by Ku et al. (1999) and the average temperature when the rate was calculated, we modified this rate as a function of temperature using the Arrhenius

Equation: $k(T) = k_0 * \exp\left(\frac{-E_a}{R*T}\right)$ with the temperature (T) converted to Kelvin (Kelvin = °C + 273), the E_a (activation energy) defined as 37800 J mol⁻¹ (King 1988) and the R value (Universal Gas Constant) of 8.314x10⁻³ kJ mol⁻¹ K⁻¹. We can calculate k_0 based on the rate (200 μmol cm⁻² yr⁻¹) and the temperature (20°C) at which the experimental measurements were made.

R_O2_sed: sulfide consumed via O₂ from the overlying water. As a minimum, we use the value for bare sediment respiration as the minimum amount of oxygen drawn through the sediment water interface. To calculate the maximum rate of oxygen uptake from the bottom water by the sediments, we have used an approximation of the diffusion equation (Fick's law $J = -D(\Delta C/d)$) with D (diffusion coefficient for water) as 10⁻⁹ m² s⁻¹ and ΔC as the difference in concentration of dissolved oxygen in the bottom water and the concentration of dissolved oxygen in the surface layers of the sediments (assuming anoxia C=0); this also assumes that all oxygen is consumed at the sediment-water interface. Using the range established between these two equations, we assume a relationship (Figure 2.8) between sediment sulfide concentrations (adjusted for area) and sediment oxygen requirements.

After calculating the net change in sulfide through our time step, using the equation

$$\frac{\partial HS}{\partial t} = R_{OC_plant} - R_{O_2_plant} + R_{OC_sed} - R_{O_2_sed}$$
 and dividing that

by a root zone depth of 40 cm (Fourqurean et al. 1992), we calculated the sulfide concentration per volume of sediment. Using the porosity of the sediments in FL Bay of 0.8 (Rude and Aller 1991), we calculated the sulfide concentration based on volume of porewater (m³) instead of total sediment volume. We account for sulfide concentration in this manner because we know that sulfide here is dissolved within the porewater. Finally, we add or subtract the sulfide produced or consumed to the sulfide concentrations for the previous time step.

Sulfide Inhibition

High sediment sulfide concentrations can inhibit photosynthesis, and if sufficiently high can kill seagrass plants (Carlson et al. 1994). Research conducted on the temperate seagrass species *Zostera marina* shows the influence of various levels of sulfide on P_{max} (Goodman et al. 1995); increasing the sulfide concentration experienced by the plant will decrease the plants P_{max} . Although we are looking at the tropical *Thalassia*, we used the data as it is the only available study with direct measures of photosynthetic rate. Using the data from the study showing an inverse relationship between P_{max} and sulfide concentration, we calculated the relative effect a given increase in sulfide concentration will have on the P_{max} . The curve was shifted from the original data to account for the fact that seagrasses in Florida Bay experience in situ sulfide concentrations that can be ten times greater than those experienced by seagrasses in Chincoteague Bay, Maryland (Figure 2.9). This allows for the higher sulfide tolerance of *Thalassia* compared to *Zostera*. Based on observations by Carlson et al. (1994),

Thalassia die-off events in Florida Bay coincided with sulfide concentrations of approximately greater than 3 mM. The adjustment of the curve shows that at a sulfide concentration of approximately 3 mM, $Q_s = 0.8$. This 20% reduction in photosynthesis coupled multiplicatively with additional nutrient limitation experienced by the plant would lead to a significant decrease in production.

Production Allocation

Once photosynthesis and respiration are accounted for, total plant production must be allocated to various compartments of the plant. The below-ground biomass of *Thalassia testudinum* makes up a large proportion of the total biomass of the plant, approximately 85%, with the rest being green leaves (Fourqurean and Zieman 1991). Considering the known proportion of biomass in each compartment of plant and the varying turnover rates for each of the compartment based on their features new production is allocated to the compartments in the following proportions:

- Production allocated to Leaf = 65%
- Production allocated to Rhizome = 26.25%
- Production allocated to Short Shoot = 5.25%
- Production allocated to Root = 3.5%

The values selected are in accordance with the findings of Kaldy and Dunton (2000) that below-ground production in *Thalassia testudinum* accounted for approximately 35% of total plant production. It is difficult deciphering the values for the various biomass divisions within the below-ground compartment; therefore, we used these estimates and conducted further discussion on this is described in Chapter 3.

Turnover

Seagrass plants lose biomass through the shedding of senescent leaves, grazing on the leaves by birds and other animals, and rhizome death. These loss processes are combined in the model and represented as turnover rates, representing the sum of loss mechanisms other than respiration. Values used for biomass turnover were a leaf loss of 2.5% per day and all other plant material loss of 0.75% per day (Duarte and Chiscano 1999).

Propagation

Vegetative propagation occurs at a slower rate than the production and allocation processes and is updated in the model on a monthly basis. Published rates of rhizome propagation indicate that the typical rates for *Thalassia testudinum* are approximately 69 cm yr⁻¹ (Hemminga and Duarte 2000). The rules for propagation developed for this model involve a threshold of rhizome biomass (200 g m⁻²) being present in a cell before rhizomes propagate into neighboring cells. The neighborhood was divided into two tiers, depending on the amount of shared boundary between the cell of interest and the neighboring cell. The first tier consists of the neighbors in the four cells sharing a complete side with the cell of interest. The second tier of the neighborhood is the four cells at the corners of the cell of interest, as they would have some interaction with the cell but not as much as those sharing a side. A specific amount of biomass was divided among the four direct neighbor cells and the four corner neighbor cells. The proportion of rhizome biomass distributed is related to the proportion of the area surrounding the cell of interest the neighbor cell occupies (Figure 2.10). There are a total of eight cells in the neighborhood. The cells that are directly next to the cell of interest (the Von Neumann

neighborhood) each receive 19.25% of the propagating biomass, while the cells at the corners of the cell of interest (the Moore neighborhood) each receive 5.75% of propagating biomass. This value was calculated by looking at a circle with a radius of 1m. Excluding the area of the cell of interest within the circle, the area within the corners is approximately 23% of the total area encompassed within the circle outside of the cell of interest and the cells on the side represent approximately 77% of the total area of the circle.

As the seagrass rhizomes propagate, they still use resources from the cell that they initially propagated from. Research indicates that resources are translocated through the rhizome system as far as 60 cm away (Marba et al. 2002). Based on the average rhizome elongation rate of 60 cm year⁻¹ (Kaldy and Dunton 2000), a rhizome growing at the standard rate would be able to use resources from the originating cell for approximately 6 months. In addition to the time limit on support from the originating cell, at each monthly time step, the portion of resources used to support the new rhizome biomass was decreased by a proportion (16.67% (one sixth) of initial propagating material), assuming a linear monthly decrease, over 6 months, in the amount of material being allocated. Within the model, biomass from the rhizomes is translocated to neighboring cells as a function of rhizome propagation. Because of this process, it is important to consider the respiratory losses of the portion of the plant that are no longer within the cell boundaries but still may share connections with the cell for energy (i.e. carbon transfer). An artifact of the development of this model structure with transport of biomass and resource between neighboring cells is that it leaves us unable to definitively differentiate between immediate neighbor cells, as these processes are constantly occurring between a given

cell and all neighbors. Additionally, the rhizomes are programmed to show no preference for propagation into environmentally favorable cells or away from occupied cells; therefore, cells may have rhizome biomass propagating both into and out of it.

Table 2.1 Plant associated parameters, symbols, units and values used in the model. (Those parameters that are calculated in the model have a * in the value column)

Symbol	Variable	Units	Value
I_{sat} [1]	Saturating Irradiance	$\mu\text{mol photon m}^{-2} \text{ s}^{-1}$	426 1.5336
P_{max} [1]	Maximum rate of photosynthesis	mg Oxygen gram dry weight leaves ⁻¹ hour ⁻¹	13.75
R_{leaf} [1]	Respiration rate of leaf biomass	mg Oxygen gram dry weight leaves ⁻¹ hour ⁻¹	0.444
R_{root} [1]	Respiration rate of root biomass	mg Oxygen gram dry weight roots ⁻¹ hour ⁻¹	0.276
$R_{\text{shortshoots}}$ [1]	Respiration rate of short shoot biomass	mg Oxygen gram dry weight short shoots ⁻¹ hour ⁻¹	0.108
R_{rhizome} [1]	Respiration rate of rhizome biomass	mg Oxygen gram dry weight rhizomes ⁻¹ hour ⁻¹	0.054
ζ [2]	Temperature effect on metabolic rates	dimensionless	0.07
Leaf_ K_m [4]	P uptake half saturation constant	$\mu\text{M Phosphorus}$	1.05-12.4 #
Root_ K_m [4]	P uptake half saturation constant	$\mu\text{M Phosphorus}$	2.69-4.05 #
Leaf _{to} [3]	Leaf Turnover	Percent biomass lost per day	2.5
Root _{to} , ShortShoot _{to} , Rhizome _{to} [3]	Biomass Turnover	Percent biomass lost per day	0.75
B	Biomass	g dry wt m ⁻²	* Model
Γ [2]	Physiological Rate	mg Oxygen gram dry weight ⁻¹ hour ⁻¹	Varies- Photosynthesis & Respiration

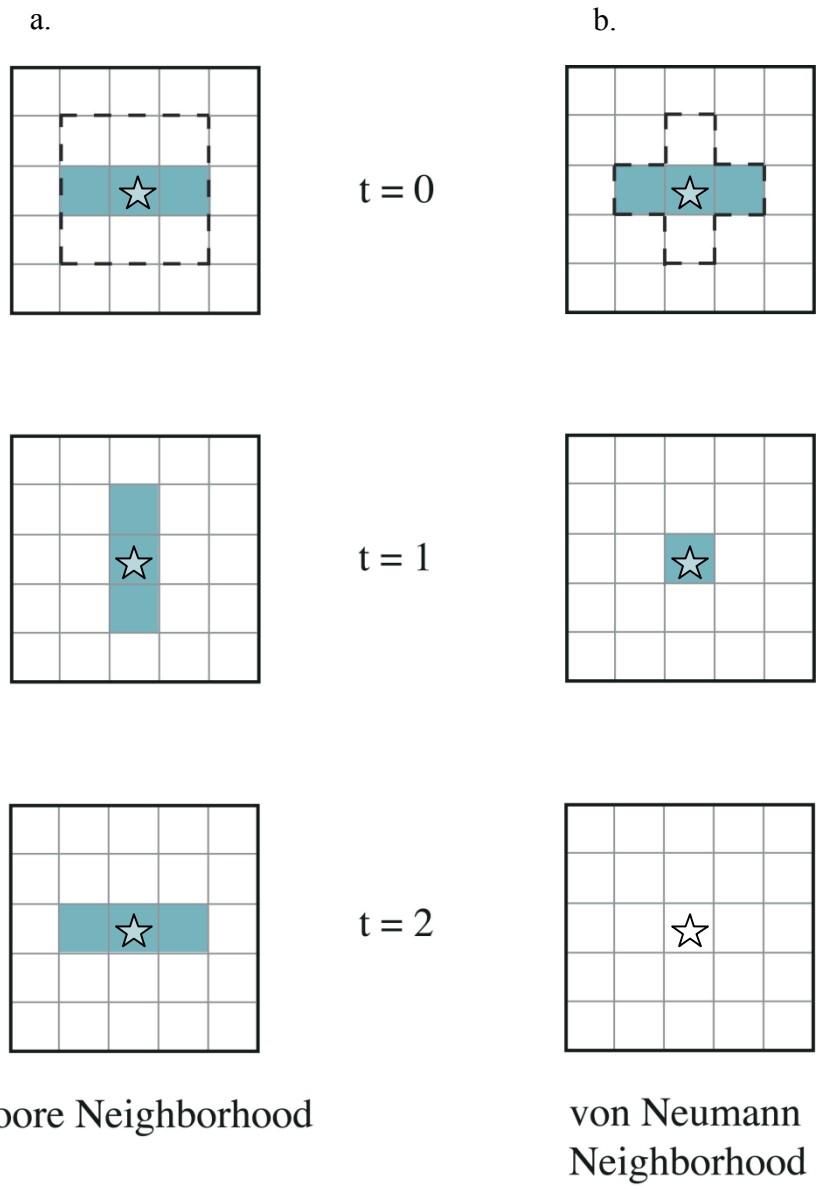
#- see Chapter 3- Sensitivity Analysis

[References for Table values: 1-Fourqurean and Zieman (1991), 2-Burd and Dunton (2001), 3-Duarte and Chiscano (1999), 4- Gras et al. (1992)]

Table 2.2 Parameters, symbols, units and values used in the model. (Those parameters that are calculated in the model have a * in the value column)

Symbol	Variable	Units	Value
H_{sat}	Hours at saturating irradiance	hours day ⁻¹	* Model
T	Temperature	°Celsius	Varies(field data)
P_i	Phosphorous concentration	µMolar	Varies(field data)
Q_p	Nutrient Limitation	dimensionless	* Model
Q_s	Sulfide Inhibition	dimensionless	* Model
HS	Sulfide concentration	µMolar sulfide	* Model
R_{OC_plant} [1]	Sulfide introduced from consumption of DOC exuded from plants	µMolar sulfide	25% Gross Primary Production
$R_{O_2_plant}$	Sulfide consumed using O ₂ exuded from plants	µMolar sulfide	*Model
R_{OC_sed}	Sulfide introduced from bare sediments	µMolar sulfide	*Model
$R_{O_2_sed}$	Sulfide consumption in bare sediments	µMolar sulfide	*Model
k [5]	Rate	µmol cm ⁻² yr ⁻¹	200
k_0	constant	µmol cm ⁻² yr ⁻¹	*model
E_a [6]	Activation Energy	J mol ⁻¹	37800
R	Universal Gas Constant	kJ mol ⁻¹ K ⁻¹	8.314x10 ⁻³
D [2]	Diffusion Coefficient for water	m ² second ⁻¹	1E-9
DBL	Diffusive boundary layer thickness	m	0.0005
Lsed [4]	Sediment Depth	m	0.4
P [3]	Porosity	dimensionless	0.8

[References for Table values: 1- Kaldy et al. (2006) 2- Boudreau (1997), 3-Rude and Aller (1991), 4-Fourqurean et al. (1992), 5- Ku et al. (1999), 6-King (1988)]



Moore Neighborhood

von Neumann Neighborhood

Figure 2.1 Two-dimensional cellular automata models through time. The time step progression, $t = 0$, $t=1$, $t=2$, of two cellular automata represented in two different neighborhoods (a. Moore Neighborhood and b. von Neumann Neighborhood) using the same rules. White cells indicate a cell state of zero, while blue cells indicate a cell state of 1. The dashed line represents the designated neighborhood.

☆The cell in the center of the grid is the cell of interest.

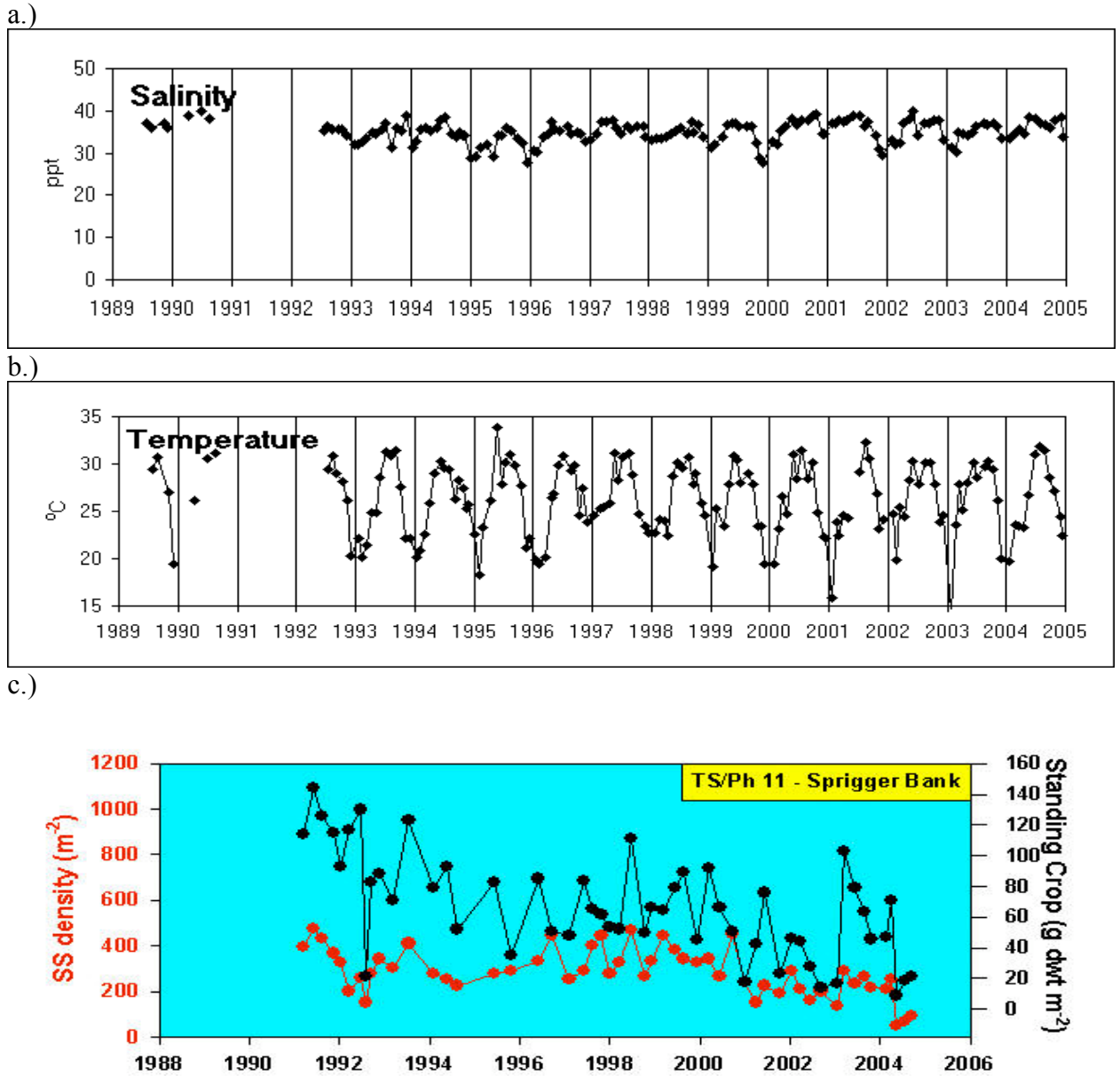


Figure 2.2 Examples of data available from long-term monitoring: a) Salinity (Southeast Environment Research Center(SERC) b) Temperature (SERC), c) Standing Crop (*Thalassia* above-ground biomass) (Florida Keys National Marine Sanctuary (FKNMS)

[SERC- <http://serc.fiu.edu/wqmnetwork/> and FKNMS- <http://serc.fiu.edu/seagrass/!CDreport/DataHome.htm>]

Model development

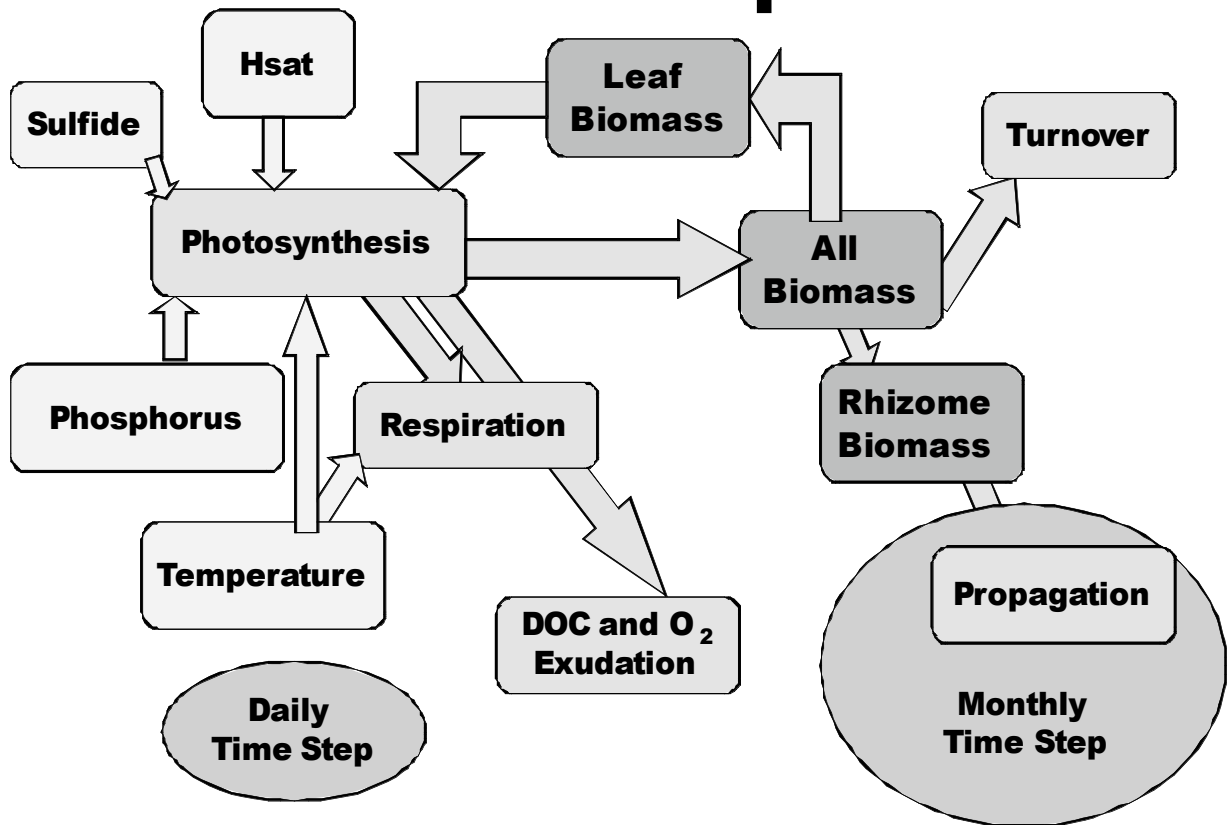


Figure 2.3 The conceptual diagram of model development showing the processes the seagrass biomass goes through (Photosynthesis, Respiration, Exudation, Turnover, Propagation) the factors affecting the processes (Hsat, Sulfide, Phosphorus, Temperature) and the time steps (Daily and Monthly).

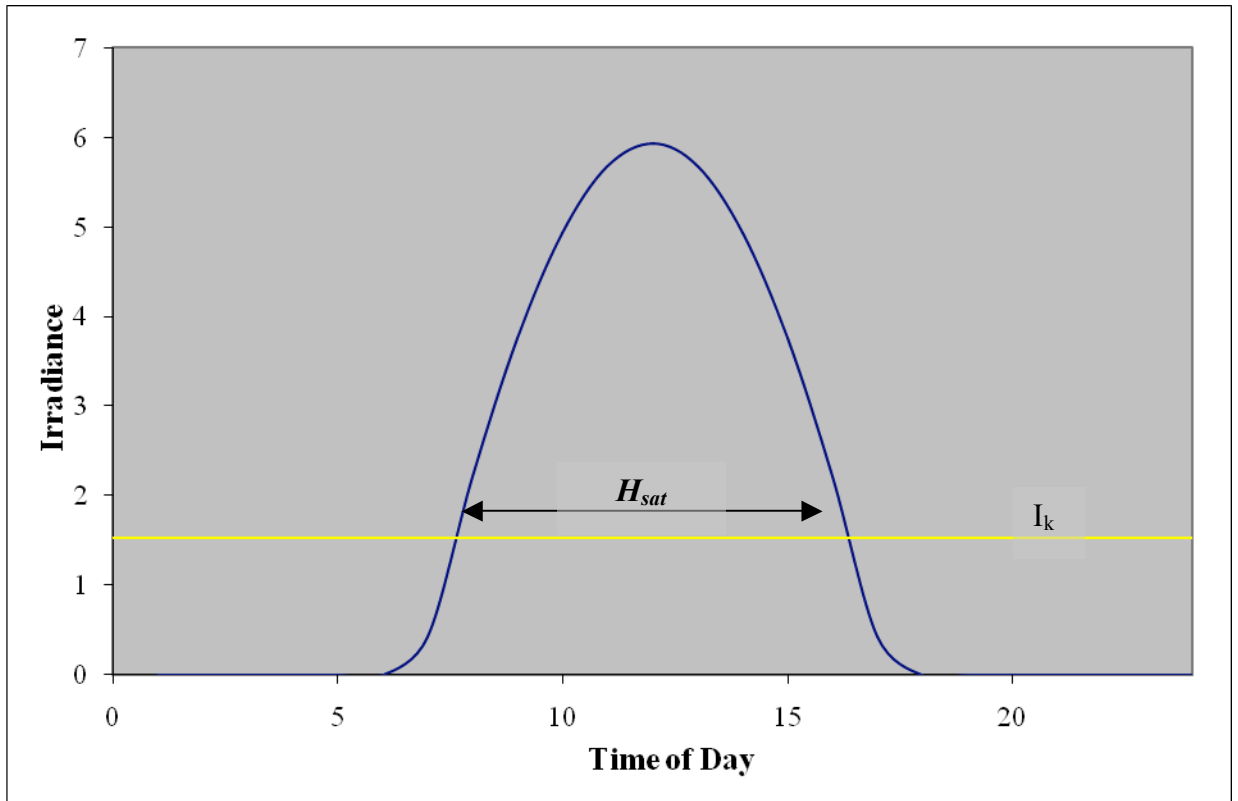


Figure 2.4 Schematic representation of H_{sat} (daily period of I-saturated photosynthesis), as defined for a cloudless day. Dark blue line is the variation in irradiance throughout the day. Yellow line indicated the value of I_k , the half-saturation values of irradiance. According to this, Photosynthesis = 0 when $I < I_k$. Adapted from Zimmerman et al. (1994).

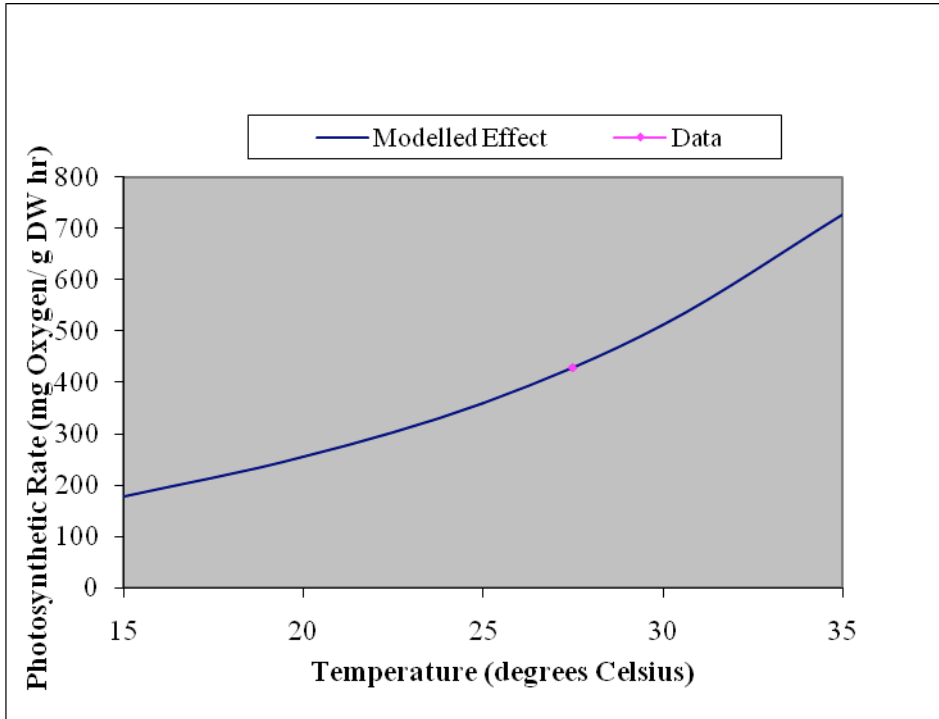


Figure 2.5 The effect of variations in temperature on P_{max} :

$P_{max}(T) = P_{max} \circ \exp(P_{max} \Delta T)$. Data point for P_{max} from Fourqurean and Zieman (1992).

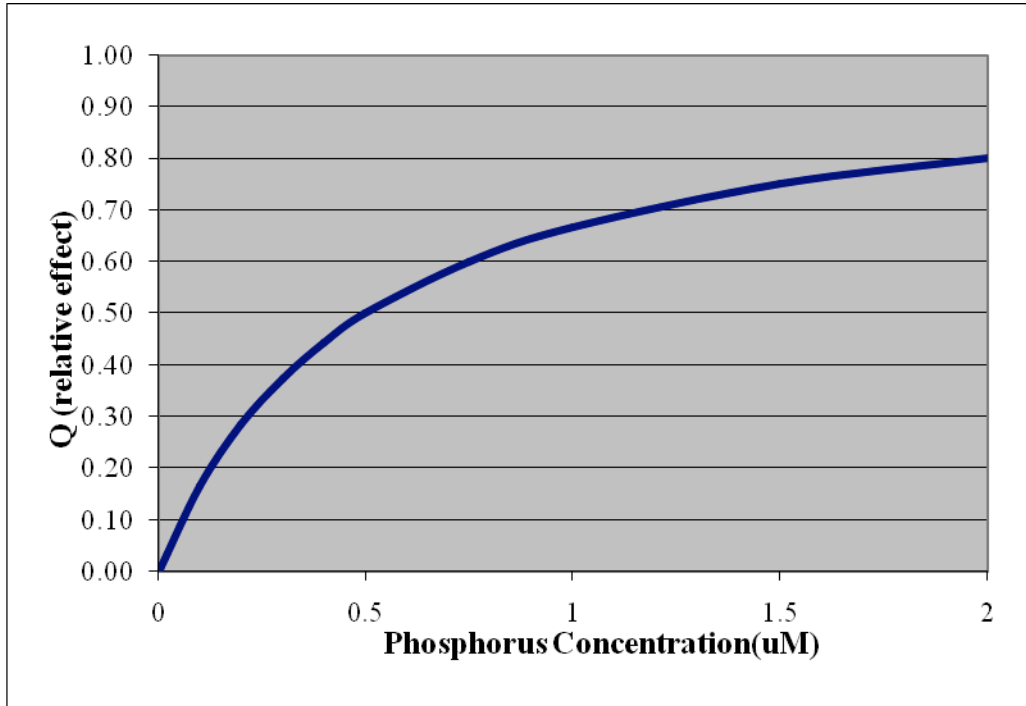


Figure 2.6 The relative effect of Phosphorus concentration on photosynthesis in

Thalassia: $Q_p = P_i / K_m + P_i$. Q_p is the factor photosynthesis is multiplied by to

show reduction in production with lower phosphorus concentrations.

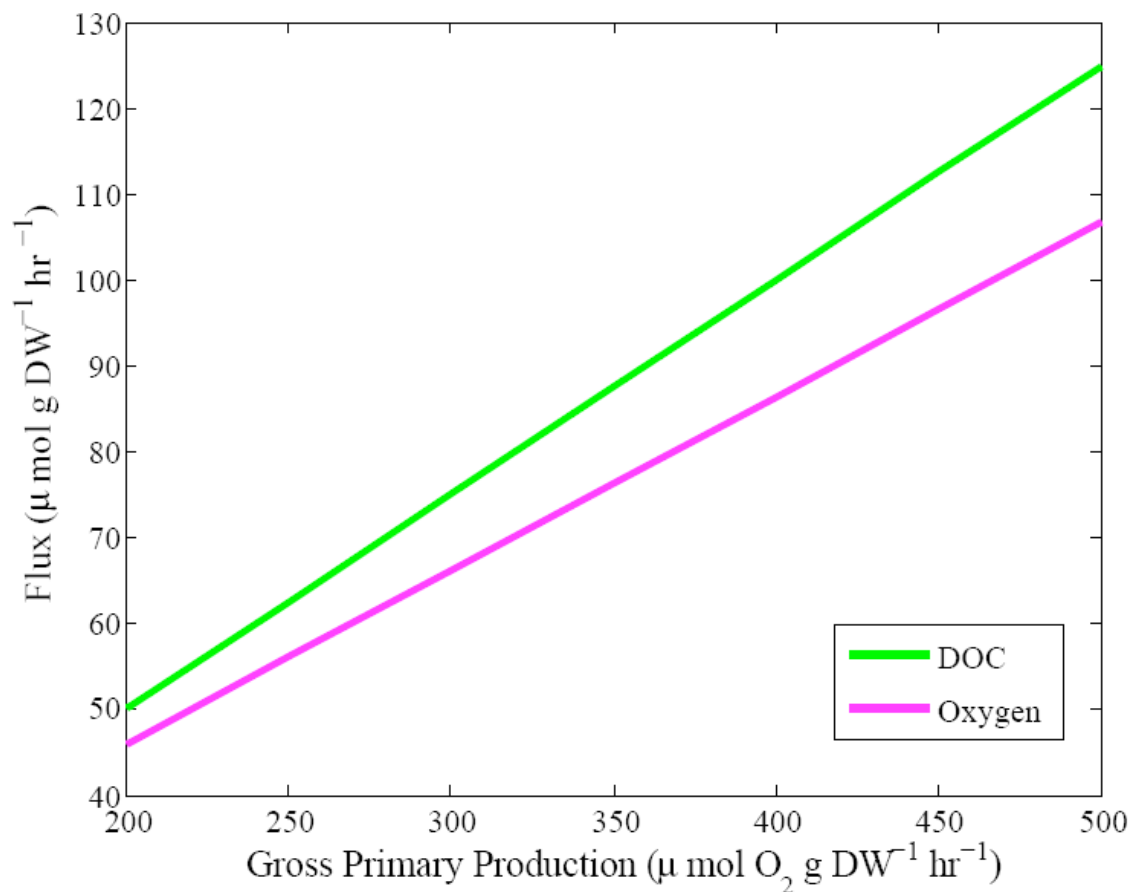


Figure 2.7 The calculated hourly flux of Oxygen and DOC from the seagrass belowground components into the surrounding sediments. Values based on a constant DOC release rate as a fixed percentage (25%) of GPP. Oxygen exuded based on equation (Based on Miller et al. 2007):

$$O_2 = ((1.0592 \times GPP) - 130.23) \times 0.25 + ((-0.062128 \times GPP) + 37.906)$$

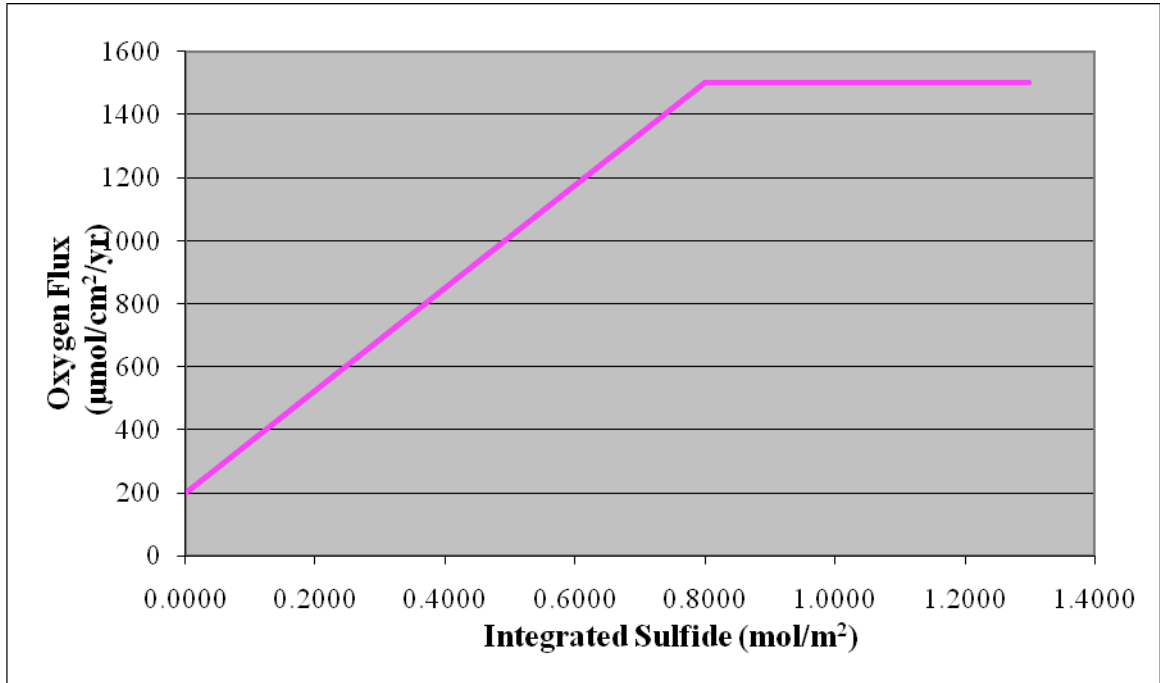


Figure 2.8 The imposed effect of Sulfide Concentration on the Oxygen Flux into the sediments from overlying bottom-water assuming high sulfide concentrations in the sediments drive the flux of oxygen from the bottom water.

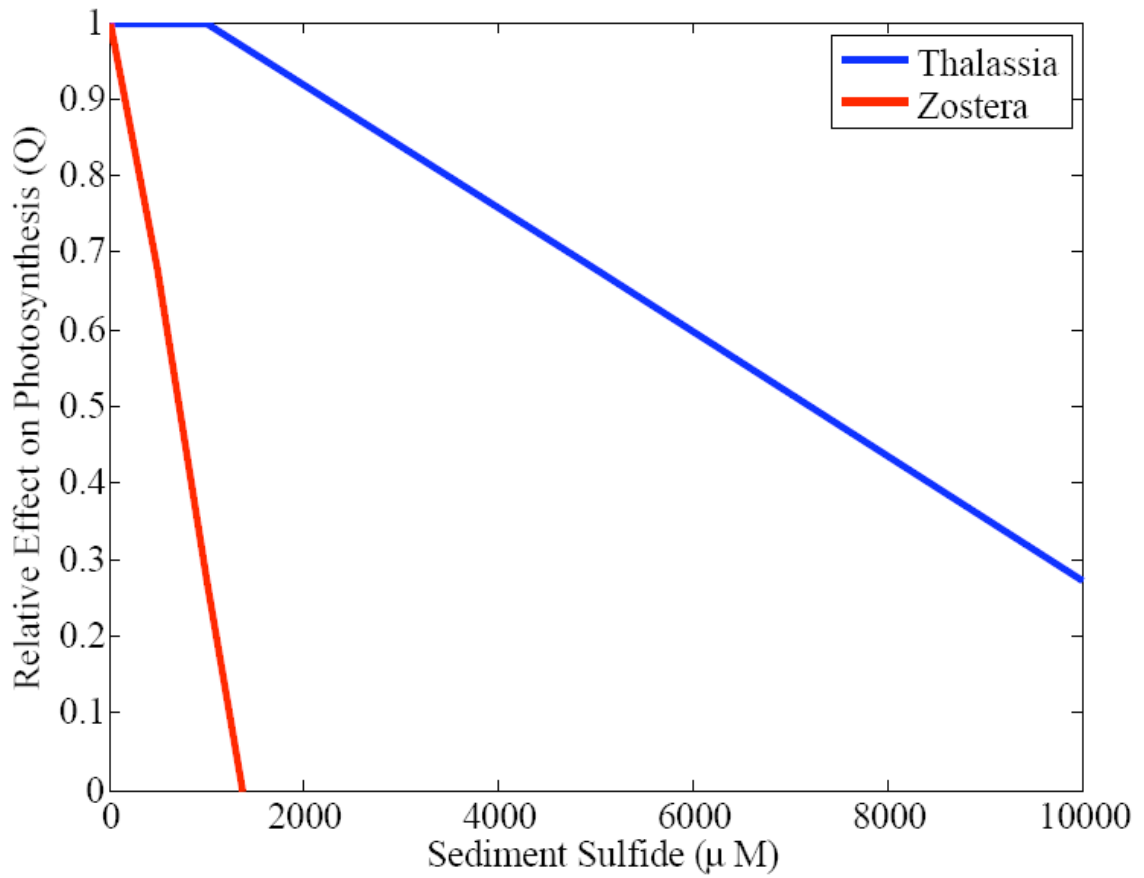


Figure 2.9 Relative Effect of Sulfide Concentration (Q_s) on the Maximum Rate of Photosynthesis of *Thalassia testudinum* derived from the work of Goodman et al. (1995) on *Zostera marina*.

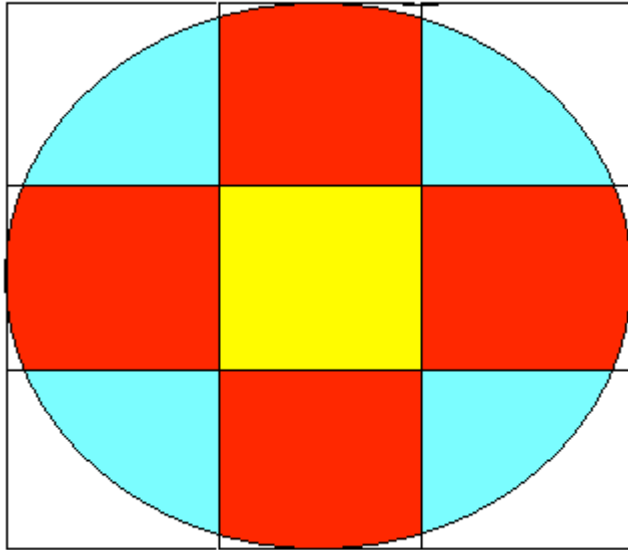


Figure 2.10 A diagram representing the spread of seagrass rhizomes into surrounding cells. The yellow cell represents the cell of interest. If the rhizome biomass in this cell reaches the threshold biomass, rhizomes will extend into the surrounding cells. Given the spread of the rhizomes is radial, the cells on the sides (red) of the cell of interest each receive approximately 19.25% of the amount of rhizome material propagating and the cells on the corners (blue) each receive approximately 5.75% of the amount of rhizome material propagating.

CHAPTER 3

SENSITIVITY ANALYSIS

Introduction

Models of natural processes require good mathematical descriptions of those processes. This implies that accurate and precise estimates of parameter values and constants are available for use in those descriptions. Sometimes, values for these parameters are either not known or have low precision, which can be important if the behavior of the model depends crucially on these particular parameters; a model may behave differently over the range of variation of a single parameter. Consequently, knowing the sensitivity of the model to variations in parameter values is crucial for interpreting model results and predictions. Sensitivity analysis is a technique for identifying those parameters, that determine the model behavior, as well as constraining their range of possible values. Knowing which parameters are controlling the model behavior can provide future research directions.

Sensitivity analysis requires selecting both the parameters and the possible model outputs. To do this, a baseline simulation and corresponding set of parameter values are chosen. The parameter values used for this simulation are typical values, and the behavior of the model should be representative of the behavior of the system the model was developed for. For example, a baseline simulation in which all seagrass plants died would be unsuitable for a sensitivity analysis aimed at determining seagrass survival. The range of model behaviors can be quantified once a suitable metric has been chosen. In the

above example, such a metric might be simulated above and below ground biomass after a fixed amount of time. If p is the parameter being varied and B is the chosen metric, then the sensitivity of the model to variations in that parameter can be quantitatively assessed using

$$S = \frac{p_b}{B_b} \left(\frac{\partial B}{\partial p} \right)$$

where p_b and B_b represent the baseline values of the parameter and metric respectively. This equation indicates that a 1% change in parameter (p) corresponds to an S % change in the metric (B) (e.g., above- or below-ground biomass).

In the sensitivity analyses presented below we chose to use the above and below ground biomass calculated after 5 years of simulation as the metric. This time period was chosen to allow the model, with the new parameter value, to reach a steady state that could be compared with the base-line model. It is important for the simulation to attain steady state conditions to ensure that transients resulting from the initial conditions are not being measured in S . All simulations were run with environmental conditions (such as light and temperature (<http://serc.fiu.edu/wqmnetwork/SFWMD-CD/Pages/FB.htm>)) representative for Rankin Lake, in north-central Florida Bay. This site was chosen as it represents a location that has experienced many changes recently including major die-off in the early 1990s.

Our initial model simulations indicated that the model was particularly sensitive to two parameters, the half-saturation constant for phosphorus uptake (K_m) and the above/below-ground allocation of production. The development of this model itself placed a significant reliance on these parameters. Additionally, these are also two areas

in which there is a lack of current research and supporting data available. In this chapter, we provide information on the sensitivity of the model to these two parameters.

Half-Saturation Constant for Phosphorus Uptake

Phosphorus is generally regarded as the limiting nutrient for seagrasses in Florida Bay (Fourqurean and Zieman 1992). Reported water column phosphorus concentrations within the Bay vary between 0.2 and 1.1 μM (Szmant and Forrester 1996, Boyer et al. 1997) and porewater concentrations vary from 0.1 to 3 μM (Fourqurean et al 1992, Szmant and Forrester 1996, McGlathery et al. 1994). Median concentrations in the water column and porewater are 0.49 μM (Boyer et al. 1997) and 0.34 μM (Fourqurean et al 1992) respectively.

Phosphorus limitation of photosynthesis is represented in the model using a Monod factor ($Q_p = P/(K_m + P)$). Consequently, photosynthesis rates will be greatly affected if phosphorus concentrations fall below K_m (Figure 3.1). In the model, phosphorus uptake limits photosynthesis ($Q_p * Photosynthesis$), however phosphorus uptake kinetics for *Thalassia testudinum* are not well known. It is known that above and below ground biomass respond differently under limiting conditions (Burd and Dunton 2001), so quantitative changes in whole-plant biomass are less obvious. Experimental studies using mesocosms give a range of K_m of 1-12 μM for a range of phosphorus concentrations between 0.5 and 25 μM (Gras et al. 2003). However, maximum phosphorus concentrations in the Bay are of the order of 0.5 μM . Such concentrations would provide severe limitation to photosynthesis using the aforementioned experimentally determined values of K_m . Indeed, Madden and MacDonald (2006) used an

assumed value of $K_m = 0.1 \mu\text{M}$ in their seagrass model to avoid complete system failure, that is seagrass decline and eventual die-off.

We used a sensitivity analysis to determine the sensitivity of modeled above and below ground biomass to the value of K_m and to also select an appropriate value for K_m . The environmental parameters for the K_m sensitivity analysis are summarized in the Appendix Table A. The baseline value of the half-saturation constant for phosphorus uptake ($0.5 \mu\text{M}$) was based on experimental studies conducted over a range of concentrations (0.5 to $25 \mu\text{M}$) (Gras et al. 2003). We ran the model using different values for K_m , ranging from 0.1 to $2.0 \mu\text{M}$ at a constant phosphorus concentration of $0.5 \mu\text{M}$ (Figure 3.1). We also ran the model at several additional concentrations (0.25 , 0.375 and $0.50 \mu\text{M}$) that are known to exist in Florida Bay and support seagrass growth (based on observations from monitoring data of seagrass and nutrient levels).

Simulations with ambient phosphorus concentrations of $0.5 \mu\text{M}$ and $K_m < 0.5 \mu\text{M}$ produced sustainable above and below ground biomass over the 5 year simulation period (Figure 3.2). Seagrass biomass was not sustainable if $K_m > 0.75 \mu\text{M}$, as expected from considering uptake kinetics (Figure 3.1) because once Q_p becomes too low, it is likely that photosynthesis becomes less than respiration. In these simulations, below ground biomass was generally greater than above ground biomass (Figure 3.3), as seen in natural systems. Steady state was reached more rapidly for lower values of K_m . For simulations with $K_m > 0.5 \mu\text{M}$, the above ground biomass declined more rapidly than the below ground biomass. This has been observed in natural situations of prolonged stress (Burd and Dunton, 2001).

These results indicate that the K_m values obtained experimentally (>1) cannot sustain seagrass biomass in our modeled representation of Florida Bay, even in regions of maximum phosphorus concentration. However, values of K_m as low as $0.1 \mu\text{M}$ (those used by Madden and MacDonald (2006)) are far lower than required for these maximum concentrations. Lower concentrations of phosphorus will be able to sustain seagrass beds with lower values of K_m . To investigate the range of possible values, we conducted additional simulations at lower phosphorus concentrations of $0.25 \mu\text{M}$ experienced in the Bay and K_m values of $0.1, 0.5, 0.75$ and $1.0 \mu\text{M}$. As seen in Figure 3.4, seagrass experienced continuous growth with the lowest K_m value indicating no nutrient limitation affecting production. However at values of $K_m \geq 0.75$ (Figures 3.5(B.)), biomass decreased to zero near the end of the first two years. The results from the analysis can be explained simply by looking at the relative effect of varying the K_m values on photosynthetic rate (Figure 3.1). The larger K_m values impose a greater influence on photosynthesis at low nutrient concentrations.

Table 3.1 summarizes the results of the sensitivity analysis using K_m of 0.5 . Phosphorus limits photosynthesis, and consequently will influence steady state above and below ground biomass. If K_m values are close to phosphorus concentrations in the Bay (e.g. 0.375), then the resulting steady-state biomass is very sensitive to the value of K_m . In this case, a 1% change in K_m , to 0.505 or 0.495 , results in a 50-81% change in above ground biomass. A 10% increase in K_m kills the plants within 2 years. If, however, K_m is less than the ambient phosphorus concentration, a 1% change in K_m results in a less than 1% change in steady-state biomass because with these values, phosphorus is not limiting production (Figure 3.1).

This sensitivity analysis has shown that model predictions of *Thalassia testudinum* production in Florida Bay will have considerable uncertainty associated with them without better knowledge of the parameters regulating phosphorus uptake. In their review, Touchette and Burkholder (2000) show that phosphorus uptake may be related to phosphorus concentrations that the seagrass experience. As stated earlier, Florida Bay has a distinct spatial gradient in phosphorus concentrations ranging from the highly oligotrophic northeast region to the less nutrient limited southwest portion. Understanding the variation of kinetic uptake parameters across the bay will be invaluable for more accurate and precise model predictions, and more effective management plans.

Evidence of acclimation of *Thalassia* uptake of phosphorus based on environmental concentrations is apparent in the results of the work of Gras et al. (2003). They tested two ranges of phosphorus concentrations: 0-25 μM and 0-5 μM . Using the Lineweaver-Burke linearization, the K_m values for the leaf was calculated for each of the two experiments represent a broad range with maximum value of 12.4 (± 4.48) μM ($R^2 = 0.94$) and a minimum value of 1.20 (± 0.63) μM ($R^2 = 0.66$). Assuming the trend represented here demonstrates the varied response of phosphorus uptake by *Thalassia* under varied ambient concentrations, it could be estimated that if the experiment were conducted with values closer to the naturally occurring range of Florida Bay, K_m values would be much lower. However, as noted by Pallud and colleagues (2007), the Lineweaver-Burke linearization, although frequently used in biological studies, may not be the most effective method of interpretation of kinetics data. Better analysis of the data presented by Gras et al. (2003) could be conducted looking at the kinetics using the

Hanes linearization method. Evaluating the results from this might give more insight variation in their K_m values and provide values closer to those that were used in the model. Using values of K_m that are too low is effective at removing phosphorus limitation from the models, but they give unrealistic results that do not capture the growth limitation these plants are known to experience.

Production Allocation

The below-ground biomass of many seagrasses plays an important role in plant propagation and survival. Below-ground biomass can act as a storage organ, thereby serving a substantial function in plant survival during prolonged reductions in resources such as light (e.g., Burd and Dunton, 2000). Also, vegetative propagation of seagrasses occurs below-ground at the apical meristems of the horizontal rhizomes and the roots are responsible for nutrient uptake from sediment pore waters. The factors affecting dynamics of seagrass below-ground biomass remain largely unquantified. This can be problematic for predicting biomass and production of *Thalassia testudinum* because the majority of the plant biomass is in the below-ground compartment, and above-ground production has to be able to support this. Models of plant production and biomass must also account for different respiratory demands of the different plant components (Fourqurean and Zieman (1991)). The development and implementation of this model and the allocation of production between respiration, carbon exudation and biomass are shown in the conceptual diagram (Figure 3.6).

Previous estimates of allocation to below-ground production have been made using models and field measurements. Burd and Dunton (2001) fitted their model of *Halodule wrightii* to data from the Laguna Madre (TX) and estimated that 34% of

primary production was allocated to below ground production. Kaldy and Dunton (2000) used field measurements of rhizome elongation to estimate that rhizome production in *Thalassia testudinum* accounted for 35% of overall production of plants from Laguna Madre (TX). In contrast, Duarte et al. (1998) used root biomass per node and the number of horizontal nodes produced annually and estimated that total below-ground production in *Thalassia* accounts for only 30% of total plant production with a majority of the production going towards the roots, not rhizomes.

Resource allocation is likely to vary seasonally. Lee and Dunton (1996) have shown seasonal changes in the soluble carbohydrate content of above and below-ground components of *Thalassia testudinum*. They hypothesize that growth during winter and early spring is supported by reserves stored in the below-ground compartments. However, existing models allocate a constant amount of primary production to the below-ground tissues and do not simulate these seasonal cycles.

The model was divided into four biomass compartments to specifically account for the difference in behavior of the specialized regions of the plant: the leaves, short shoots, roots and rhizomes. Unfortunately, we were unable to use the experimentally determined values of resource allocation in the model. There are several reasons for this. First, different authors use different definitions of above and below-ground biomass, and these do not correspond to the divisions in the model. For example, the short-shoot of *Thalassia* is the vertical rhizome and technically consists of both below- and above-ground tissue. Many authors refer to “above-ground biomass” as being only the photosynthetic parts of the plant, while other authors refer to below-ground components as being only the roots and horizontal rhizomes. Secondly, resource allocation in the

model differs qualitatively from estimates of resource allocation made from field measurements. The latter are integrative measures, often made using leaf and rhizome marking techniques (e.g., Kaldy and Dunton, 2000) to measure elongation rates, and hence production. In the model however, resources allocated to growth were calculated at each time step and did not allow for storage and remobilization of resources.

We used a sensitivity analysis to determine the sensitivity of the model results to the allocation of primary production to below-ground biomass, as well as to determine a value for the ratio of the above to below-ground production suitable for this species. The environmental parameters for the production allocation sensitivity analysis are summarized in the Appendix Table B. We again used simulated above and below-ground biomass after 5 years as metrics for the sensitivity analysis. The model classifies only photosynthetic tissue (leaf material) as above-ground biomass (Fourqurean and Zieman 1992) with the relative proportion of production allocated to the above-ground compartment varying between 60 and 70%. Below-ground production was allocated in fixed proportions to short shoots (10%), roots (15%) and rhizomes (75%).

If too little production (30-32.5%) is allocated to the below-ground structure of the plant, the above-ground biomass can exceed the below-ground biomass (Figure 3.7). This tends to occur in late summer in the model and is not observed in natural, healthy seagrass systems where below-ground biomass is typically much greater than above-ground biomass (e.g., Kaldy and Dunton, 2000). These simulations show qualitatively that a greater proportion of production needs to be allocated to the below-ground compartment in the model.

If 37.5-40% of the production is allocated to the below-ground compartment, the biomass cannot be sustained and dies-off within 3 years (Figure 3.8). There is a steady decline in the below-ground biomass during the simulation even though with the smaller value of production allocation, the above-ground biomass shows a very slight recovery (Figure 3.8(A.)). This indicates that the model is sensitive to the proportion of production allocated to the below-ground tissues.

Given the above results, we chose a value of 35% of production allocated below-ground for subsequent simulations and a baseline for sensitivity analysis (Table 3.2). These results confirm the previous analysis that if too small a proportion of production is allocated to the below-ground biomass, the above-ground biomass can be greater than the below-ground biomass. For example, with 28.5% of production being allocated below-ground, the ratio of above to below ground biomass is 1.3. Conversely, if too much production is allocated below-ground, then the plant dies. A value of 35% of production being allocated below-ground produces steady-state biomasses that are in general agreement with those observed in Florida Bay. Therefore, subsequent simulations use this value.

Conclusions

Sensitivity analysis is an integral part of any modeling exercise as it examines the effect that varying values of given parameters will have on the behavior and output of a model. This allows for a better understanding of where further research is most needed and can be useful when interpreting model results. In this work, we have also used sensitivity analysis to better constrain the ranges of certain parameters by requiring that model output be qualitatively and quantitatively consistent with field observations.

The two parameters we chose to examine were the half-saturation constant for phosphorus uptake by the seagrass and the proportion of production that is allocated to below-ground biomass. Values for both these parameters remain uncertain and the model results are sensitive to both of them.

There is little information known about seagrasses nutrient uptake kinetics, and in particular about the spatial and temporal variations in plant uptake rates. Lee and Dunton (1999) measured uptake kinetics for NH_4^+ and NO_3^- for both the roots and leaves of *Thalassia testudinum*. They found both spatial and temporal variations in both the half-saturation constants and the maximum uptake rates. For example, K_m for NO_3^- uptake by the leaves varied from 38.5 μM to 2.2 μM between February and October and K_m for root uptake of NH_4^+ varied between 34.4 μM and 649.5 μM between February and May respectively. The high end value for root uptake of NH_4^+ is well outside the range of values observed for other seagrass species (Touchette and Burkholder 2000). Curiously, water column ($\text{NO}_3^- + \text{NO}_2^-$) concentrations remained below 1.2 μM throughout the year and pore water NH_4^+ concentrations remained below 40 μM at the same site. The fact that ambient concentrations were less than the half-saturation constants suggests that nitrogen demands of the plant could be met with even uptake at a less than maximum rate, or, although less likely, that the plant had responded to ambient conditions that had passed.

By contrast, the model suggests that K_m for phosphorus uptake should be close to or less than the ambient concentration of inorganic phosphorus. If it is greater, then the model cannot sustain the plant biomass. This contradicts the results from mesocosm experiments that suggest that K_m is greater than the ambient phosphorus concentration in Florida Bay. Temporal variations in the half-saturation constants have not been taken into

account in the model. Yet, if phosphorus uptake kinetics displays the same degree of variability as inorganic nitrogen, then we would expect at least an order of magnitude variation in K_m during the year. However, without a proposed mechanism for these changes, they will be difficult to model.

The contrast between the value of K_m obtained in this study and those obtained from experimental mesocosms indicates that further work is required. Experimental studies using ambient phosphorus concentrations more typical of Florida Bay should be made.

In addition, new model formulations that capture variations, seasonal or regional, in uptake kinetics should be investigated. This will be particularly important if models are to be used for management purposes. Lack of an adequate model representation of nutrient uptake kinetics limits the predictive ability of the model in its current form.

The second parameter we investigated was the percentage of production allocated to below-ground production. Little is known quantitatively or mechanistically about resource allocation and translocation within seagrasses. The sensitivity analysis suggests that the model is very sensitive to the proportion of net primary production (NPP) is passed to the below ground biomass. This value selected based on this analysis, 35% of NPP, is in general agreement with published literature values (Kaldy and Dunton 2000 and Duarte et al. 1998). However, these proportions allocated to the above- versus the below-ground biomass also vary seasonally (Figure 3.9, adapted from Kaldy, 1997) and such variation is not built into the model. However, the model could be extended by incorporating both structural and non-structural carbohydrate. The latter is known to vary seasonally (Lee and Dunton, 1996) and presumably forms a resource for plant growth

during times of limited resources. This indicates that the below-ground material can supplement photosynthesis, and that there can be an allocation of resources from the below-ground compartment to the above ground compartment.

The model of *Halodule wrightii* developed by Burd and Dunton (2001) also contains allocation of production from above to below ground biomass, but not in the opposite sense. That model was successful at reproducing trends in above and below-ground biomass, but failed to adequately reproduce the recovery at the end of a period of prolonged light limitation. In this case, after a die-back, the below-ground biomass recovered more rapidly than the above-ground biomass, a feature not captured in the model. This difference between above and below-ground recovery rates indicates a variation in the amount of production allocated to below-ground, providing another reason for concentrating on this aspect of seagrass dynamics.

Table 3.1 Summary of results from the quantitative sensitivity analysis of the model to variations in the phosphorus half-saturation constant, K_m .

Parameter Value K_m (μM)	Indicator I (Maximum in Year 4) Above-Ground Biomass (g DW m^{-2})	Indicator II (Maximum in Year 4) Below-Ground Biomass (g DW m^{-2})	Percent Change in parameter	S above (%)	S below (%)	P (μM)
0.5	78	111	0%			0.375
0.505	37	55	+1%	-53	-50	0.375
0.495	141	194	-1%	-81	-75	0.375
0.55	0	0	+10%	NA	NA	0.375
0.45	1304	1369	-10%	-158	-114	0.375
0.5	4109	6927	0%			1.0
0.505	4091	6888	+1%	-0.42	-0.57	1.0
0.495	4126	6967	-1%	-0.43	-0.57	1.0

Table 3.2 Summary of results from the quantitative sensitivity analysis of the model to variations in the proportion of production allocated to above and below-ground biomass.

Percentage of production allocated to below-ground	Indicator I (Maximum in Year 4) Above-Ground Biomass (g DW m ⁻²)	Indicator II (Maximum in Year 4) Below-Ground Biomass (g DW m ⁻²)	Percent Change in parameter	S above (%)	S below (%)
35	78	111	0%		
35.65	24	39	-1%	69.10	65.05
34.35	181	238	1%	132.73	115.70
41.5	0	0	-10%	NA	NA
28.5	2057	1586	10%	254.44	133.46

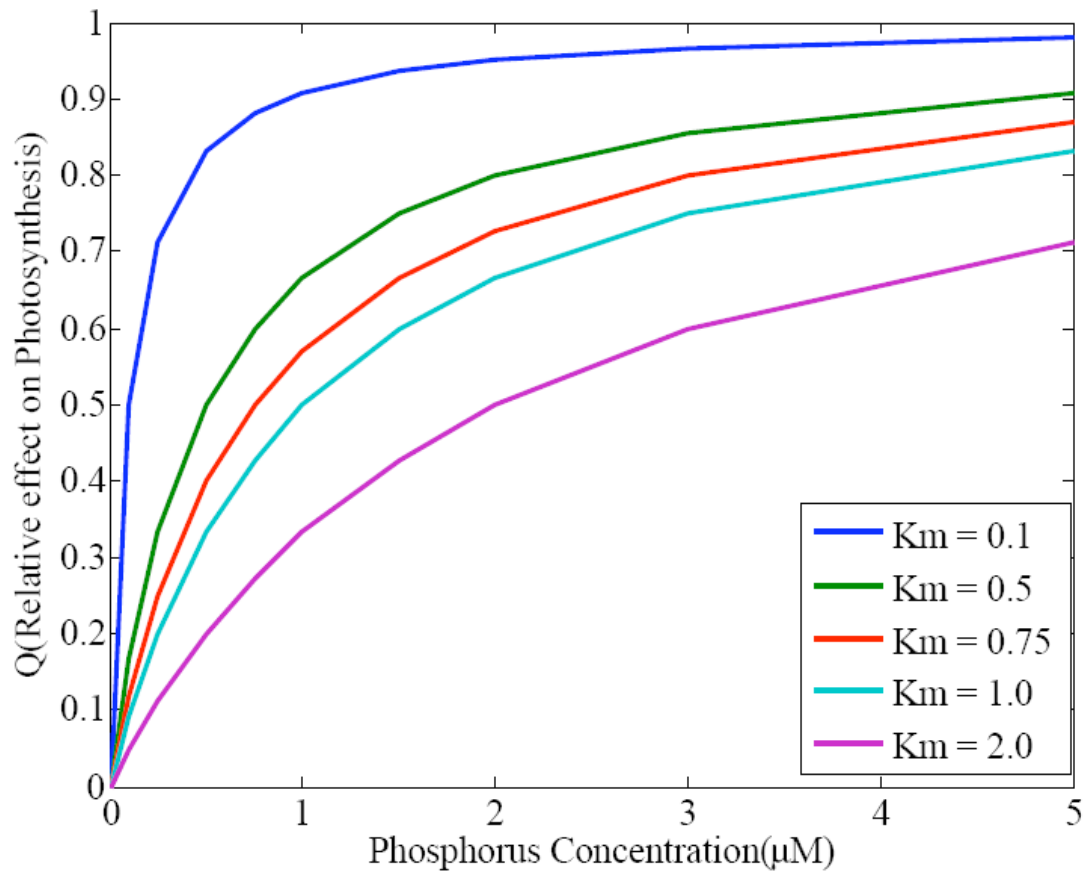


Figure 3.1 Variation of phosphorus uptake limitation on photosynthesis with phosphorus concentration and half-saturation constant (K_m) for phosphorus uptake; K_m is given in units of μM .

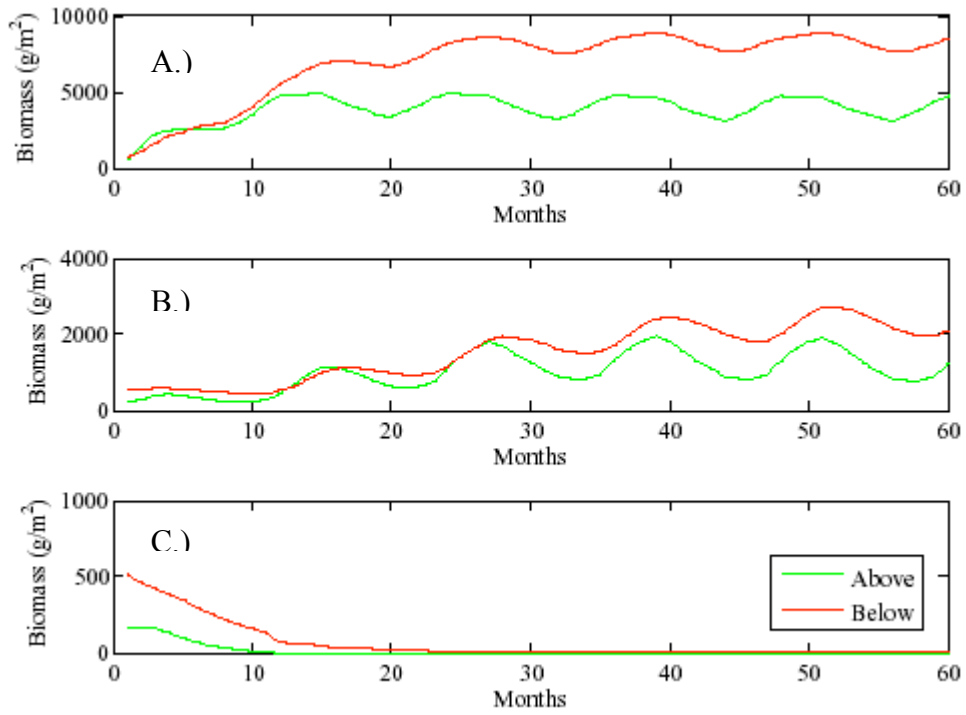


Figure 3.2 Above- and Below-ground biomass over 5 years with K_m values of 0.1 (A.), 0.5 (B.) and 0.75 (C.) μM and phosphorus concentration = 0.5 μM .

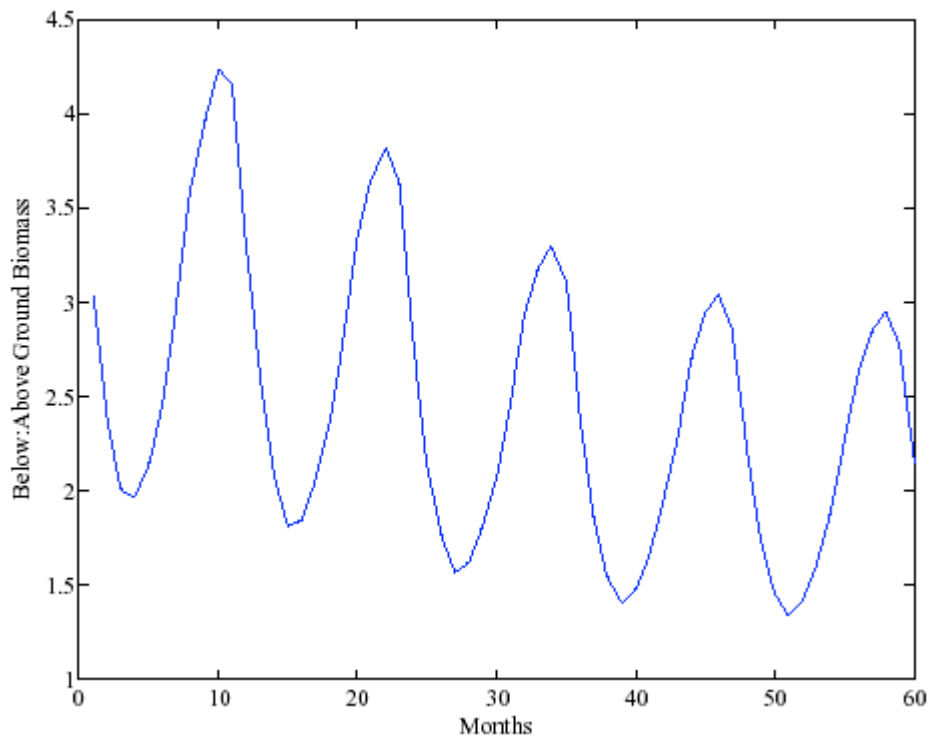


Figure 3.3 The ratio of below: above ground biomass (areal averages) over time from model output.

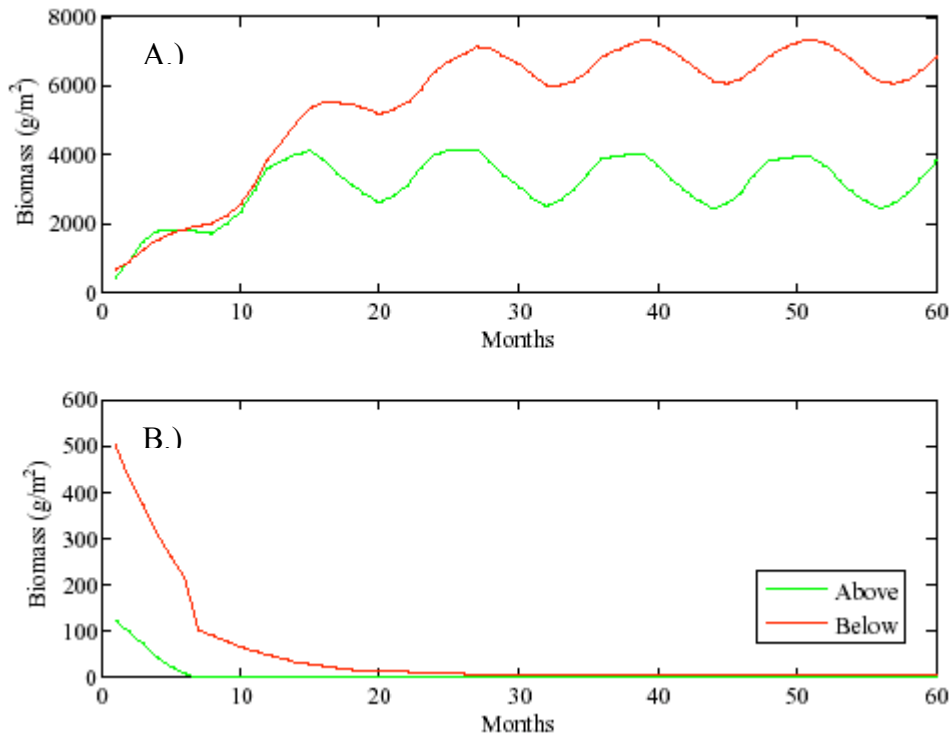


Figure 3.4 Above- and Below-ground biomass over 5 years with K_m values of 0.1 (A.) and 0.5 (B.) μM and phosphorus concentration = $0.25 \mu\text{M}$.

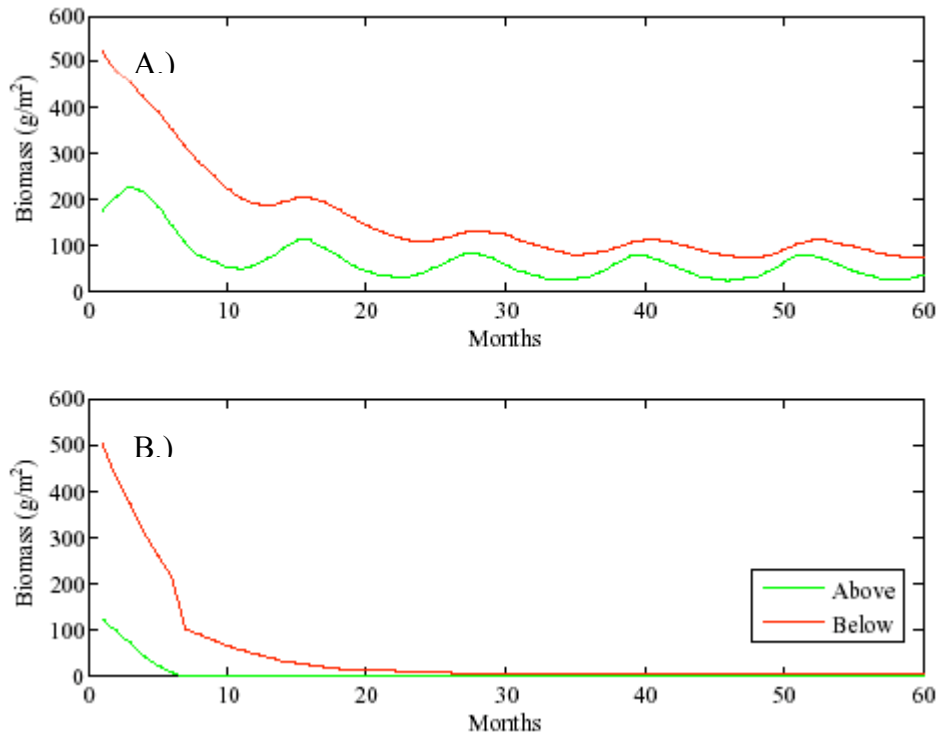


Figure 3.5 Above- and Below-ground biomass over 5 years with K_m values of 0.5 (A.) and 0.75 (B.) μM and phosphorus concentrations = $0.375 \mu\text{M}$.

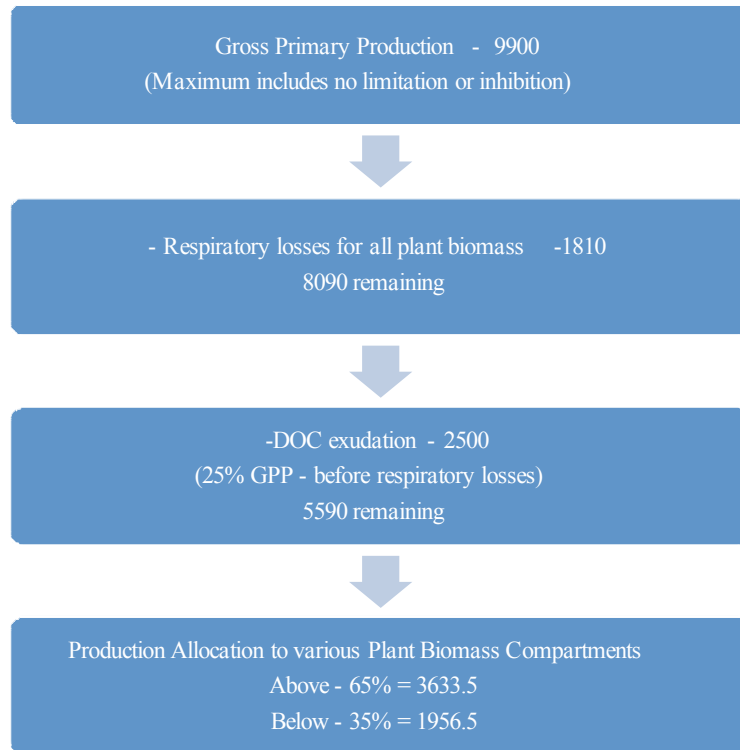


Figure 3.6 A conceptual diagram showing the flow of photosynthetically derived product through the seagrass. The values shown here represent a summer day, with maximum photosynthesis occurring (i.e. no phosphorus limitation or sulfide inhibition). The units for all values above are $\text{mg O}_2 \text{ m}^{-2} \text{ day}^{-1}$

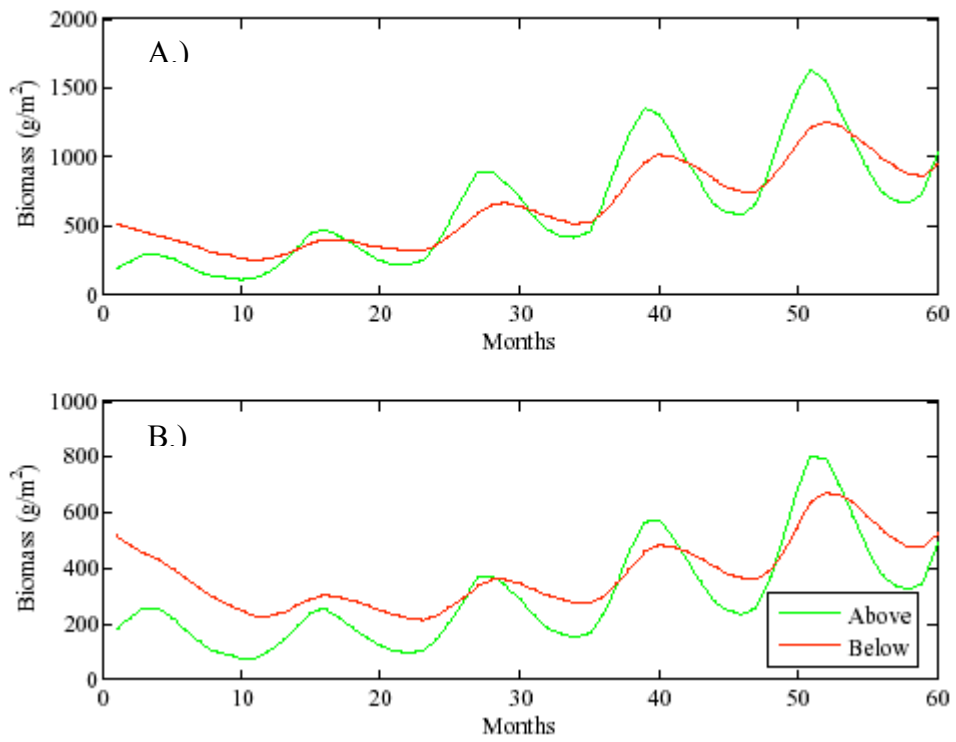


Figure 3.7 Biomass over time varying the allocation of production to above and below compartments (70/30(A.) and 67.5/32.5(B.)).

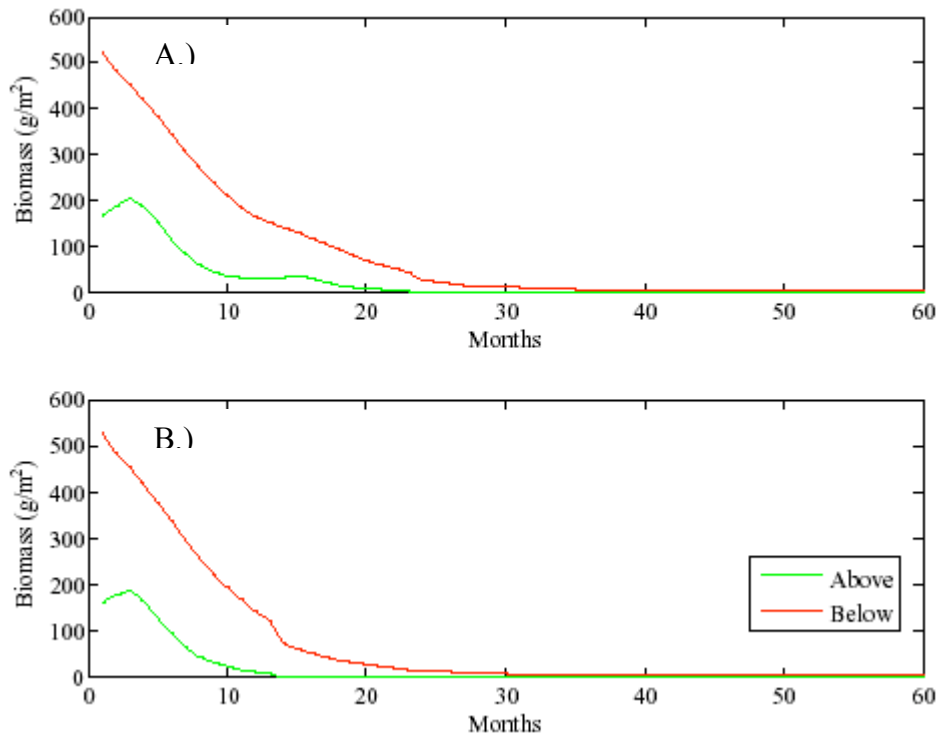


Figure 3.8 Biomass over time varying the allocation of production to above and below compartments (62.5/37.5(A.) and 60/40(B.)).

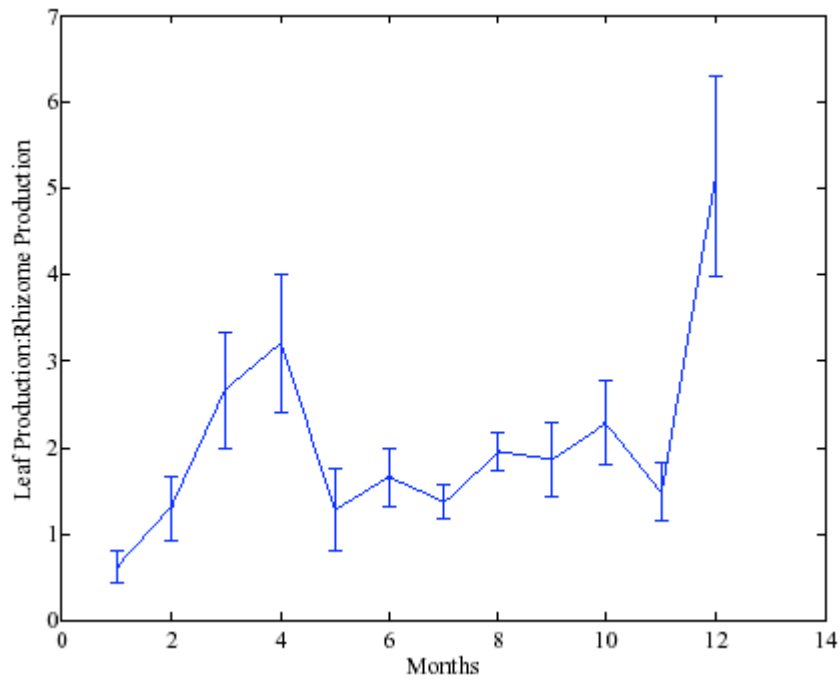


Figure 3.9 Seasonal variation in ratio of leaf:rhizome production as seen in *Thalassia testudinum* in Lower Laguna Madre Texas (created using data available from Kaldy 1997).

CHAPTER 4

CASE STUDIES

Introduction

Most existing seagrass models simulate spatially uniform seagrass growth within a given area (Fong and Harwell 1994, Burd and Dunton 2001, Madden and MacDonald 2006). Such models cannot easily deal with spatial variations in growth and propagation, which makes it difficult to use them to examine spatial processes such as recovery from prop-scar damage and patch dynamics. A seagrass patch is a small area of seagrass surrounded by bare sediments or different species of seagrasses. Natural seagrass populations are able to tolerate and recover from moderate disturbances. Recovery from extreme disturbances, arising from both natural processes (e.g., erosion, storms and other high energy events) and human impacts (propeller scars and blow-outs), is less certain and depends on a combination of seedling recruitment and vegetative propagation (Duarte and Sand-Jensen 1990). Seedling recruitment is most important for the initial colonization of unvegetated areas, which, once colonized, become established and grow laterally via the extension of below-ground horizontal rhizomes. However, the natural rate of patch formation is low because seedlings have high mortality rates and low densities (Duarte and Sand-Jensen 1990). Patch formation has not been measured for *Thalassia testudinum*, but formation rates for *Zostera marina* are approximately 5×10^{-3} patches $\text{ha}^{-1} \text{y}^{-1}$ (Olesen and Sand-Jensen 1994).

Once a patch has been formed, its growth depends on the clonal nature of the plants through their rhizome elongation. Similarly, the rate at which a gap in seagrass cover is filled will depend on rhizome elongation. In this chapter, various case studies were examined where spatial dynamics are important and a comparison is made between the model results and field measurements obtained from the literature.

Four classes of case studies were chosen in order to study the effects of heterogeneous biomass distributions and rhizome propagation on patch and gap evolution.

1. Random spatial patterns.
2. Idealized spatial patterns,
3. Patterns resulting from boat damage.

These were chosen for the insights they cast on the model behavior and for the amount of field data available to compare with model results. Particular attention was given to rates and patterns of seagrass recovery and factors contributing to spatial patch dynamics.

Random Spatial Distributions

The spatial distribution of biomass within a healthy seagrass bed is not uniform, but displays variation arising from diverse factors. For example, changes in sediment depth can affect seagrass growth (Zieman et al. 1989), as will distributions of epifaunal biomass and sediment sulfide concentrations. The small scale dynamics created by inhomogeneity in biomass cannot be examined using traditional models, but can be examined using a cellular automata model. Such models can be used to ask questions concerning the spatial distributions that arise from purely vegetative propagation.

Methods

To simulate spatial variation in biomass, the initial leaf-biomass for each cell of the model was chosen from a normal distribution of given mean and standard deviation. An initial mean biomass was chosen (150 and 200 g DW m⁻²). Any negative values were multiplied by -1 to give positive values. Initial biomasses of short-shoot, rhizome and root for each cell were then calculated as shown in Chapter 2. Irradiance, calculated from the PAR model, and nutrient concentrations were spatially uniform but sulfide concentrations were allowed to vary (according to the formulation in Chapter 2). The environmental parameters for the random spatial distribution case studies are summarized in the Appendix Table C. The simulation was run for a period of 5 years. Results from simulations with random initial biomass were compared with field data from Florida Bay.

Results

The average modeled biomass reached a quasi steady state within 2-3 years (Figure 4.1). The above-ground biomass decreased by over a factor of two, from an initial value of 150 or 200 g DW m⁻² to a peak steady state value of approximately 60 g DW m⁻² – note that average standing crop of *Thalassia* in Florida Bay varies from about 30 g DW m⁻² in the northeastern region of the bay to 125 g DW m⁻² in the western region (Zieman et al. 1989 and Hall et al. 1999). If an initial average biomass of less than 150 g DW m⁻² was chosen, then the seagrass population died within the 5 years of the simulation. Sediment sulfide concentrations also reached a quasi steady state within 2-3 years of the simulation with peak values of 800 μM (Figure 4.2), which is consistent with values measured in Florida Bay (Carlson et al. 1994).

Leaf biomass within cells also reached a quasi steady state. Comparison of the biomass within each cell at the end of 3 years with that at the end of 5 years reveals a one-to-one relationship for all cases except those with very low biomass at the end of 3 years (Figure 4.3). Cells with less than approximately 3 g DW m^{-2} at the end of three years were not able to sustain biomass during the following two years.

The frequency distribution of biomass also changes during the simulation, indicating a change in the spatial biomass distributions (Figures 4.4 – 4.7). In all cases the initial normal distribution is shifted to lower values and its width is decreased. For an initial distribution with a mean leaf biomass of $150 \pm 15 \text{ g DW m}^{-2}$ the final distribution is approximately normal except for an increase in the frequency of cells having zero biomass (Figure 4.4). Broader initial biomass distribution however, show deviations in the final biomass distribution from a normal distribution are apparent in both the high and the low tails (Figures 4.5 – 4.7).

Comparison of initial and final within-cell biomass showed the existence of three distinct populations (Figure 4.8). For sufficiently large (in this case, greater than about 160 g DW m^{-2}) initial within-cell leaf biomass, the final biomass is lower than the initial value but related to it in an approximately linear manner. Two populations are evident for initial leaf biomass below 160 g DW m^{-2} . The first population is characterized by final leaf biomass being less than the initial leaf biomass and the second is characterized by final leaf biomass being greater than the initial leaf biomass for that cell.

The model results using an initial random distribution of above-ground biomass, with an average of $150 \pm 15 \text{ g DW m}^{-2}$, were compared with those measured at Sprigger Bank and Duck Key (Figure 4.9), both sites of the Florida Coastal Everglades Long Term

Ecosystem Research Program (data obtained from the Seagrass Ecosystem Research Lab website <http://serc.fiu.edu/seagrass/!CDreport/DataHome.htm>). These two sites were chosen because they represent regions of maximum and minimum seagrass standing stock in the Bay and long time-series are available for both sites. The comparison of simulated leaf biomass with field measurements from Florida Bay shows that leaf biomass at Sprigger Bank and Duck Key bracket the quasi steady state biomass given by the model (Figure 4.10). Seasonal changes in biomass at the two sites and the model do not always agree, possibly indicating variation in an environmental parameter affecting plant growth. In 1995-1996, the model predicts a peak in biomass, but the data from both Sprigger Bank and Duck Key show a minimum. However, in 1994-1995, the peak in the model biomass corresponds to a minimum at Sprigger Bank and is close to a maximum at Duck Key.

Discussion

These results indicate that model transients last for approximately 2 years, but that after 3 years, quasi steady state conditions hold. The quasi steady state is determined by environmental conditions (such as irradiance and nutrient concentrations) rather than the initial conditions (this can be seen in Figure 4.1 where different initial biomasses result in almost the same quasi steady state). The seagrass biomass decline observed with an initial biomass of less than 150 g DW m^{-2} indicates that the model works toward some ratio of biomass values that is slightly different than our initializing conditions. These values are influenced by the processes included in the model and the parameters that represent them. This suggests that any major conclusions drawn from the model behavior

should be taken from the activity of the model following the first two years after this stabilization has occurred.

The shift in frequency distribution of biomass might also indicate that the relative patchiness of the biomass distribution matters. Further examination of frequency distributions of the specified neighborhoods surrounding cells of interest may provide an explanation.

Model results also indicate that the more spatially uniform a distribution of biomass is, the more stable the seagrass bed is. This could have consequences for replanting, where the aim would be to have a uniform distribution of seedlings or transplant units. In replanting studies, a success rate of 68% in 15 months was achieved using a uniform spatial distribution of one transplant every 20 cm (Ehrlinger and Anderson 2002). Similarly, research has shown that the more short shoots present on a transplanted plant fragment, the greater the survival of the transplant (Tomasko et al. 1991).

The magnitude of the modeled leaf biomass is consistent with the monitoring data indicating that our model is appropriately capturing the general behavior of the plant biomass. However, the model results exhibit a slight delay in the peaks of leaf biomass when compared with data from the monitoring sites (Figure 4.10). This may indicate the need for more modification of the model, possibly by incorporating a seasonality, in the values of parameters for processes such as resource allocation.

Idealized Patterns

The spatial distribution of seagrass biomass is determined largely by the vegetative production of the below ground tissues. For example, Burd and Dunton (2001) showed the importance of the rhizomes for recovery of *Halodule wrightii* after

prolonged, chronic light limitation. In addition, it is known that the rate at which a newly formed patch increases in size is determined in part by the elongation and branching rates of rhizomes (Vidondo et al. 1997 and Marbà and Duarte 1998).

The seagrass model implemented here does not incorporate the structure of the rhizomes, but instead models their propagation as a linear advance dependent on resource translocation from existing seagrass tissue. In this case, one would expect that the rate of increase in coverage would depend on the linear dimensions of the coverage gap being filled, as well as its shape. In particular, the number of vertices will be important. This is because at a corner, more cells can contribute to the propagation of rhizomes into the gap. The consequences of this simplification need to be examined. To do that, a series of simulations were performed with initial conditions chosen to represent gaps and patches having known, simple geometries.

Methods

As previously stated, these simulations were run for five years with an initial uniform distribution of leaf biomass of 150 g DW m^{-2} . The environmental parameters for the idealized patterns case studies are summarized in the Appendix Table D-G. A series of initial gap and patch geometries were set up and are summarized in Tables 4.1 – 4.4 and Figures 4.11 and 4.12. Within the overall grid, patches or gaps of varying sizes were created using rectangles, squares and multi-sided polygons. The different gap sizes and shapes were selected to examine both the difference in perimeter-to-area ratio and the influence of multiple corners on seagrass propagation. For gap geometries, an area of zero biomass was created in the initial biomass distribution. For patch geometries, a region of uniform leaf biomass (of 150 g DW m^{-2}) was created, with the remaining grid

cells containing zero biomass. Changes in seagrass coverage were calculated using changes in rhizome biomass only, not above ground biomass, because we are only interested here in coverage changes resulting from vegetative propagation.

Results

The rate at which gaps are filled as a function of the perimeter-to-area ratio is shown in Figure 4.13. There is an approximately linear relationship between the gap perimeter-to-area ratio and the proportion of the gap area filled in during the simulation.

The effect of varying the shape of the gap was inconclusive. The fill-in rate for the 20-sided polygon was the same as that of a rectangle having the same perimeter-to-area ratio (Table 4.2). However, the fill-in ratio for these two shapes is greater than that expected from the regression relationship. Curiously, the fill-in rate for a 12-sided polygon has a lower than expected fill-in rate.

Contrary to our expectations, there was no clear relationship between the number of corners that a gap possessed and the fill-in rate of that gap. For example, cases B and C in Table 4.2 have the same perimeter-to-area ratio and rhizome fill-in rate but different numbers of corners and different leaf fill-in rates. For both these cases, the rhizome fill-in rate was faster than expected. However, case D in Table 4.2 has more corners than a simple quadrilateral, but has a lower than expected rhizome fill-in rate (Figures 4.14 – 4.15).

The evolution of patches followed a similar pattern to the fill-in of gaps in the seagrass distribution (Tables 4.3 and 4.4 and Figures 4.16 and 4.17). Both leaf and rhizome coverage increased with increasing perimeter-to-area ratio, but with the increase in leaf coverage being lower than that of the rhizomes (Table 4.3). As with the gap fill-in

rate, the rectangle and polygon with identical perimeter-to-area ratios (cases B and C, Table 4.4) had the same increase in rhizome coverage, but the rectangle had a smaller increase in leaf coverage.

Discussion

In examining the results from the idealized pattern runs, the model behaves as would be expected given the way in which rhizome propagation has been represented although we are unable to explain all of the observed results. Colonization from one cell to another occurs, for the most part, along the edges of the cell, and at a constant rate. Patches and gaps with a greater perimeter:area ratio generally exhibited faster colonization. This correlates with observation in temperate seagrass species in Australia (Kendrick et al. 1999). Additional analysis could be conducted over the temporal scale of the simulations to analyze the change in perimeter:area ratio as the simulation progresses and to see if that, in turn, correlates to any variation in propagation. Corners and vertices in the patch or gap geometry produce faster colonization rates because of the larger number of neighboring cells that can contribute to the colonization. This simple representation of rhizome propagation adequately captures the geometry of the rhizome network for *Thalassia testudinum*.

Patterns of leaf fill-in of gaps lag behind those of the rhizomes (Figures 4.14 and 4.15). This is most evident in cases with more complex geometry (Figure 4.15). The reason for this is that the plant must first colonize a region with below-ground material before building above ground material.

Although our analysis looked at varying geometries, the focus was placed on polygons with 90° angled vertices. To expand this analysis, various other shapes could be

incorporated, such as circles and triangles. Following these lines may lead to more conclusive results in terms of what parameters of patch or gap shapes have the largest impact for propagation.

Motor Vessel Injuries

Motor vessel injuries such as propeller scarring and the more serious blow-out, are the most common form of human disturbance to seagrass beds. Whitfield and colleagues (2004) made observations of a large-scale disturbance that occurred in a mixed species (*Thalassia* and *Syringodium*) seagrass bed in Red Bay Bank in southwest Florida Bay. A 7200 m² ‘blowhole’ was created when a tugboat ran aground in the bed, completely destroying the above- and below-ground seagrass community structure. The perimeter of the initial injury was mapped in May 1993 and a follow-up was conducted in January 1998 (Figure 4.18). During the recovery a succession of seagrass species typical for tropical regions was observed: *Syringodium* made up approximately 7.1% of the recovery propagating into the injured regions during those 4.8 years, while *Thalassia* only accounted for 5.9% of the seagrass recovery. The remainder of the recovery area was colonized by various forms of macro-algae (Whitfield et al. 2002).

Propeller scars are more common than large-scale damage caused by motor boats. Although little published information exists for incidence and recovery rates of propeller scarring in Florida Bay, some information does exist for nearby Tampa Bay, Florida (Dawes et al. 1997). Initial injuries to *Thalassia testudinum* beds were rectangular in shape and approximately 5 m x 1.25 m in size. Recovery into these injuries was found to take 1.7 to 7.3 years with a mean recovery rate of 3.5 years, where recovery was defined as re-growth to average densities of the surrounding standing crop (Dawes et al. 1997).

In this series of simulations, initial conditions were set up to represent typical prop-scar damage (Dawes et al. 1997) and the blowout examined by Whitfield et al. (2004). The aim was to examine if the model could replicate some of the large-scale features of seagrass recovery from these events. Of particular interest is whether or not environmental parameters (such as nutrient and sulfide concentrations) can significantly alter the recovery rates. This is important because we know that phosphorus is the limiting nutrient for seagrasses in Florida Bay, and from the model sensitivity tests we know that the model is highly sensitive to the phosphorus concentration.

Methods

Initial conditions were created for a blowhole that had a similar size and shape as that observed by Whitfield et al. (2004) (Figure 4.19). The region surrounding the blowhole was assumed to be unaffected by the disturbance and contained healthy plants. Average phosphorus concentrations in the region during this time varied between 0.2 μM and 0.4 μM (Boyer et al. 1997). To represent this, various simulations were run with either spatially constant phosphorus concentrations, or spatially random concentrations chosen from a normal distribution (parameters summarized in Table 4.5 and 4.6, and Appendix Table H). If random numbers were generated less than zero, the absolute value was used.

To simulate recovery from propeller scarring, initial biomass (150 g DW m^{-2}) distributions were created containing rectangular gaps of length 10 m and width 2 m. These gaps were twice as wide as observed propeller scars. This was done because the spatial resolution of the model was only 1 m and rhizome propagation rates would require

that re-growth would occur immediately from both sides of the scar if the dimensions were 10 m by 1 m.

Simulations were run for five years. Sulfide and phosphorus concentrations were either constant or allowed to vary spatially, with phosphorus concentrations chosen from the range measured by Boyer et al. (1997). The environmental parameters for the propeller case studies are summarized in the Appendix Table I. The damage caused by motor-vehicle damage can also increase sediment sulfide concentrations by suddenly removing the above-ground biomass. The below-ground biomass is no longer supported and can die; releasing dissolved organic carbon into the sediments that can in turn fuel microbial production of sulfide. To mimic this process, we varied background sulfide concentrations in the propeller scarring simulations.

Results

Recovery of *Thalassia* into the simulated blowhole depended on the phosphorus concentration (Table 4.5, Figure 4.20). Rhizome recovery coverage was always greater than leaf recovery coverage, though for case A (Table 4.5), the difference was slight. Rhizome coverage always increased, with increases ranging from 6.5% to 19.9%. Changes in leaf coverage on the other hand were both positive and negative, with loss of leaf coverage occurring for phosphorus concentrations of 0.3 μM and lower.

Recovery of both rhizome and leaf coverage was increased if the phosphorus concentration was spatially variable (compare cases A – C in Table 4.5). Indeed, variable phosphorus concentrations produced greater recovery than cases with constant phosphorus concentrations (compare cases A and C, Table 4.5). Leaf coverage recovery of 6.5%, similar to that observed by Whitfield et al. (2004), was obtained using a

spatially variable phosphorus concentration with mean value of 0.3125 μM (case G, Table 4.5).

The results for the propeller scarring simulations are summarized in Table 4.6. At constant high nutrient concentrations (0.375 μM) full rhizome recovery occurred but no leaf recovery took place after 5 years (case A, Table 4.6). However, when the nutrient concentration was allowed to vary spatially, full recovery of both above- and below-ground biomass was observed after 5 years (cases B and C, Table 4.6).

High background sulfide concentrations affected the plant recovery. For initial background sulfide concentrations greater than 4000 μM , there was a full recovery of both rhizome and leaf coverage, but the biomass densities did not recover to that of the surrounding region, as they had for lower sulfide concentrations (cases G and H, Table 4.6).

Discussion

The simulations of motor vessel injuries demonstrated that the model can give estimates of gap behavior in seagrass beds with realistic time scales. The model possesses the ability, using the parameters it was developed with, to provide rough estimates of recovery into these regions using vegetative propagation. Propeller scar simulations showed that full recovery took place within the five years, which is consistent with the mean recovery rate of 3.5 years observed by Dawes et al. (1997). This indicates that the method we have selected for modeling *Thalassia* propagation is accurate at the same spatial and temporal scales that are observed in nature.

Conclusion

The development of this model was a proof-of-concept project to see if a cellular automaton could be used to simulate the spatial evolution of a seagrass bed. It is difficult to incorporate processes leading to spatial dynamics in traditional seagrass unit models (e.g., Burd and Dunton 2001), which predict spatially uniform biomass densities. This is because the processes giving rise to spatial variation (such as vegetative propagation and resource translocation) are not easily translated into rates per unit area as would be required in these models. It would be possible to add a diffusive term to these traditional models to represent spatial growth, however solving these models would require numerically solving the resulting reaction-diffusion equations. Using a cellular automaton for below-ground vegetative propagation incorporates spatial processes without resorting to sophisticated numerical approaches. The simulations reported in this chapter were designed to test the capabilities of the cellular automata approach, and to suggest improvements and alternative approaches.

Spatial dynamics within a seagrass bed arises from two sources: environmental processes such as variations in sediment depth or spatial variation in nutrient concentrations, and plant-related processes such as seed dispersal and rhizome elongation. This model, and the test cases examined in this chapter, concentrates on rhizome elongation and variations in nutrient concentration.

The model was parameterized for the general region of Florida Bay. This region is relatively oligotrophic in the eastern part of the bay (e.g., Duck Key) which is characterized by low seagrass biomass densities, and high seagrass biomass occurring in the central and western regions of the bay (Boyer et al. 1999 and Hall et al. 1999). Clear

sky irradiance was calculated for the latitude of the bay, and typical nutrient concentrations found within the bay were used in the model. Given this, the model predicts quasi steady state seagrass biomass densities that fall between the high values measured at Sprigger Bank and the low values of Duck Key. Interannual variations could not be modeled because neither surface nor underwater irradiance is regularly measured in the region and such measurements are crucial for model validation (Burd and Dunton 2001). What is more, the quasi steady state appears to be robust to variations in the initial biomass.

Additional factors, apart from irradiance, would be needed to make the model applicable to specific regions of Florida Bay. It is known that seagrass distributions in the bay reflect changes in sediment depth, with shallow sediments in the eastern region preventing extensive stable seagrass meadows from being established (Zieman et al. 1989). Phosphorus concentrations also vary spatially and temporally throughout the Bay (Boyer et al. 1999), with lower concentrations in the eastern part of the bay. As discussed in Chapter 3, the model is sensitive to the parameter values used to represent phosphorus uptake kinetics. Values for these parameters that have been measured in mesocosm experiments are higher than ambient phosphorus concentrations in the bay, and consequently lead to mortality when used in simulations. If ambient phosphorus concentrations vary across the bay, then it is also possible that values of the uptake parameters also vary and this would need to be taken into account in any model that aimed to accurately represent seagrass productivity in the bay.

The distribution of leaf-biomass per cell in the quasi steady state is not a normal distribution. Initializing the model with a normal distribution of within-cell biomass

resulted in non-normal distributions with lower means. The lower mean reflects the lower sustainable biomass in the quasi steady state and the larger number of cells that have zero biomass leading to a non-normal distribution in the quasi steady state.

The quasi steady state biomass distributions also show deviations from a normal distribution at the high biomass end. This is particularly evident when the initial distribution was broad (e.g. Figure 4.7). Broad distribution of biomass initially would contain more cells within the high biomass range. Given this, it would be expected that these cell would lead to more cells after the five year simulation remaining with a higher biomass value. However, the final biomass distribution has fewer than expected cells with high biomass. This could indicate that individual cells lose biomass at rates that depend on the amount of biomass in the cell. For example, biomass in one cell interacts with its neighboring cells through self-shading of leaf biomass and through resource translocation and rhizome propagation. It is therefore unclear what determines the final steady state biomass distribution, and ultimately it may depend on the properties of the neighboring regions.

A similar conundrum is apparent when the initial and final within-cell biomasses are plotted against each other (Figure 4.8). There are apparently two distinct populations that both have low initial biomass ($< 150 \text{ g DW m}^{-2}$). For one group, the within-cell biomass decreases, in many cases to zero. However, within-cell biomass increases for the other group. Again, interactions between the biomass of one cell and its neighbors might explain this. For example, a cell with low initial biomass that is surrounded by cells with high biomass would be colonized by its neighboring cells. However, a plot of initial within-cell biomass against the sum of the biomass in surrounding cells does not show

any pattern that might explain the difference between these populations (Figure 4.22); therefore, further examination would be required to establish the relationship, if any.

The simulations of idealized spatial patterns provide an indication of patch growth and gap fill-in rates in the model. In particular, these model simulations show the importance of patch and gap geometry. Through testing various shapes, it was shown that corners and vertices in the patch or gap geometry produce faster colonization rates because of the larger number of neighboring cells that can contribute to the colonization.

Seagrass rhizomes form a branched network with a rate of horizontal growth that varies considerably between species. For example, rhizomes of *Posidonia oceanica* grow at rates of only a few centimeters a year, whereas those of *Halophila ovalis* can grow at more than 5 m per year (Duarte 1991 and Marbà and Duarte 1998). This range in rates also affects the rate of production of new shoots and above-ground material, because the below-ground structure must be in place before the plant can produce new above-ground material. The rate at which seagrass rhizomes branch also varies widely between species: *Heterozostera tasmanica* branches every four nodes whereas *Thalassia testudinum* has, on average, one branch every 1600 nodes, i.e. approximately every 20 m, (Hemminga and Duarte 2000). In general, smaller seagrasses tend to have higher branching rates and consequently are more able to rapidly colonize regions (Marbà and Duarte 1998 and Duarte 1991).

Given the slow rate of rhizome branching in *Thalassia testudinum*, the modeled approximation of a linear expansion of the below-ground tissue is probably reasonable. However, this representation does neglect the relationship between above- and below-ground structures, so the assumption of a constant rate of expansion may not be correct.

Vertical shoots producing leaves are only formed at discrete spatial intervals along the rhizome (the plastochrone interval) and this interval varies between species. Rhizomes grow faster when colonizing unvegetated areas than when growing within a seagrass bed. This is not taken into account in the model because explicit rhizome growth only occurs when cells are colonizing other cells and does not occur within the cell. Rhizome biomass does increase within the cell, but each plant is not explicitly represented and so lateral growth of an individual rhizome is not modeled.

The representation of rhizomes through biomass only could be a problem when trying to model the growth rates of patches. Seagrass patches are known to grow at an accelerating rate with the number of shoots in a patch increasing with the elapsed time (t) according to $t^{2.3}$ (Vidondo et al. 1997). However, the model presented here would predict a linear increase in rhizome coverage. To see this, consider a square patch of seagrass with sides of length L ($L \gg 1$) and the lateral increase in rhizome coverage of 1 unit per year (e.g., one cell per year). Then, after N years, the total coverage, C , would be

$$C = L^2 + 4 \sum_{n=1}^N (L + n)$$

For large patches (L much larger than the annual lateral increase) C increases approximately linearly with time (n). However, for small patches (L similar in size to the annual lateral increase), C is a non-linear function of time (n).

Alternatives to the cellular automata may provide more realistic propagation of rhizomes. Individual-based-models (Haefner 1996), which represent the growth of individual clones within the seagrass bed, could be parameterized using rhizome branching and variable rhizome propagation rates. Such a model could also make explicit connections between the above- and below-ground structures of the seagrass meadow.

Given the nature of this project, the cellular automata model is able to approximate spatial patterns of seagrass propagation. Propagation rates and biomass values determined from these case studies are within realistic magnitude both spatially and temporally. Additionally, it is useful for investigating areas where our knowledge needs to be improved.

Table 4.1: Simulation results for model runs examining the influence of the perimeter-to-area ratio on gap fill-in rates.

Number of Gaps	Gap Dimensions	Initial Total Gap Size (m ²)	Final Total Gap Size (m ²)	Change in Total Gap Size (m ²)	Perimeter (m)	P:A ratio (m ⁻¹)
1	40m x 40m	1600	1444	156	160	0.1
1	30m x 30m	900	784	116	120	0.133
2	45m x 10m	900	688	212	220	0.244
9	10m x 10m	900	576	324	360	0.4
22	10m x 4m	880	352	528	616	0.7

Table 4.2: Simulation results for model runs examining the effect of shape on the gap fill-in rate. All initial gaps are 100m^2 in area.

Model ID	Size/Shape	P:A ratio (m^{-1})	Final gap size (m^2)-Rhizome	Final gap size (m^2)-Leaf	Change in Gap (m^2)-Rhizome	Change in Gap (m^2)-Leaf
A	Square (10m x 10m)	0.4	64	100	36	0
B	Rectangle(25m x 4m)	0.58	46	100	54	0
C	20-sided polygon	0.58	46	80	54	20
D	12-sided polygon	0.6	54	88	46	12

Table 4.3 Simulation results for model runs examining the spread of rhizome and leaf biomass radiating from a central square patch of seagrass in the center of the grid. Initial and final areas are given as the areas that contain no biomass (hence B=0).

Patch Size	Patch Area (m ²)	P:A ratio (m ⁻¹)	Initial (m ²) B=0	Final Rhizome (m ²) B=0	Final Leaf (m ²) B=0	Change Rhizome (m ²)	Change Leaf (m ²)
30m x 30m	900	0.133	9100	8976	9088	124	12
9(10m x 10m)	900	0.4	9100	8704	8992	396	108
22(10m x 4m)	880	0.7	9120	8416	8856	704	264

Table 4.4 Simulation results for model runs examining the spread of rhizome and leaf biomass radiating from various shapes of seagrass placed at the center of the grid. All initial patches are 100m²; initial area with zero biomass is 9900 m².

Size/Shape	P:A ratio (m ⁻¹)	Final Rhizome (m ²) B=0	Final Leaf (m ²) B=0	Change in Gap (m ²) Rhizome	Change in Gap (m ²) Leaf
Square (10m x 10m)	0.4	9856	9888	44	12
Rectangle (25m x 4m)	0.58	9838	9888	62	12
20-sided polygon	0.58	9838	9864	62	36
12-sided polygon	0.6	9846	9876	54	24

Table 4.5: Simulation results from model runs examining the effect of varying phosphorus concentrations (μM) on the recovery of *Thalassia* into a large-scale boat propeller blowout.

Model ID	Initial gap size (m^2)	Final rhizome gap (m^2)	Final leaf gap (m^2)	Change in rhizome gap area (%)	Change in leaf gap area (%)	P concentration (μM)
A	7279	5834	5850	19.9	19.6	0.35 ± 0.1
B	7279	7279	16384	0	-125	0.35
C	7279	6807	7255	6.5	0.3	0.375
D	7279	6750	13129	7.3	-80.4	0.25 ± 0.1
E	7279	6491	7690	10.8	-5.6	0.3 ± 0.1
F	7279	6331	6446	13.0	11.4	0.325 ± 0.1
G	7279	6352	6807	12.7	6.5	0.3125 ± 0.1

Table 4.6: Simulation results for model runs examining the effect of varying phosphorus concentrations (μM) and sediment sulfide concentrations (μM) on the recovery into a gap in a seagrass bed.

Model Run ID	Change in leaf area (m^2)	Change in rhizome area (m^2)	Sulfide Concentration (μM)	P concentration (μM)
A	0(gap remained)	20	0	0.375
B	20	20	0	0.375 ± 0.1
C	20	20	0	0.3125 ± 0.1
D	20	20	0	0.4
E	20	20	1000	0.4
F	20	20	2000	0.4
G	20*	20*	4000	0.4
H	20*	20*	6000	0.4

*Filled in the entire gap, but does not reach the same density as surrounding area

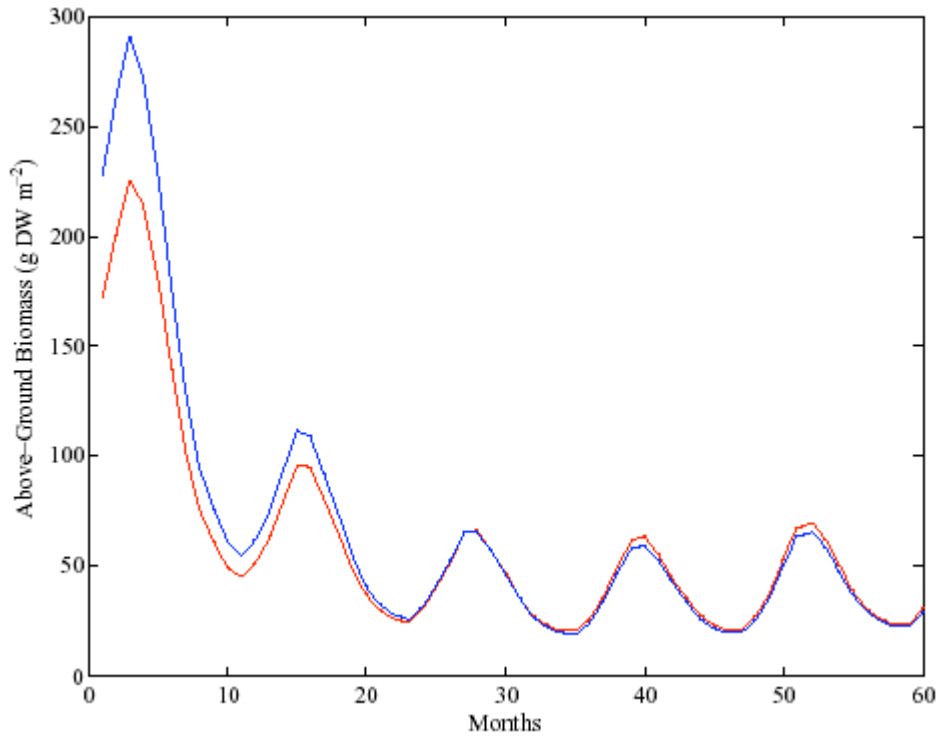


Figure 4.1: Model results of above-ground biomass over a five year period using two different initial conditions: 150 ± 30 g DW m⁻² (red curve) and 200 ± 40 g DW m⁻² (blue curve). The modeled biomass reaches a quasi steady state in the third year of the simulation.

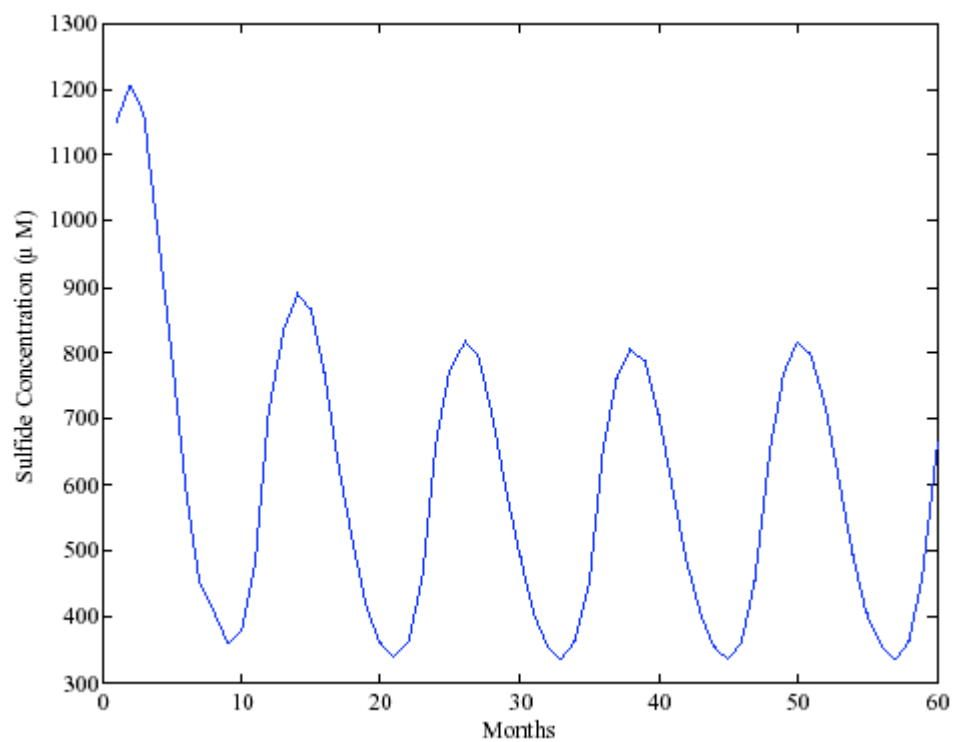


Figure 4.2: Graph showing the median sediment sulfide concentration (μM) reaching steady state after 3 years.

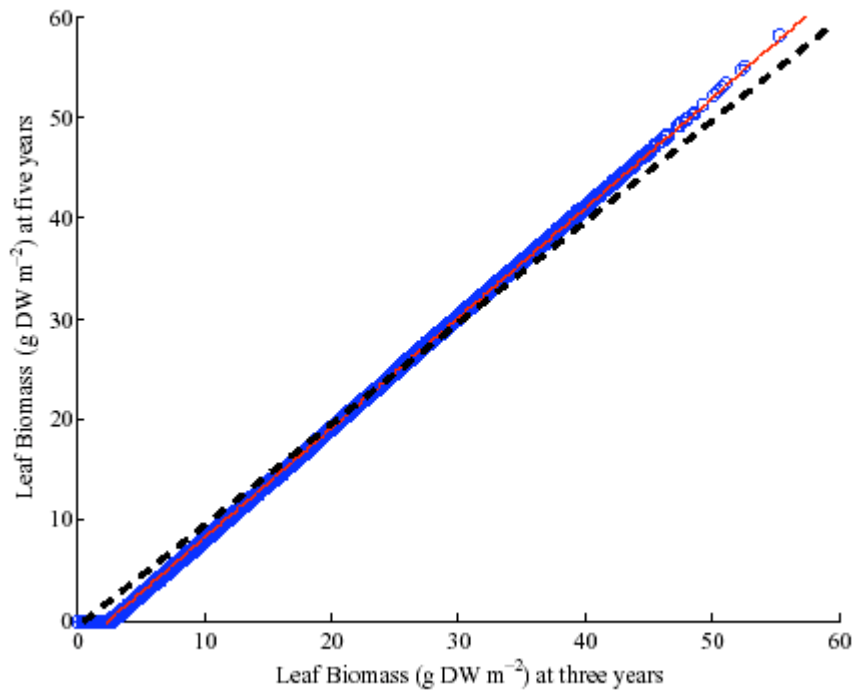


Figure 4.3: The relationship between the leaf biomass at the end of three years and at the end of five years (blue dots). The red line represents a least squares fit to the data (including zero data points) and the black dashed line is the one-to-one line.

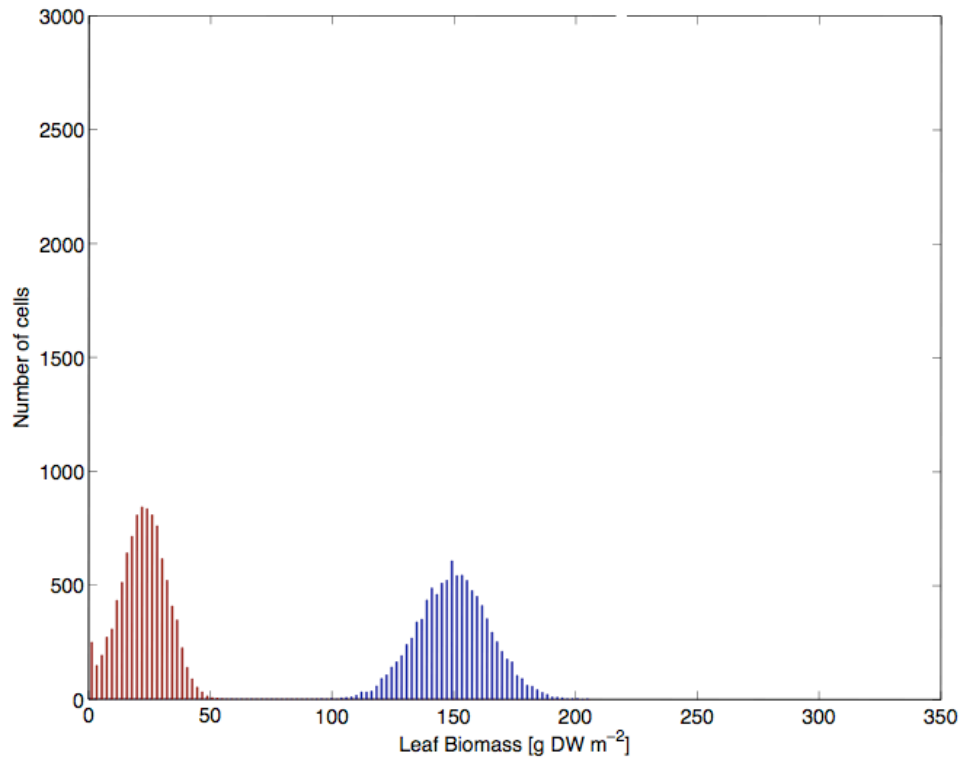


Figure 4.4: Frequency distribution of leaf biomass in each cell within the grid. The initial distribution (blues bars) was imposed and was a normal distribution with biomass of 150 ± 15 g DW m⁻². The final distribution (red bars) is the one obtained after the model was run for 5 years. The final distribution for leaf biomass greater than 0 can be fit to a normal distribution with a mean of 22.5 (22.3, 22.7) g DW m⁻² and standard deviation of 9.3 (9.2, 9.4) g DW m⁻² (numbers in parentheses represent the 95% confidence interval).

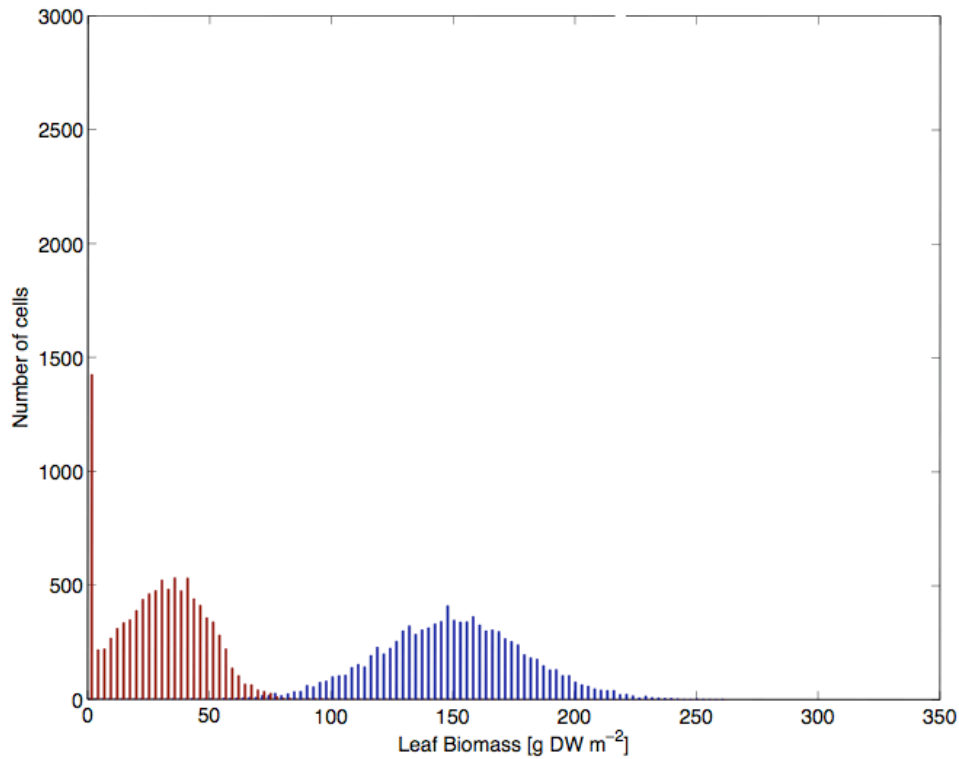


Figure 4.5: Frequency distribution of leaf biomass in each cell within the grid. The initial distribution (blues bars) was imposed and was a normal distribution with biomass of 150 ± 30 g DW m⁻². The final distribution (red bars) is the one obtained after the model was run for 5 years. The final distribution for leaf biomass greater than 0 can be fit to a normal distribution with a mean of 32.5 (32.3, 32.8) g DW m⁻² and standard deviation of 16.4 (16.1, 16.6) g DW m⁻² (numbers in parentheses represent the 95% confidence interval).

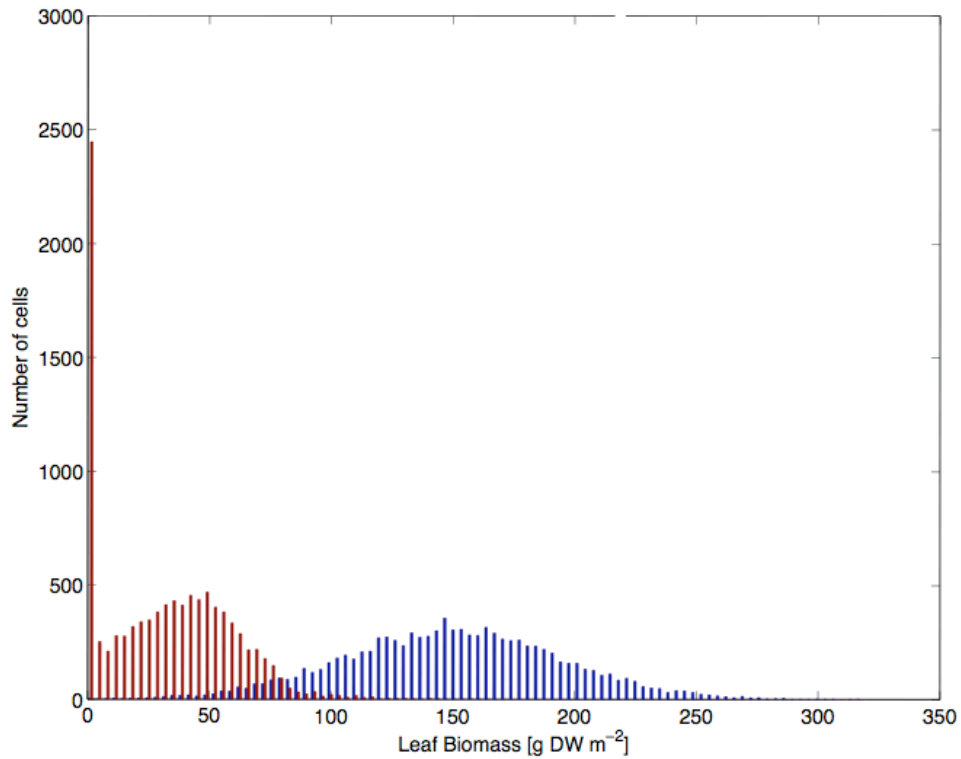


Figure 4.6: Frequency distribution of leaf biomass in each cell within the grid. The initial distribution (blues bars) was imposed and was a normal distribution with biomass of 150 ± 45 g DW m⁻². The final distribution (red bars) is the one obtained after the model was run for 5 years. The final distribution for leaf biomass greater than 0 can be fit to a normal distribution with a mean of 38.5 (38.0, 39.0) g DW m⁻² and standard deviation of 23.5 (23.1, 23.8) g DW m⁻² (numbers in parentheses represent the 95% confidence interval).

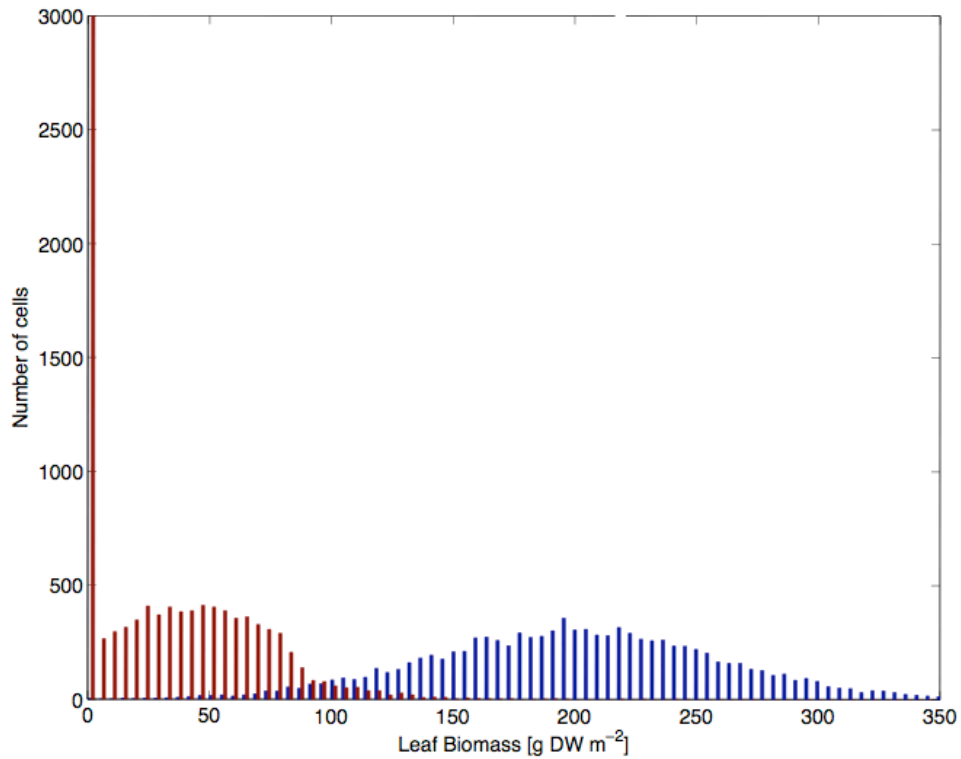


Figure 4.7: Frequency distribution of leaf biomass in each cell within the grid. The initial distribution (blues bars) was imposed and was a normal distribution with biomass of 200 ± 40 g DW m^{-2} . The final distribution (red bars) is the one obtained after the model was run for 5 years. The final distribution for leaf biomass greater than 0 can be fit to a normal distribution with a mean of 41.4 (40.7, 42.1) g DW m^{-2} and standard deviation of 32.3 (31.8, 32.7) g DW m^{-2} (numbers in parentheses represent the 95% confidence interval).

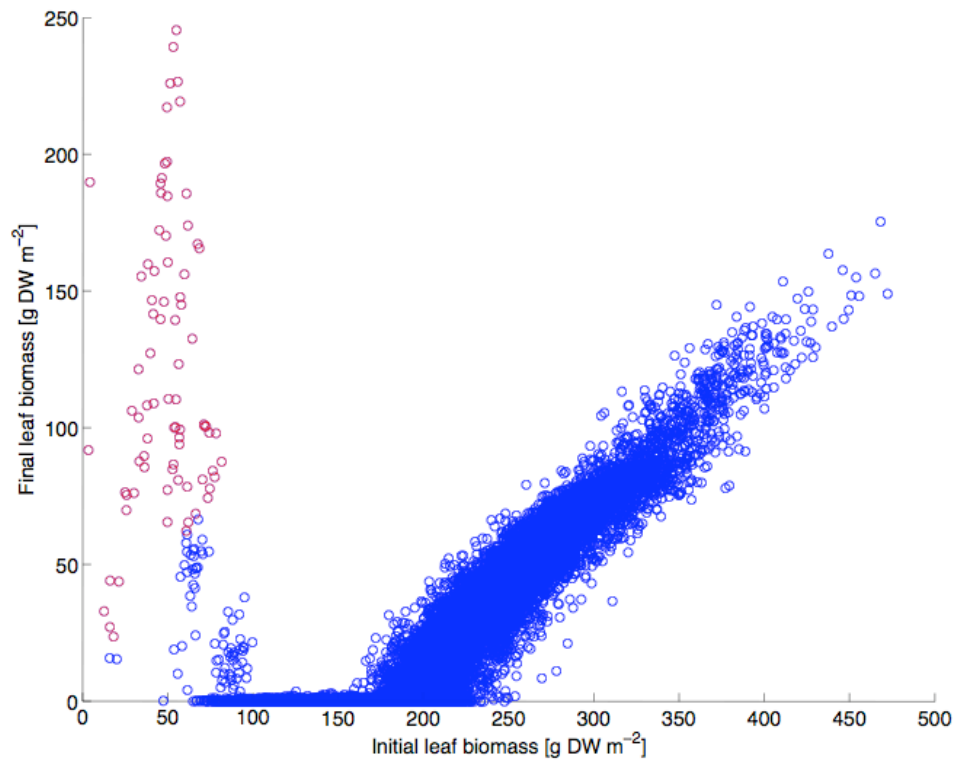


Figure 4.8: The relationship between initial and final leaf biomass and after a five year simulation with an initial above-ground biomass of 200 ± 40 g DW m⁻². Each circle represents the leaf biomass contained within a single cell of the model grid. Red circles show those cells for which the final biomass is greater than the initial biomass, and blue circles depict cells for which the final biomass is lower than the initial biomass.

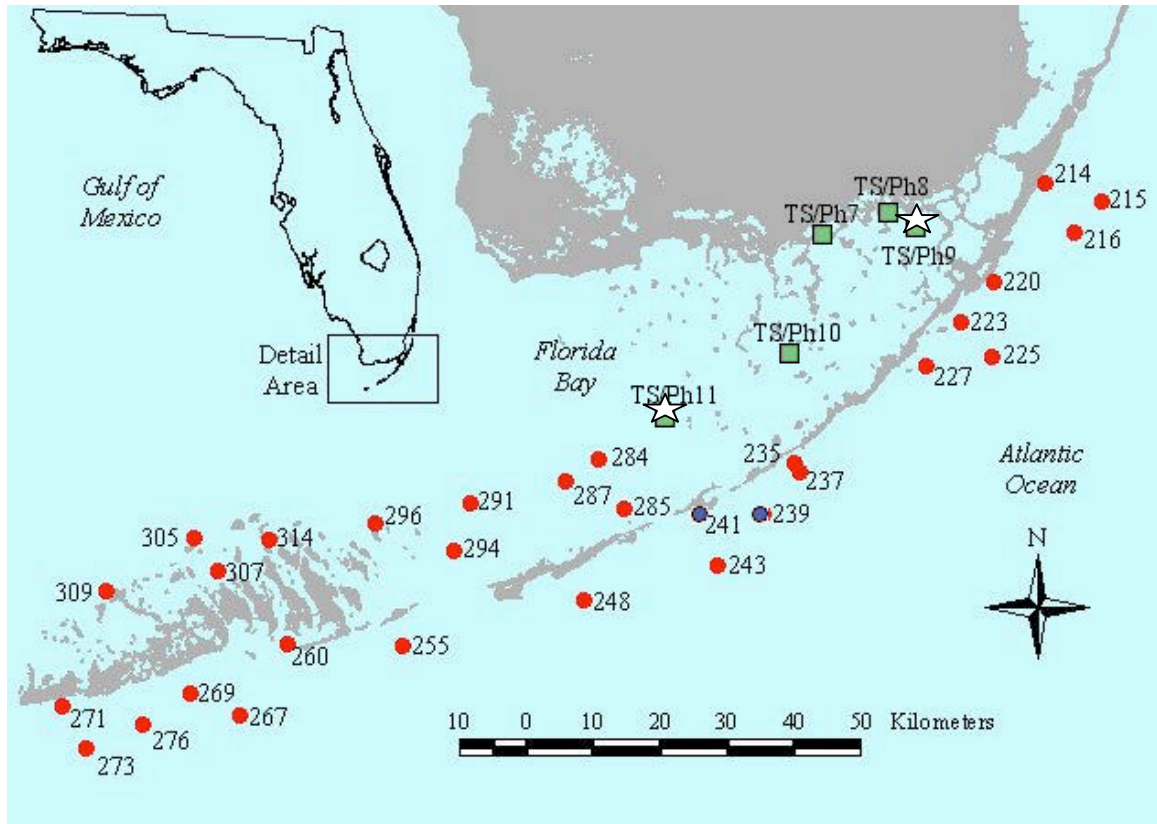


Figure 4.9 The two sites that were selected for model comparison [TS/Ph 9-Duck Key- and TS/Ph 11-Sprigger Bank] located within Florida Bay (<http://serc.fiu.edu/seagrass/!CDreport/DataHome.htm>)

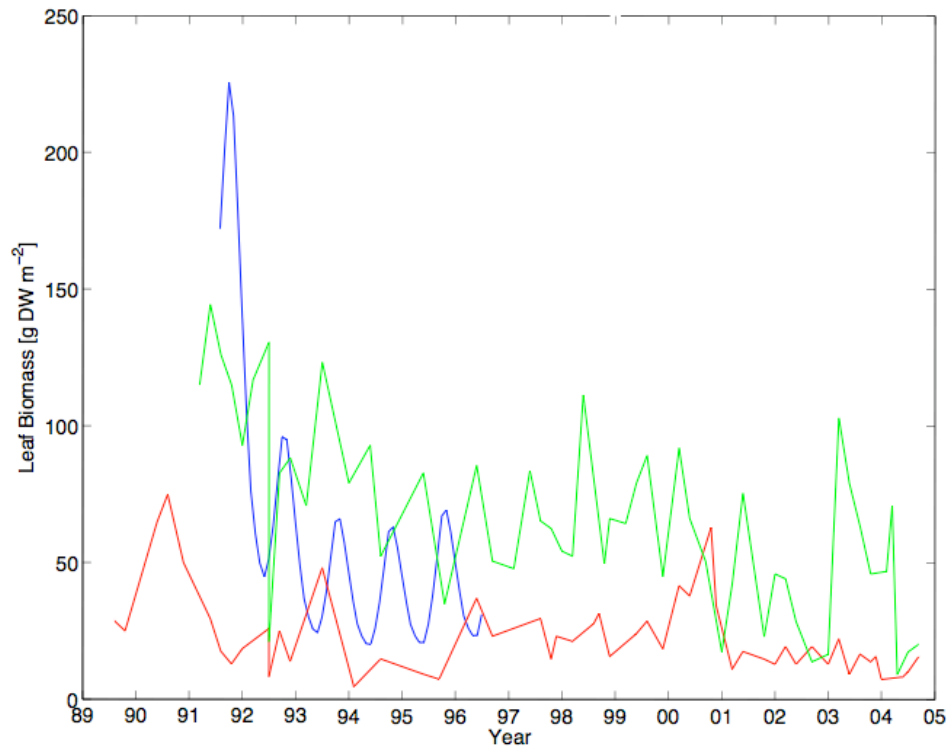


Figure 4.10: Comparison of the model leaf biomass (blue) with field measurements from Sprigger Bank (green) and Duck Key (red).

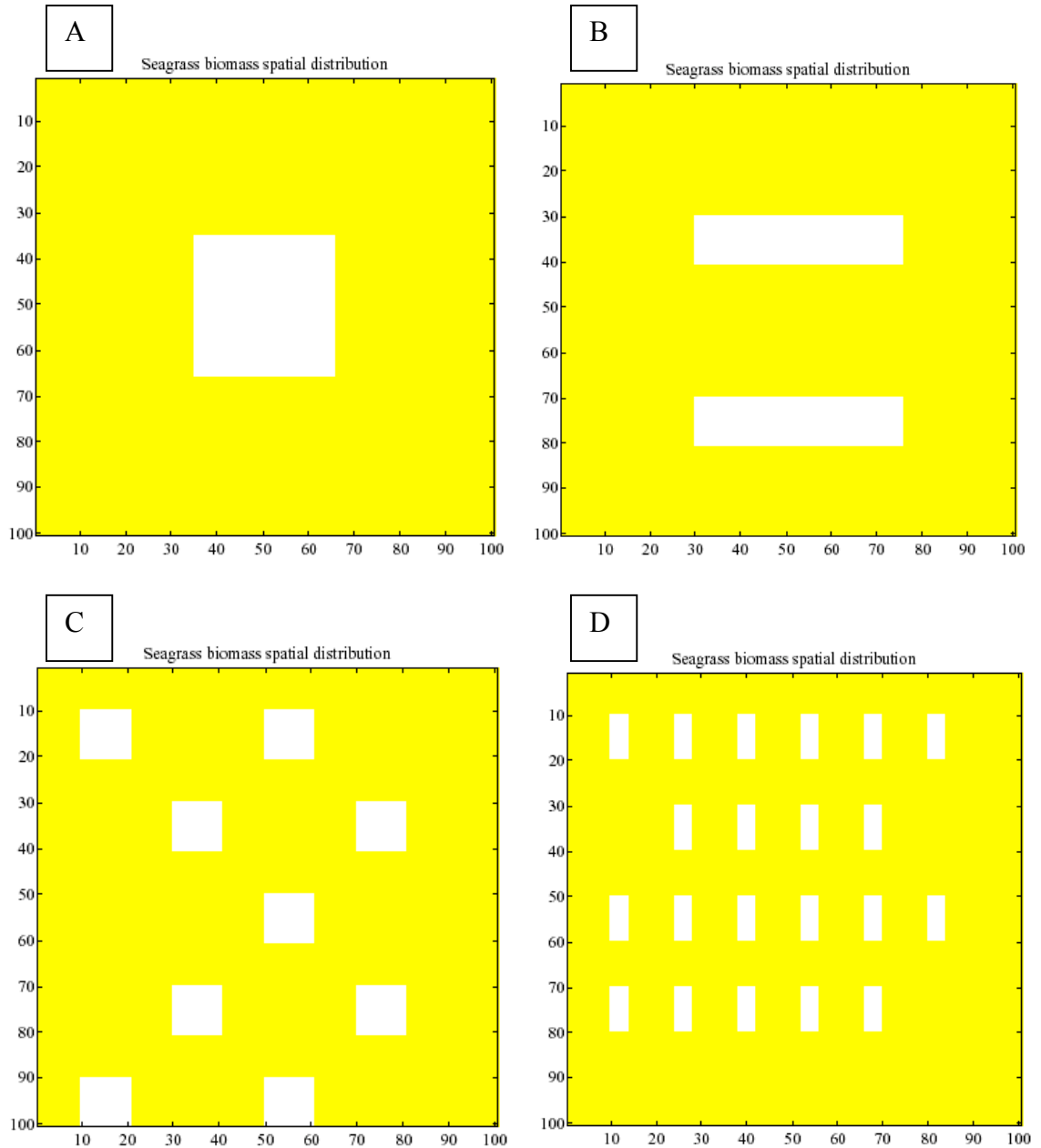


Figure 4.11 Initial Spatial Distribution of seagrass biomass within the model domain.

White areas represent Biomass = 0.

A.) 30 m by 30 m square gap (900 m^2). Perimeter to Area ratio of 0.133.

B.) 2- 15 m by 10 m rectangular gaps (900 m^2). Perimeter to Area ratio of 0.244.

C.) 9- 10 m by 10 m square gaps (900 m^2). Perimeter to Area ratio of 0.400.

D.) 22- 10 m by 4 m square gaps (880 m^2). Perimeter to Area ratio of 0.700.

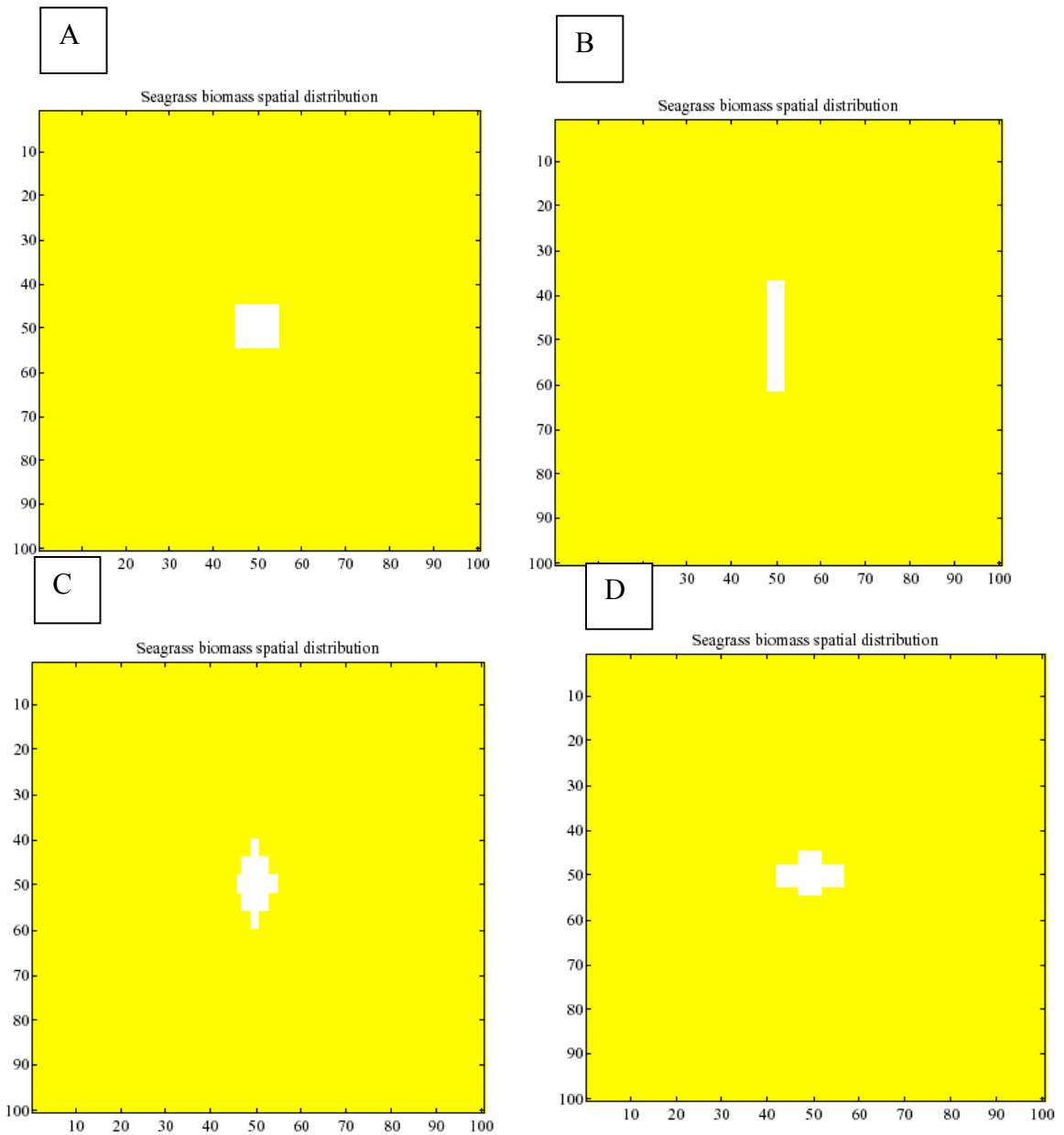


Figure 4.12 Initial Spatial Distribution of seagrass biomass within the model domain

(refer to Table 4.2). White areas represent Biomass = 0.

- A.) 10m x 10m with a Perimeter to Area ratio of 0.40.
- B.) 25m x 4m with a Perimeter to Area ratio of 0.58.
- C.) 20-sided polygon with a Perimeter to Area ratio of 0.58.
- D.) 12-sided polygon with a Perimeter to Area ratio of 0.60.

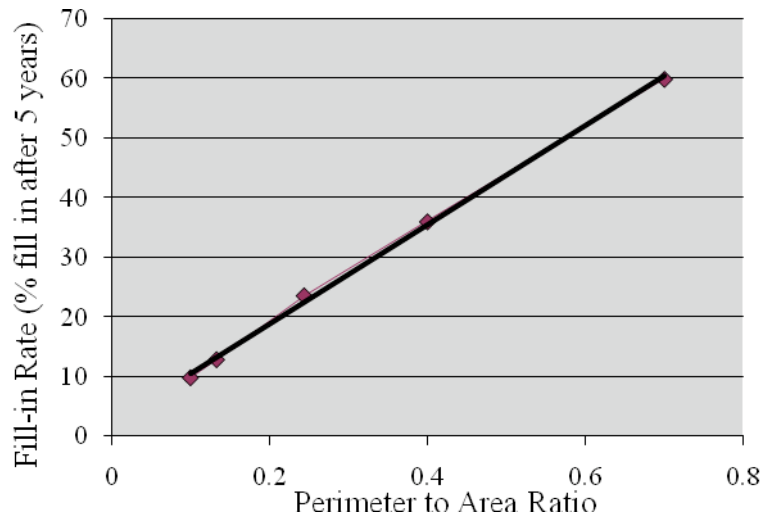


Figure 4.13 The effect of the perimeter to area ratio of the seagrass gap to the rate of fill into the gap after five years. ($y = 83.411x + 2.1121$ $R^2 = 0.9986$)

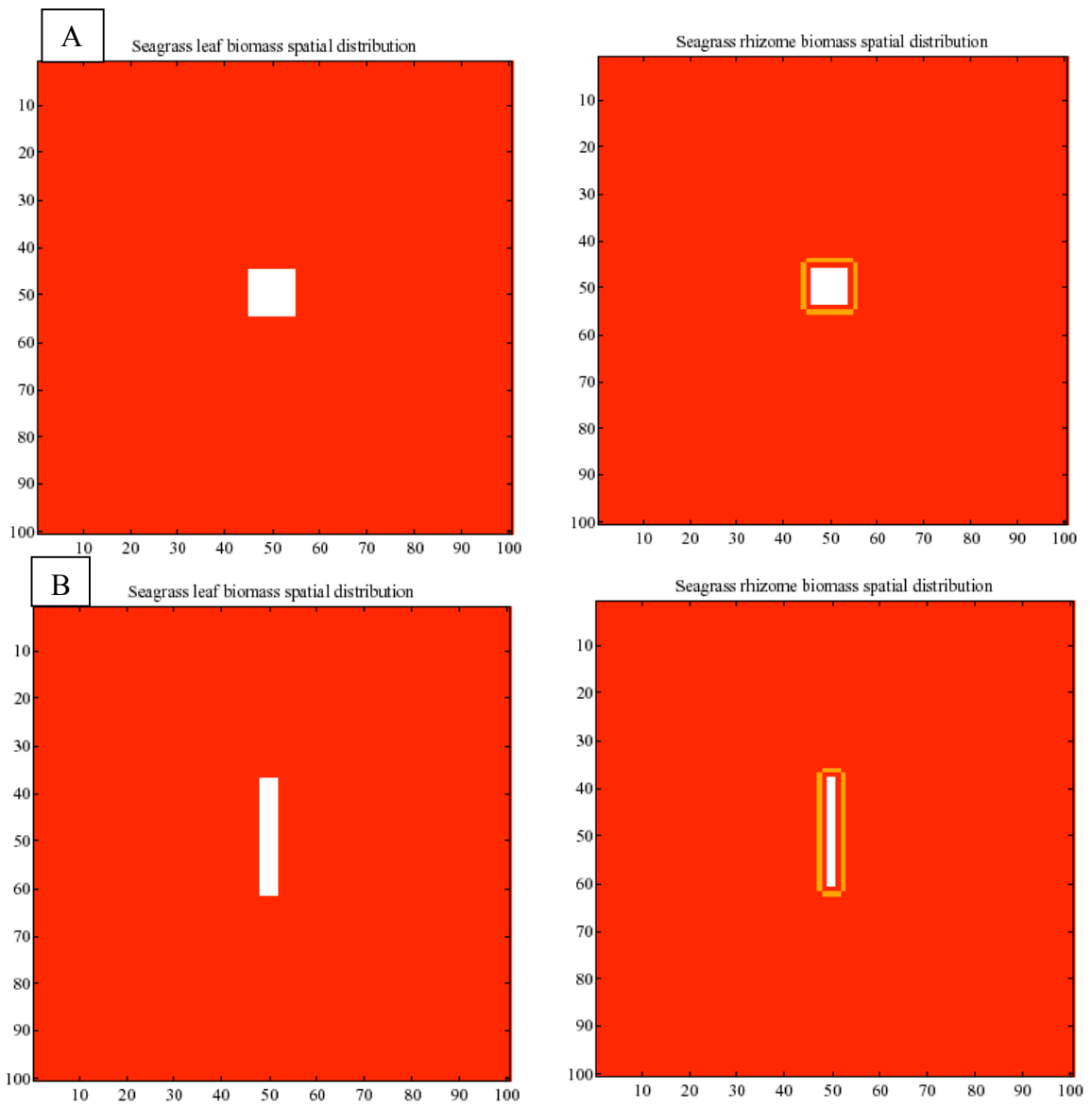


Figure 4.14: Final spatial distribution of seagrass biomass, leaf (left hand frames) and rhizomes (right hand frame) after 5 years for initial conditions A (top row) and B (bottom row) from Table 4.2. The red cells represent areas with biomass from 1 to 50 g DW m^{-2} , the orange cell represent areas with biomass from 50-100 g DW m^{-2} .

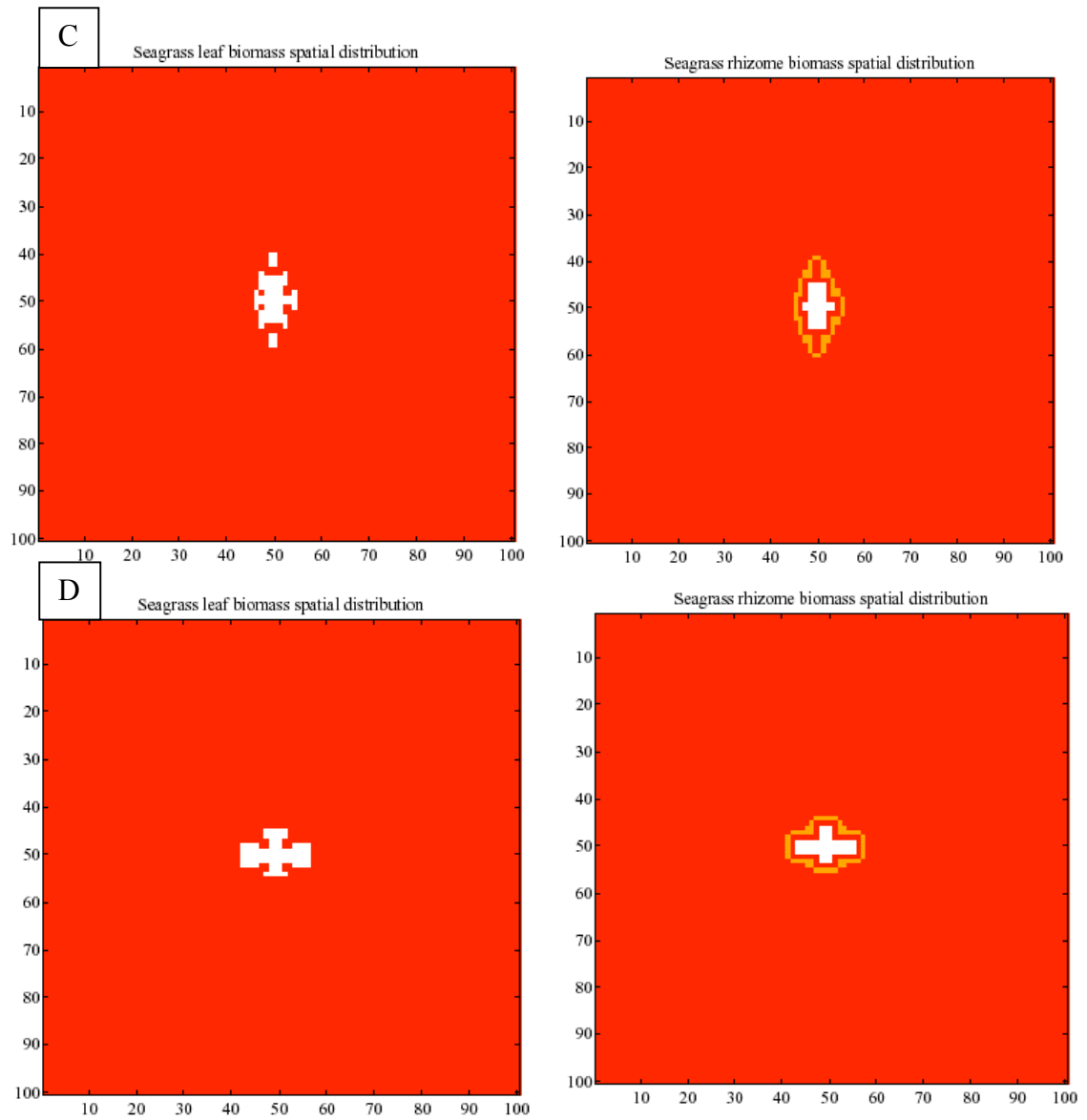


Figure 4.15: Final spatial distribution of seagrass leaf (left hand frames) and rhizome (right hand frames) biomass after 5 years for initial conditions C (top row) and D (bottom row) from Table 4.2. The red cells represent areas with biomass from 1 to 50 g DW m^{-2} , the orange cell represent areas with biomass from 50-100 g DW m^{-2} .

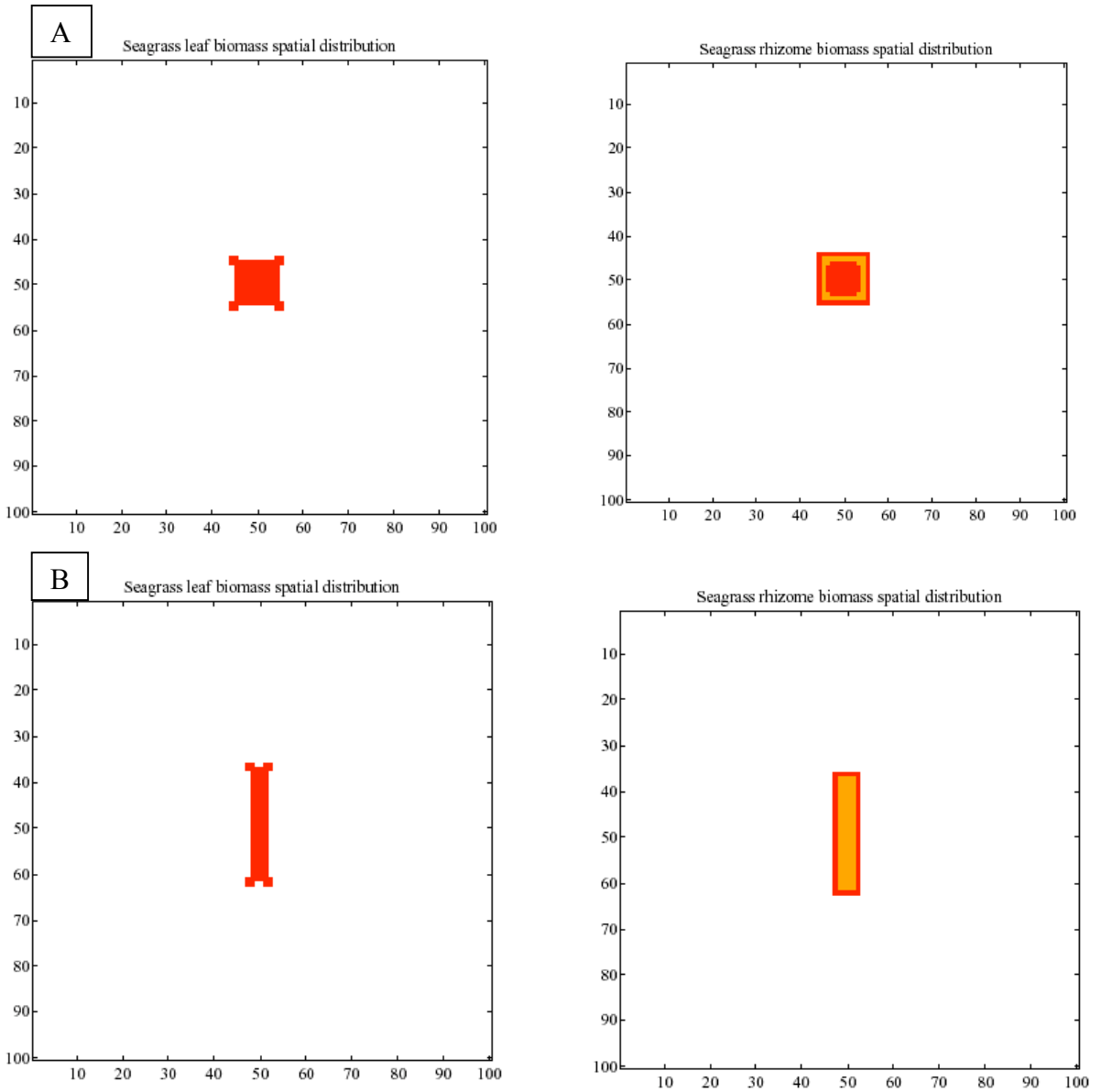


Figure 4.16: Final spatial distribution of seagrass leaf (left hand panels) and rhizome (right hand panels) biomass after 5 years of simulation for patch evolution cases A and B (Table 4.4). The red cells represent areas with biomass from 1 to 50 g DW m⁻², the orange cell represent areas with biomass from 50-100 g DW m⁻².

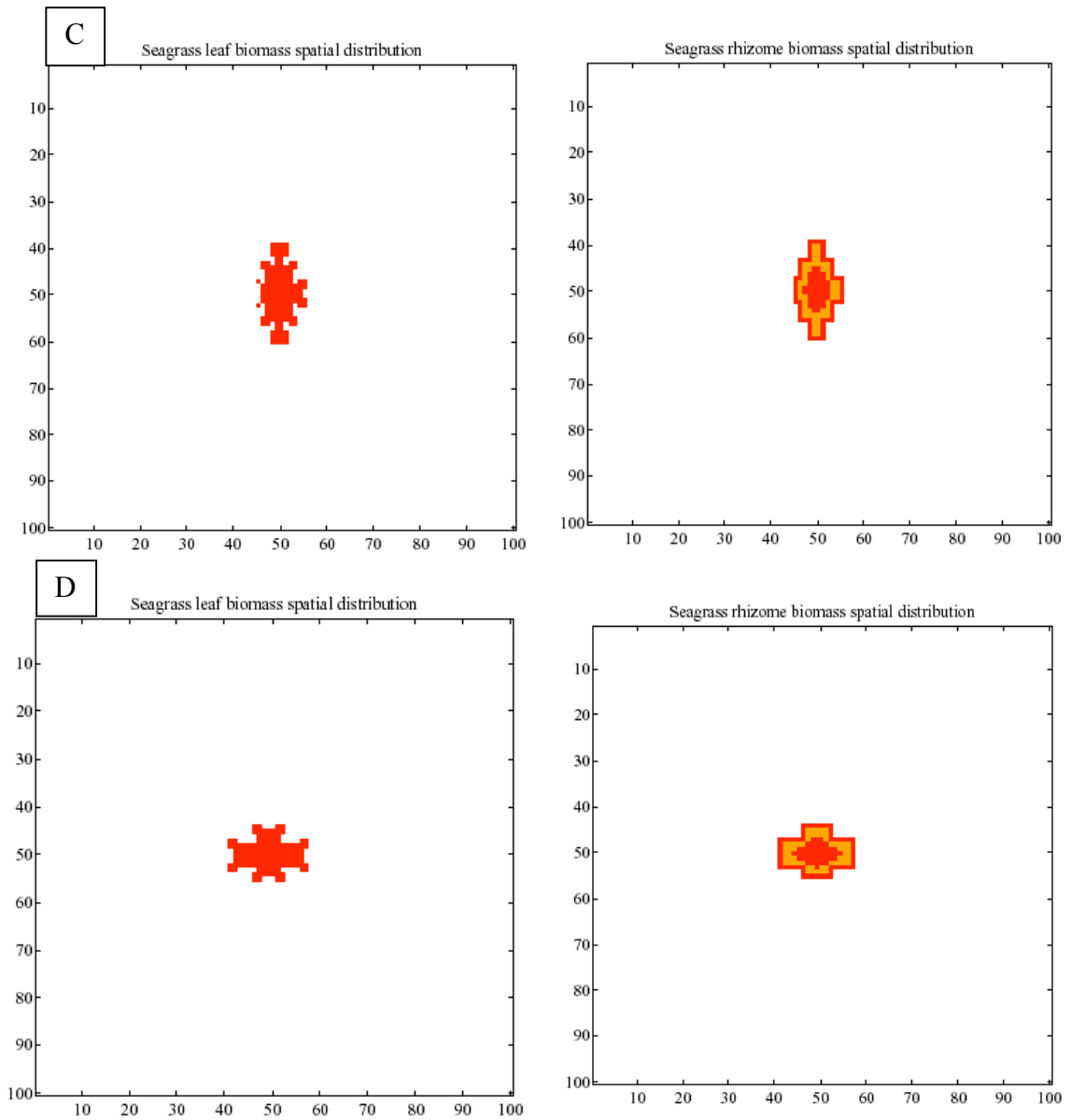


Figure 4.17: Final spatial distribution of seagrass leaf (left hand panels) and rhizome (right hand panels) biomass after 5 years of simulation for patch evolution cases C and D (Table 4.4). The red cells represent areas with biomass from 1 to 50 g DW m⁻², the orange cell represent areas with biomass from 50-100 g DW m⁻².

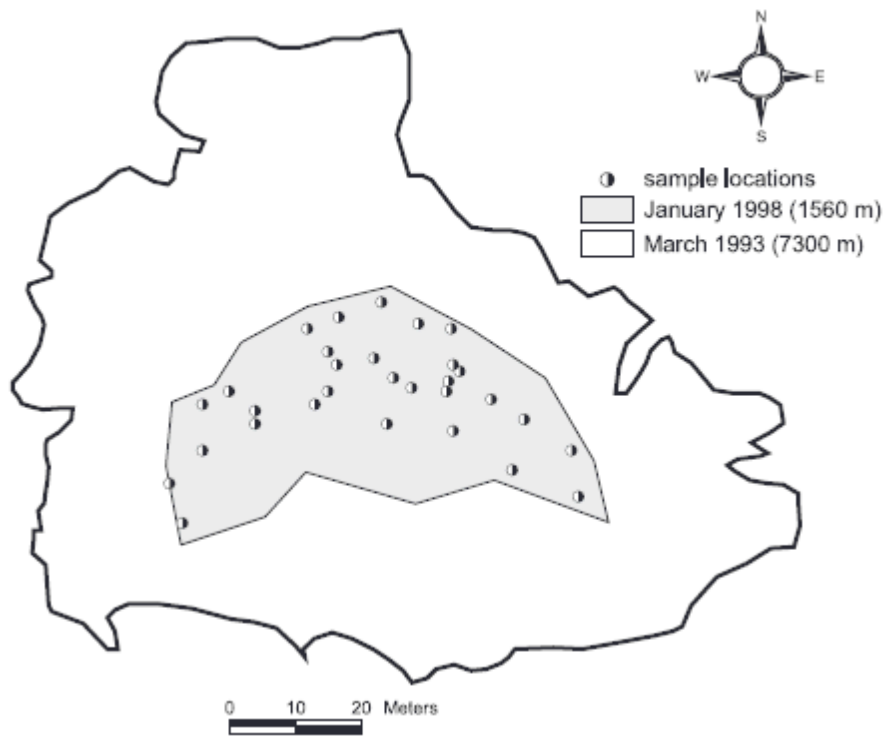


Figure 4.18 Two perimeters mapped from the large-scale study shortly after the boat grounding occurred in May 1993 (area $\sim 7300 \text{ m}^2$) and 4.8 yr later, when the site was sampled for presence of *Thalassia testudinum* seedlings in January 1998 (area $\sim 1560 \text{ m}^2$). White area indicates recovery by *Syringodium filiforme* and gray area represents the remaining unrecovered area. Sample locations are indicated inside the January 1998 Perimeter. (From Whitfield et al. 1994)

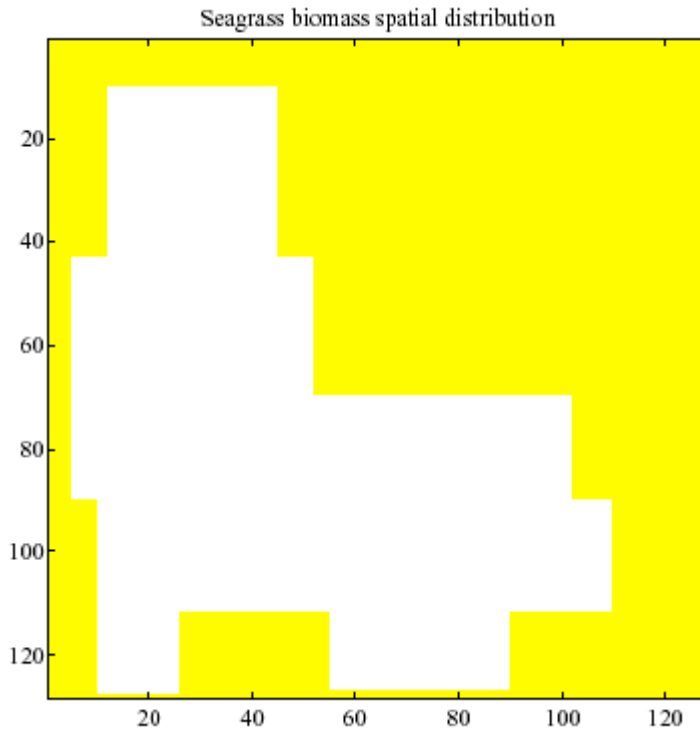


Figure 4.19: Initial spatial distribution of seagrass biomass showing the gap created by the boat grounding documented in Whitfield et al. (2004). An attempt was made to capture the geometry as best possible when converting from real-world to the square grid model domain. The white region represents zero biomass above- and below-ground; the yellow region represents biomass of 150 g DW m⁻².

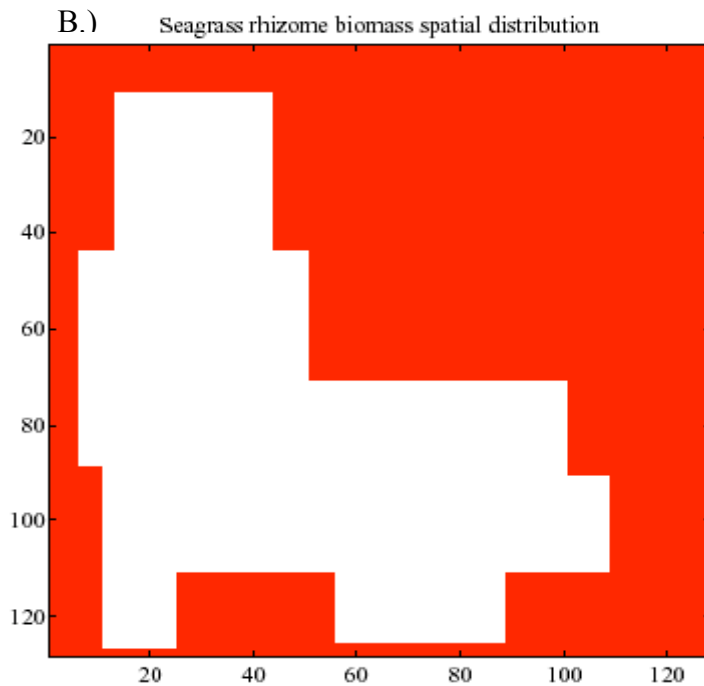
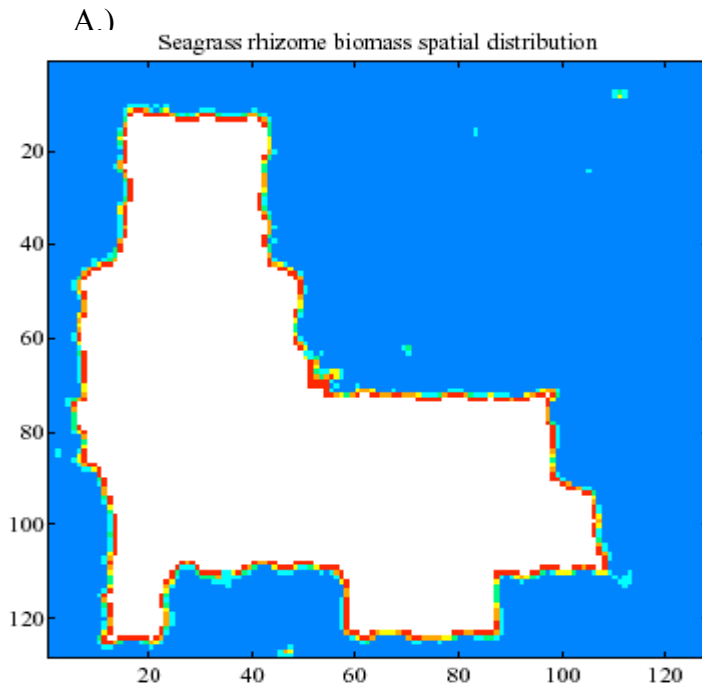


Figure 4.20: Final biomass distribution of rhizome after various simulations. (See Table 4.5 for details of conditions (A and B)) The colors represent different biomass categories: White = 0 g DW m⁻², Red = 1-50 g DW m⁻², Orange = 50-100 g DW m⁻², Yellow = 100-150 g DW m⁻², Green 150-200 g DW m⁻², Turquoise 200-250 g DW m⁻², Blue 250-300 g DW m⁻².

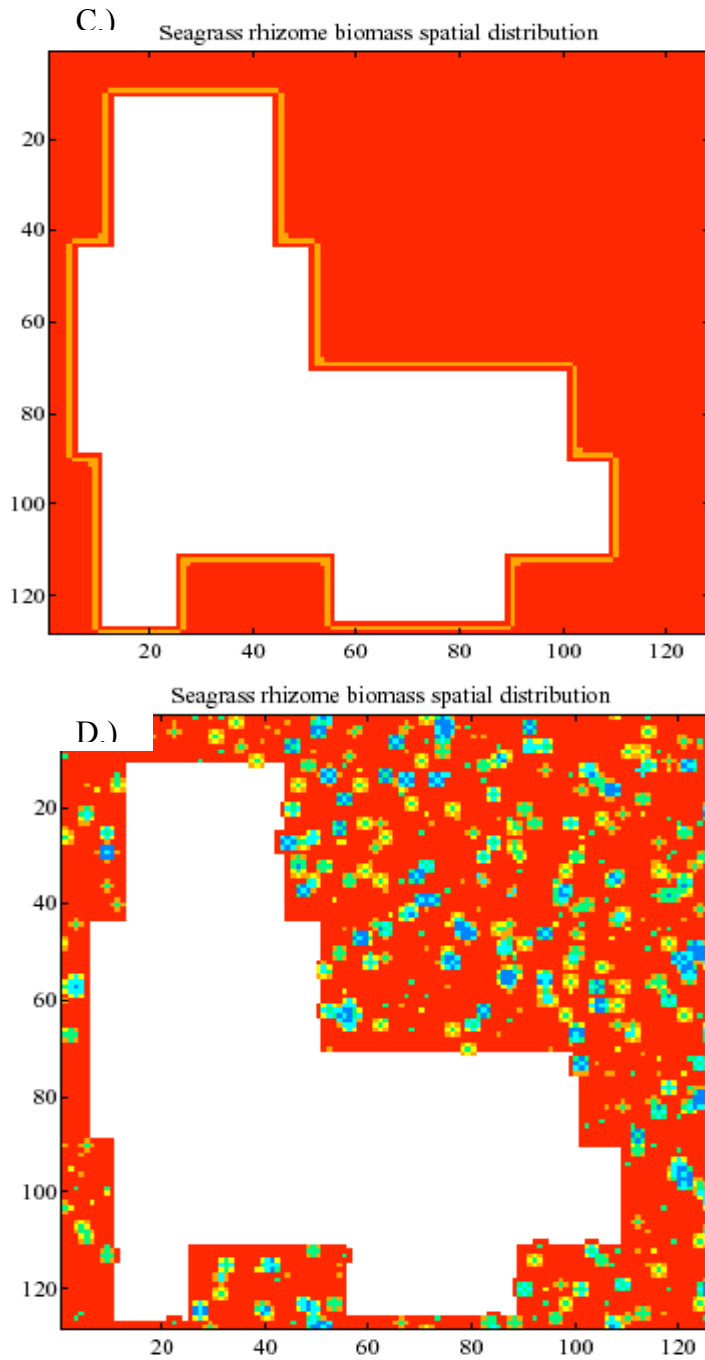


Figure 4.20 (cont'd) Final biomass distribution of rhizome after various simulations. (See Table 4. 5 for details of conditions (C and D)) The colors represent different biomass categories: White = 0 g DW m⁻², Red = 1-50 g DW m⁻², Orange = 50-100 g DW m⁻², Yellow = 100-150 g DW m⁻², Green 150-200 g DW m⁻², Turquoise 200-250 g DW m⁻², Blue 250-300 g DW m⁻².

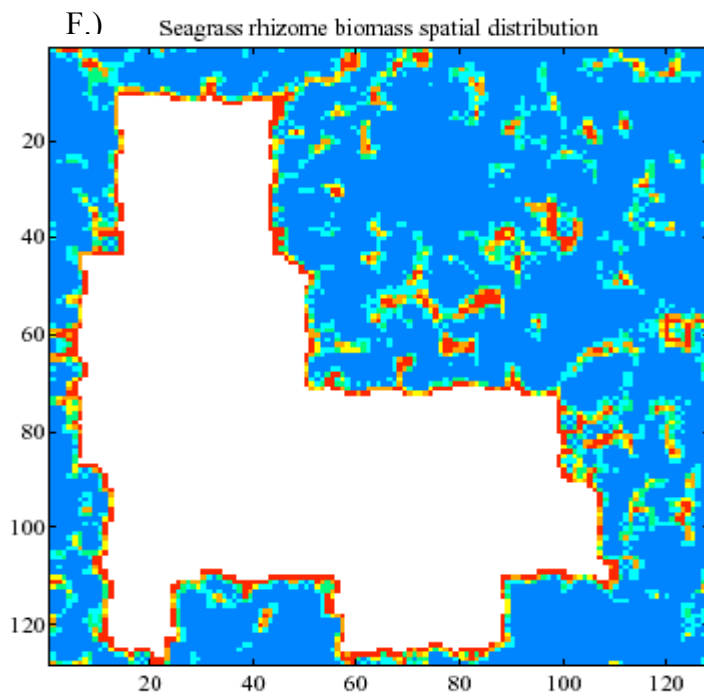
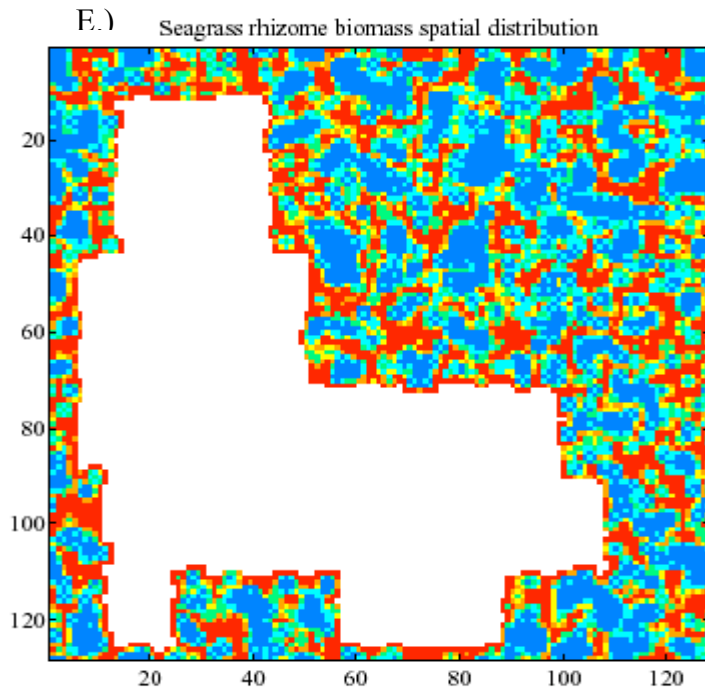


Figure 4.20 (cont'd) Final biomass distribution of rhizome after various simulations.

(See Table 4. 5 for details of conditions (E and F)) The colors represent different biomass categories: White = 0 g DW m⁻², Red = 1-50 g DW m⁻², Orange = 50-100 g DW m⁻², Yellow = 100-150 g DW m⁻², Green 150-200 g DW m⁻², Turquoise 200-250 g DW m⁻², Blue 250-300 g DW m⁻².

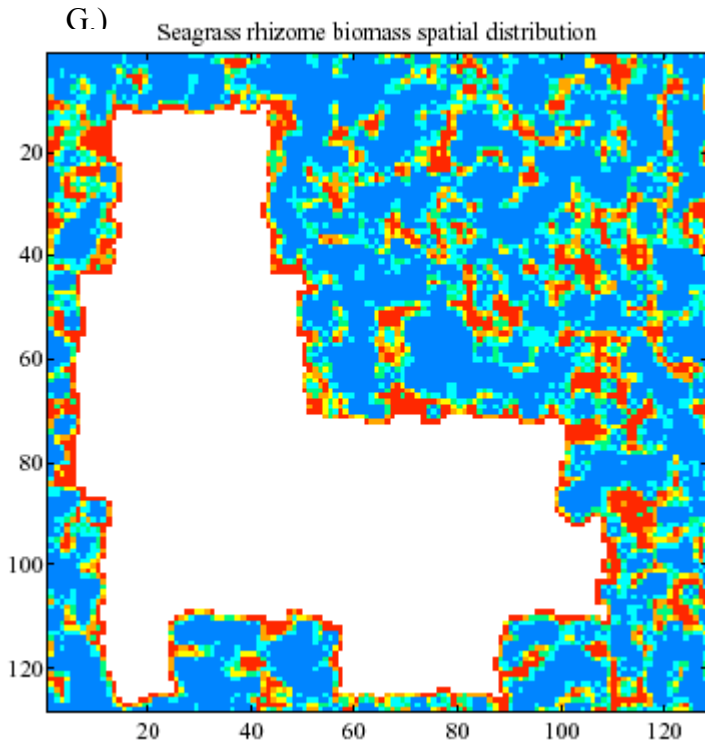


Figure 4.20 (cont'd) Final biomass distribution of rhizome after various simulations.

(See Table 4. 5 for details of conditions (G)) The colors represent different biomass categories: White = 0 g DW m⁻², Red = 1-50 g DW m⁻², Orange = 50-100 g DW m⁻², Yellow = 100-150 g DW m⁻², Green 150-200 g DW m⁻², Turquoise 200-250 g DW m⁻², Blue 250-300 g DW m⁻².

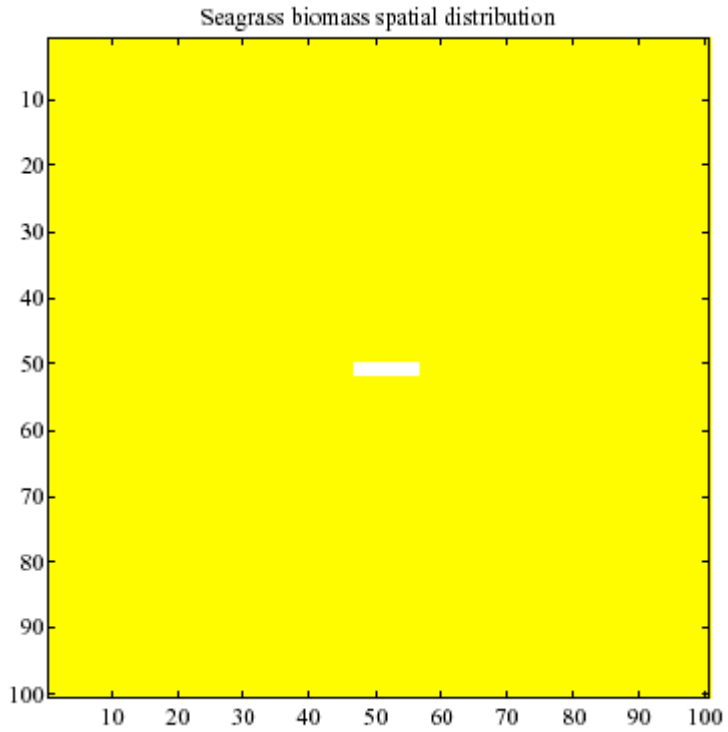


Figure 4.21 Initial spatial distribution of seagrass biomass in the model grid showing a simulated prop scar (10m x 4m). The white region represents zero biomass above- and below-ground; the yellow region represents biomass of 150 g DW m⁻².

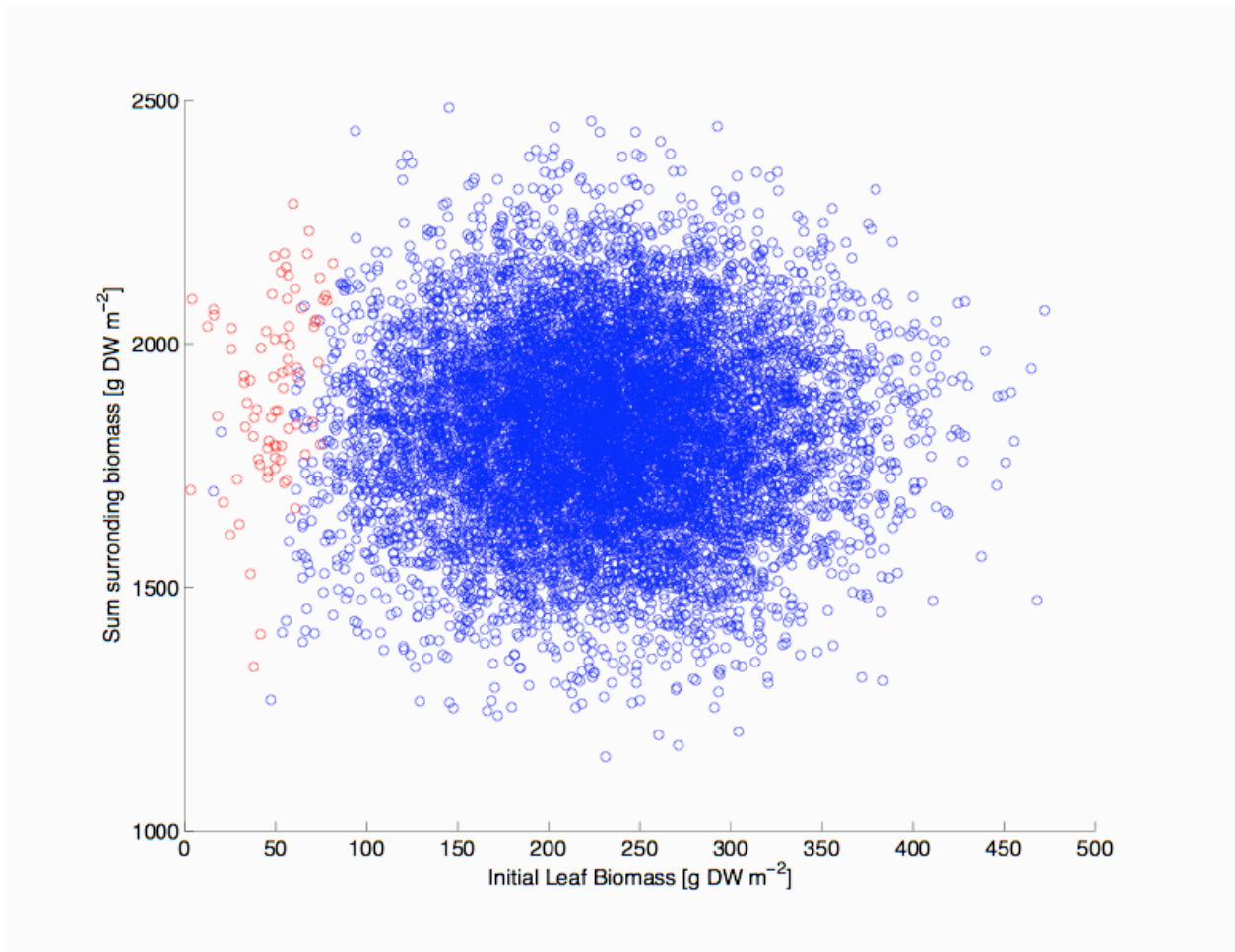


Figure 4.22: Scatter plot of initial leaf biomass of an individual cell against total leaf biomass in surrounding cells for the simulation with initializing biomass 200 ± 40 g DW m^{-2} . The red circles represent those values for which, after a 5 year model run, the final biomass is greater than the initial biomass.

CHAPTER 5

DISCUSSION

Summary

Seagrasses are important in coastal ecosystems (Zieman and Wetzel 1980). Through their complex root systems, they stabilize sediments (Fonseca and Fisher 1986), while their above-ground components provide food and shelter for a wide range of organisms (Larkum et al. 1989 and Phillips and McRoy 1980). They also play an important role as nurseries for juveniles of species from surrounding habitats (Heck et al. 2003).

Declines in seagrass populations globally have caused concern among managers of coastal marine systems (Short and Wyllie-Echeverria 1996). They have also highlighted the need for good management tools, among which will be models. For example, Bortone (2000) noted that there is a need for a connection between monitoring programs, current research and modeling efforts.

Florida Bay is a prime target for research as it hosts a variety of important marine habitats: coral reefs, mangrove islands, and most importantly, seagrass beds. The dominant species of seagrass throughout Florida Bay is *Thalassia testudinum*, also known as turtle grass, with *Halodule wrightii*, *Syringodium filiforme* and *Ruppia maritima* also present in many locations. The environmental monitoring of seagrass sites within Florida Bay makes it an ideal location for model development. The natural beauty of Florida Bay makes it a recreational boating destination, which also increases the vulnerability of seagrass beds to significant losses resulting from motor boat damage. Other, large-scale losses of seagrasses experienced in the

Bay have been connected to a variety of stressors, both natural and anthropogenic (Robblee et al 1991).

Most models of seagrass production focus on primary production. A few have included nutrient uptake (Zimmerman et al 1987) and some later models include simplified descriptions of resource allocation and below-ground production (e.g., Burd and Dunton, 2001). However, these models do not explicitly incorporate spatial dynamics and propagation of plants, and are usually constrained by the lack of information on resource allocation.

Seagrass propagation occurs mainly through vegetative propagation of the below-ground tissue. This means that resource allocation within the plant is important, because production of new below-ground biomass must come from primary production. The complex interplay between above and below-ground biomass, production and resource allocation has been demonstrated in observations of *Halodule wrightii* during prolonged stress resulting from light limitation (Burd and Dunton, 2001). However, few measurements have been made of either below-ground production or resource allocation in other species, particularly *Thalassia testudinum*.

Cellular Automata are rule-based models that do not use differential equations to describe the spatial dynamics of the system. They have been successfully used in models of forests, erosion, and population dynamics (Schlicht and Iwasa 2006, Rammig et al. 2006 and D'Ambrosio et al. 2001). Without a firm knowledge of the mechanisms involved in resource allocation and spatial propagation of seagrasses, a rule-based description is potentially a good approach. Similar approaches have been used in studies of terrestrial plant distributions (Silvertown et al. 1992, Schwinning and Parsons 1996) and more recently introduced in the field of seagrass propagation (Giusti and Marsili-Libelli 2005). This project was developed as a

proof-of-concept to show that we can devise reasonable rule-based descriptions of spatial propagation in seagrasses.

An important use of models is to identify areas where our knowledge does not allow for accurate predictions to be made. In this case, through our sensitivity analysis we have identified two such areas: phosphorus uptake kinetics and plant resource allocation. Through our implementation of the Monod kinetics, we were able to determine that our model is particularly sensitive to the experimentally derived K_m values. Other more simplified approaches to nutrient modeling exist, such as the approach used by Fong and Harwell (1994), in which the model was parameterized with optimum growth occurring under specified nutrient regimes and reduced growth at any sub-optimal levels. However, the use of Monod kinetics is able to capture more dynamics within the system, which is a main objective of this model and the reason for the continued use of the Monod method. Additional field studies of nutrient uptake kinetics at nutrient concentrations experienced in-situ may lead to more certainty in the selection of the method for modeling nutrient limitation in addition to the values chosen for the half-saturation constant for phosphorus uptake. Furthermore, more investigations on the specific mechanisms of plant uptake of phosphorus would lend itself to better implementation in the model and the determination as to whether the Monod formulation is the most appropriate method.

Plant resource allocation also demonstrated sensitivity to experimental values. Having a strong base of experimental values to determine the model parameter values would give us a better grasp of the values to use and how to effectively model production allocation. As seen in the case study analysis of our model results compared to time-series data from Florida Bay, the peaks in model leaf biomass are slightly delayed compared to measured values. If more

measurements of resource allocation were made seasonally, we could implement a seasonal component to resource allocation that may produce better model fit to the data.

The case studies that we have run indicate that, in its present form, the model produces realistic results in terms of biomass values and propagation rates that can give insight to seagrass spatial dynamics and be used to formulate hypotheses that can be tested in the field. The model produces seasonal above-ground biomass that falls between the maximum and minimum found in Florida Bay.

Over 85% of the overall biomass of *Thalassia* lies below the sediments (Fourqurean and Zieman 1991). Regular measurements of the production of the biomass below-ground at the seagrass monitoring sites would also contribute greatly to better understanding of this system. It would also be an important contribution for practical use of this model by managers in order to make important decisions regarding the status of the seagrass community.

The model can also be used to examine re-growth of gaps and evolution of patches. We cannot fully explain the trends in the model results with respect to geometry, but it would seem that the shape and number of vertices are important. Altering the dimensions of a gap, by giving it more sides or a greater perimeter-to-area ratio, can greatly influence the rate of re-growth. This would help managers target which gaps would be the most effective to target for fertilization or transplantation assistance. The model also shows that to properly gauge the success of a re-growth, one needs to look at the rhizome distribution because the leaf distribution can lag behind it by as much as 64%. This again stresses the importance of monitoring below-ground biomass and understanding resource allocation to having a better understanding of the system. Propagation of seagrasses from a patch, or re-vegetation of a gap, will be affected by

seasonal changes in resource allocation to below-ground tissue and changes in environmental conditions.

Future Research

Several aspects of the model presented here may be further developed and additional processes included to enhance its predictive ability.

The model was set up with initial spatial distributions of nutrient concentrations that remained constant throughout the model run. However, nutrient concentrations at monitoring sites in Florida Bay show some variability, although not a pronounced annual cycle (<http://serc.fiu.edu/wqmnetwork/>). This variability can be caused by the plants themselves or other factors in the system, such as microbial activity. Future modifications of the model implementation of nutrient conditions could be two-fold. One direction may be to initialize the spatial distribution of phosphorus and then allow a feedback between the plants and the phosphorus in the system, thereby allowing the seagrass to regulate its own nutrient availability through organic matter release and nutrient recycling. McGlathery et al (2001) showed that, although nutrient concentrations are often used to demonstrate nutrient availability, they are often only a small portion of the nutrients cycling within the system. Another approach would be to impose a time varying phosphorus concentration, using daily or monthly variations according to the sampling frequency of the monitoring data. Although this would allow for temporal variation, at this time data are not available on the spatial scale of each cell within our grid. Therefore there would be temporal variability but not true spatial variability.

Berns (2003) found that seagrass maintained a normal healthy appearance in response to varying salinities until a threshold of values over 50 and below 20 PSU. The reason we chose not to include a salinity response in our study was that a majority of Florida Bay currently does

not experience such large salinity fluctuations, except during extreme events. During the period of hypersalinity in 1989-1990, average Bay concentrations were 41 PSU with peak salinity values near 70 PSU. In cases such as these, it would be important to include a salinity response in modeling efforts. Incorporating salinity effects into the model will enable it to be used to address questions arising from the Comprehensive Everglades Restoration Plan (CERP) which contains proposals that may increase fresh water flows into Florida Bay. For a manager looking at the implications of water management, it would be worthwhile to include the salinity response.

Seedling recruitment is not the primary source of revegetation into disturbed areas, although we do know that it occurs, albeit infrequently (Whitfield et al. 2004). Kaldy and Dunton (1999) looked at the expansion of seagrass meadows and found that the combined effect of both seedlings and rhizomes was an important factor. Including the dynamics of seedling production and propagation would be a significant future development of the cellular automata model; however, this would require a much better understanding of the mechanisms involved and amount of resources allocated to reproduction.

Additional environmental heterogeneity could be added as well. For example, sediment depth is known to be important for seagrass colonization and growth, especially for *Thalassia testudinum*. Hall et al (1999) showed that there exists a positive correlation between sediment depth and seagrass standing crop in Florida Bay. Peak *Thalassia* standing crop, approximately 200 g DW m⁻², was present in deeper sediments, approximately 200 cm. Indeed, the seagrass distribution in Florida Bay matches closely the east-west gradient of sediment depth. Also, small-scale changes in sediment depth arising from small depressions, as well as sediment modification by marine vessel, which could displace up to 50 cm of sediments, could be included in the model.

The rate of rhizome propagation is typically not uniform. Instead, rhizomes grow faster in directions where there are no seagrasses (Marba and Duarte 1998). However, once rhizomes have experienced some type of damage (i.e. boat propeller) they are unlikely to begin propagation as normal until some amount of lag or recovery time has occurred (Dawes and Andorfer 2002). We have assumed a uniform, outward rhizome expansion from cells in the model. In reality, rhizome propagation is a branching process and it may be that an individual based model should be used to adequately simulate the dynamics of vegetative propagation. The model could benefit from the development of a more complex rhizome propagation component that includes these features; however, more information on rhizome biomass would be an important factor in making such a development successful.

Conclusions

Seagrass growth and production can be better represented by including the spatial aspects of the processes involved. This work has used a cellular automata approach, and is one of the first to model the spatial aspects of seagrass growth. The aim was to represent as many known processes as possible to make the model realistic while not overburdening the user with too many inputs. This model could successfully approximate the annual cycle of above-ground biomass seen in Florida Bay and was used to examine the behavior of propagation into gaps and the evolution of patches in the seagrass distribution.

A sensitivity analysis of our model indicates that a greater understanding of three factors will greatly improve the ability of any seagrass model to accurately represent natural conditions. These factors are an improved knowledge of phosphorus uptake kinetics, sulfide dynamics and resource allocation within the plant. The latter is especially important for vegetative growth and survival during periods of resource limitation. Although we have found some areas of

improvement that would enhance the model results, we have concluded that this model, even in its current state, may be of use to help make predictions on the spatial behavior of the seagrass

Thalassia testudinum.

REFERENCES

- Berns, D., 2003. Physiological responses of *Thalassia testudinum* and *Ruppia maritima* to experimental salinity levels. Master's Thesis, University of South Florida.
- Bodensteiner, L. B., 2006. The impact of light availability on benthic oxygen release by the seagrasses - *Thalassia testudinum* (Banks ex König) and *Zostera marina*. Master's Thesis, California State University.
- Bortone, S. (Ed.), 2000. Seagrasses Monitoring, Ecology, Physiology, and Management. CRC Press.
- Borum, J., Pederson, O., Greve, T., Frankovich, T., Zieman, J., Fourqurean, J., and Madden, C., 2005. The potential role of plant oxygen and sulphide dynamics in die-off events of the tropical seagrass, *Thalassia testudinum*. *Journal of Ecology* 93: 148–158.
- Boudreau, B., 1997. Diagenetic Models and Their Implementation. Springer.
- Boyer, J., Fourqurean, J., and Jones, R., 1997. Spatial characterization of water quality in Florida Bay and Whitewater Bay by multivariate analyses: zones of similar influence. *Estuaries* 20: 743–758.
- Burd, A., and Dunton, K., 2001. Field verification of a light-driven model of biomass changes in the seagrass *Halodule wrightii*. *Marine Ecology Progress Series* 209: 85-98.
- Cain, M., 1990. Models of Clonal Growth in *Solidago altissima*. *Journal of Ecology* 78: 27-46.
- Carlson, P., Yarbrow, L., and Barber, T., 1994. Relationship of sediment sulfide to mortality of *Thalassia testudinum* in Florida Bay. *Bulletin of Marine Science* 54:733-746.
- Carlson, P., Yarbrow, L., Peterson, B., Ketron, A., Arnold, H., and Madely, K., 2002. The influence of sediment sulfide on the structure of south Florida seagrass communities. In: *Seagrass Management: It's not just nutrients*. 2002 August 22-24; Greening, H.S., editor. St. Petersburg, FL. Tampa Bay Estuary Program.
- Chen, Q., Mynett, A., and Minns, A., 2002. Application of cellular automata to modelling competitive growths of two underwater species *Chara aspera* and *Potamogeton pectinatus* in Lake Veluwe. *Ecological Modelling* 147: 253-265.
- Connolly, R., Hindell, J., and Gorman, D., 2005. Seagrass and epiphytic algae support nutrition of a fisheries species, *Sillago schomburgkii*, in adjacent intertidal habitats. *Marine Ecology Progress Series* 286: 123–136.

- D'Ambrosio, D., Di Gregorio, S., Gabriele, S., and Gaudio, R., 2001. A Cellular Automata model for soil erosion by water. *Physics and Chemistry of the Earth, Part B: Hydrology, Oceans and Atmosphere* 26: 33-39.
- Dawes, C., Andorfer, J., Rose, C., Uranowski, C., and Ehringer, N., 1997. Regrowth of the seagrass *Thalassia testudinum* into propellar scars. *Aquatic Botany* 59: 139-155.
- Dawes, C., and Andorfer, J., 2002. Production of Rhizome Meristems by *Thalassia testudinum*. In: *Seagrass Management: It's not just nutrients*. 2002 August 22-24; Greening, H.S., editor. St. Petersburg, FL. Tampa Bay Estuary Program.
- Den Hartog, C., 1970. *The Seagrasses of the World*. Amsterdam, North-Holland Publishing Company.
- Dennison, W., and Orth, R., 1993. Assessing water quality with submerged aquatic vegetation. *Bioscience* 43.
- Dewdney, A., 1989. *The Turing Omnibus: 61 Excursions in Computer Science*. Rockville, MD: Computer Science Press.
- Duarte, C., 1991. Allometric scaling of seagrass form and productivity. *Marine Ecology Progress Series* 77: 289-300.
- Duarte, C., Marine, M., Agawin, N., Uri, J., Fortes, M., Gallegos, M., Marba, N. and Hemminga, M. 1998. Root production and belowground seagrass biomass. *Marine Ecology Progress Series* 171: 97-108.
- Duarte, C., and Chiscano, C., 1999. Seagrass biomass and production: a reassessment. *Aquatic Botany* 65: 159-174.
- Duarte, C., and Sand-Jensen, K., 1990. Seagrass colonization: patch formation and patch growth in *Cymodocea nodosa*. *Marine Ecology Progress Series* 65: 193-200.
- Durako, M., and Moffler, M., 1987. Factors affecting the reproductive ecology of *Thalassia testudinum* (Hydrocharitaceae). *Aquatic Botany* 27: 79-95.
- Ehringer, J., and Anderson, J., 2002. Seagrass Transplanting and Restoration in Tampa Bay. In: *Seagrass Management: It's not just nutrients*. 2002 August 22-24; Greening, H.S., editor. St. Petersburg, FL. Tampa Bay Estuary Program.
- Enriques, S., Marba, N., Duarte, C., Van Tussenbroek, B., and Reyes-Zavala, G., 2001. Effects of seagrass *Thalassia testudinum* on sediment redox. *Marine Ecology Progress Series* 219: 149-158.

- Fong, P., Harwell, M., 1994. Modeling seagrass communities in tropical and subtropical bays and estuaries: A mathematical model synthesis of current hypotheses. *Bulletin of Marine Science* 54(3): 757-781.
- Fong, P., Jacobson, M., Mescher, M., Lirman, D., and Harwell, M., 1997. Investigating the management potential of a seagrass model through sensitivity analysis and experiments. *Ecological Applications* 7(1): 300-315.
- Fonseca, M., and Fisher, J., 1986. A comparison of canopy friction and sediment movement between four species of seagrass with reference to their ecology and restoration. *Marine Ecology Progress Series* 29: 15-22.
- Fourqurean, J., Jones, R., and Zieman, J., 1993. Processes influencing water column nutrient characteristics and phosphorus limitation of phytoplankton biomass in Florida Bay, FL, USA: Inferences from spatial distributions. *Estuarine, Coastal and Shelf Science* 36(3): 295-314.
- Fourqurean, J., Willsie, A., Rose, C., and Rutten, L., 2001. Spatial and temporal pattern in seagrass community composition and productivity in South Florida. *Marine Biology* 138: 341–354.
- Fourqurean, J., and Zieman, J., 1991. Photosynthesis, respiration and whole plant carbon budget of the seagrass *Thalassia testudinum*. *Marine Ecological Progress Series* 69: 161–170.
- Fourqurean, J., and Zieman, J., 1992. Phosphorus limitation of primary production in Florida Bay: Evidence from C:N:P ratios of the dominant seagrass *Thalassia testudinum*. *Limnology and Oceanography* 37: 162–171.
- Fourqurean, J., Zieman, J., and Powell, G., 1992. Relationships between porewater nutrients and seagrasses in a subtropical carbonate environment. *Marine Biology* 114: 57-65.
- Fourqurean, J., and Zieman, J., 2002. Nutrient content of the seagrass *Thalassia testudinum* reveals regional patterns of relative availability of nitrogen and phosphorus in the Florida Keys USA. *Biogeochemistry* 61(3): 229-245.
- Gacia, E., Granata, T., and Duarte, C., 1999. An approach to measurement of particle flux and sediment retention within seagrass (*Posidonia oceanica*) meadows. *Aquatic Botany* 65(1): 255-268.
- Giusti, E., and Marsili-Libelli, S., 2005. Modelling the interactions between nutrients and the submersed vegetation in the Orbetello Lagoon. *Ecological Modelling* 184: 141-161.
- Goecker, M., Heck, J., Valentine, J., 2005. Effects of nitrogen concentrations in turtlegrass *Thalassia testudinum* on consumption by the bucktooth parrotfish *Sparisoma radians*. *Marine Ecology Progress Series* 286: 239-248.

- Goodman, J., Moore, K., and Dennison, W., 1995. Photosynthetic responses of eelgrass (*Zostera marina* L.) to light and sediment sulfide in a shallow barrier island lagoon. *Aquatic Botany* 50: 37-47.
- Gras, A., Koch, M., and Madden, C., 2003. Phosphorus uptake kinetics of a dominant tropical seagrass *Thalassia testudinum*. *Aquatic Botany* 76: 299-315.
- Haefner, J., 1996. *Modeling Biological Systems: Principles and Applications*. Chapman and Hall, New York.
- Hall, M., Durako, M., Fourqurean, J., and Zieman, J., 1999. Decadal Changes in Seagrass Distribution and Abundance in Florida Bay. *Estuaries* 22(2): 445-459.
- Heck, J. K., Hays, G., and Orth, R., 2003. Critical evaluation of the nursery role hypothesis for seagrass meadows. *Marine Ecology Progress Series* 253: 123-136.
- Hemminga, M., and Duarte, C., 2000. *Seagrass Ecology*. Cambridge University Press.
- Herzka, S., and Dunton, K., 1997. Seasonal photosynthetic patterns of the seagrass *Thalassia testudinum* in the western Gulf of Mexico. *Marine Ecology Progress Series* 152: 103-117.
- Herzka, S., and Dunton, K., 1998. Light and carbon balance in the seagrass *Thalassia testudinum*: evaluation of current production models. *Marine Biology* 132: 711-721.
- Iqbal, M., 1983. *An Introduction to Solar Radiation*. Academic Press, New York.
- Jensen, H., McGlathery, K., Marino, R., and Howarth, R., 1998. Forms and Availability of Sediment Phosphorus in Carbonate Sand of Bermuda Seagrass Beds. *Limnology and Oceanography* 43(5): 799-810.
- Kaldy, J., 1997. Production dynamics, reproductive ecology and demography of *Thalassia testudinum* (Turtle Grass) from the Lower Laguna Madre, Texas. Doctor of Philosophy Dissertation, University of Texas.
- Kaldy, J., and Dunton, K., 1999. Ontogenetic photosynthetic changes, dispersal, and survival of *Thalassia testudinum* (turtle grass) seedlings in a sub-tropical lagoon. *Journal of Experimental Marine Biology and Ecology* 240: 193-212.
- Kaldy, J., Dunton, K., Kowalski, J., and Lee, K., 2004. Factors controlling seagrass revegetation onto the dredged material deposits: A case study in lower Laguna Madre, Texas. *Journal of Coastal Research* 20 (1): 292- 300.
- Kendrick, G., Eckersley, J., and Walker, D., 1999. Landscape-scale changes in seagrass distribution over time: a case study from Success Bank, Western Australia. *Aquatic Botany* 65: 293-309.

- Kenworthy, W., Fonseca, M., Whitfield, P., and Hammerstrom, K., 2002. Analysis of seagrass recovery in experimental excavations and propellar scar disturbances in the Florida Keys National Marine Sanctuary. *Journal of Coastal Research* 37: 75-85.
- King, G., 1988, Patterns of sulfate reduction and the sulfur cycle in a South Carolina salt marsh. *Limnology and Oceanography* 33(3): 376–390.
- Koch, E., 2001. Beyond light: Physical, geological and geochemical parameters as possible submerged aquatic vegetation habitat requirements. *Estuaries* 24: 1–17.
- Koch, M., and Erskine, J., 2001. Sulfide as a phytotoxin to the tropical seagrass *Thalassia testudinum*: interactions with light, salinity and temperature. *Journal of Experimental Marine Biology and Ecology* 266: 81-95
- Ku, T., Walter, L., Coleman, M., Blake, R., and Martini, A., 1999. Coupling between sulfur recycling and syndepositional carbonate dissolution: Evidence from oxygen and sulfur isotope composition of pore water sulfate, South Florida Platform, U.S.A. *Geochimica et Cosmochimica Acta* 63(17): 2529 –2546.
- Kuo, J., McComb, A., and Cambridge, M., 1981. Ultrastructure of the seagrass rhizosphere. *New Phytologist* 89(1): 139-143.
- Larkum, A., McComb, A., and Sheperd, S. (Eds.), 1989. *Biology of Seagrasses*. Elsevier Science Publishers.
- Lapointe, B., and Barile, P., 2004. Comment on J.C. Zieman, J.W. Fourqurean, and T.A. Frankovich. 1999. Seagrass die-off in Florida Bay: Long-term trends in abundance and growth of turtle grass; *Thalassia testudinum*. *Estuaries*. 22:460–470. *Estuaries* 27: 157-178.
- Lee, K., and Dunton, K., 1996. Production and carbon reserve dynamics of the seagrass *Thalassia testudinum* in Corpus Christi Bay, Texas, USA. *Marine Ecology Progress Series* 143: 201–210.
- Lee, K., and Dunton, K., 1999. Inorganic nitrogen acquisition in the seagrass *Thalassia testudinum*: Development of a whole-plant nitrogen budget. *Limnology and Oceanography*. 44(5): 1204-1215.
- Madden, C., and MacDonald, A. 2006. An ecological model of the Florida Bay seagrass community: Model Documentation Version II. South Florida Water Management District: Coastal Ecosystems Division.
- Marbà, N., and Duarte, C., 1998. Rhizome elongation and seagrass clonal growth. *Marine Ecology Progress Series* 174: 269-280.

- Marbà, N., Hemminga, M., Mateo, M., Duarte, C., Mass, Y., Terrados, J., and Gacia, E., 2002. Carbon and nitrogen translocation between seagrass ramets. *Marine Ecology Progress Series* 266: 287-300.
- McGlathery, K., Marino, R., and Howarth, R., 1994. Variable rates of phosphorus uptake by shallow marine carbonate sediments: mechanisms and ecological significance. *Biogeochemistry* 25(2): 127-146.
- McGlathery, K., Berg, P., and Marino, R., 2001. Using porewater profiles to assess nutrient availability in seagrass-vegetated carbonate sediments. *Biogeochemistry* 56(3): 239-263.
- Miller, H., Meile, C., and Burd, A., 2007. A novel 2D model of internal O₂ dynamics and H₂S intrusion in seagrasses. *Ecological Modelling* 205: 365–380.
- Olesen, B., and Sand-Jensen, K., 1994. Patch dynamics of eelgrass *Zostera marina*. *Marine Ecology Progress Series* 106: 147-156.
- Pallud, C., Meile, C., Laverman, A., Abell, J., and Van Cappellen, P., 2007. The use of flow-through sediment reactors in biogeochemical kinetics: Methodology and examples of applications. *Marine Chemistry* 106: 256-271.
- Phillips, R., and McRoy, C. (Eds.), 1980. *Handbook of Seagrass Biology: An Ecosystem Perspective*. Garland Publishing, Inc.
- Powell, G., Kenworthy, W., and Fourqurean, J., 1989. Experimental evidence for nutrient limitation of seagrass growth in a tropical estuary with restricted circulation. *Bulletin of Marine Science* 44(1): 324-340.
- Rammig, A., Fahse, L., Bugmann, H., and Bebi, P., 2006. Forest regeneration after disturbance: A modelling study for the Swiss Alps. *Forest Ecology and Management* 222: 123-136.
- Robblee, M., Barber, T., Carlson, P., Durako, M., Fourqurean, J., Muehlstein, L., Porter, D., Yarbrow, L., Zieman, R., and Zieman, J., 1991. Mass mortality of the tropical seagrass *Thalassia testudinum* in Florida Bay USA. *Marine Ecology Progress Series* 71: 297–299.
- Rude, P., and Aller, R., 1991. Fluorine mobility during early diagenesis of carbonate sediment: An indicator of mineral transformations. *Geochimica Et Cosmochimica Acta* 55: 2491-2509.
- Ruxton, G., and Saravia, L., 1998. The need for biological realism in the updating of cellular automata models. *Ecological Modelling* 107: 105–111.
- Sargent, F., Leary, T., Crews, D., and Kruer, C., 1995. Scarring of Florida's Seagrasses: Assessment and Management. Technical report. FMRI 1h/94, St. Petersburg, Florida: Florida Marine Research Institute. 62 p.

- Sarkar, C., and Abbasi, S., 2006. Cellular automata-based forecasting of the impact of accidental fire and toxic dispersion in process industries. *Journal of Hazardous Materials* 137: 8-30.
- Schlicht, R., and Iwasa, Y., 2006. Direction of regeneration waves in grid-based models for forest dynamics. *Journal of Theoretical Biology* 242: 363-371.
- Schwinnig, S., and Parsons, A., 1996. A spatially explicit population model of stoloniferous N-fixing legumes in mixed pasture with grass. *Journal of Ecology* 84: 815-826.
- Short, F., and Wyllie-Echeverria, S., 1996. Natural and human-induced disturbance of seagrasses. *Environmental Conservation* 23: 17-27.
- Silvertown, J., Holtier, S., Johnson, J., and Dale, P., 1992. Cellular automaton models of interspecific competition for space - the effect of pattern on process. *Journal of Ecology* 80: 527-534.
- Smith, S., 1984. Phosphorous versus nitrogen limitation in the marine environment. *Limnology and Oceanography* 29: 1149-1160.
- Sommer, U., 1991. A comparison of the Droop and the Monod Models of nutrient limited growth applied to natural populations of phytoplankton. *Functional Ecology* 5(4):535-544.
- Szmant, A., and Forrester, A., 1996. Water column and sediment nitrogen and phosphorus distribution patterns in the Florida Keys, USA. *Coral Reefs* 15: 21-41.
- Tomasko, D., and Dawes, C., 1989. Evidence for physiological integration between shaded and unshaded short shoots of *Thalassia testudinum*. *Marine Ecology Progress Series* 54: 299-305.
- Touchette, B., and Burkholder, J., 2000. Review of nitrogen and phosphorus metabolism in seagrasses. *Journal of Experimental Marine Biology and Ecology* 250: 133-167.
- Vidondo, B., Middleboe, A., Stefansen, K., Lutzen, K., Nielsen, S., and Duarte, C., 1997. Dynamics of a patchy seagrass (*Cymodocea nodosa*) landscape. Size and age distributions, growth and demography of seagrass patches. *Marine Ecology Progress Series* 158: 131-138.
- Weidner, S., Arnold, W., and Puhler, A., 1996. Diversity of uncultured microorganisms associated with the seagrass *Halophila stipulacea* estimated by restriction fragment length polymorphism analysis of PCR-amplified 16S rRNA genes. *Applied and Environmental Microbiology* 62(3): 766-771.
- Whitfield, P., Kenworthy, W., Hammerstrom, K., and Fonseca, M., 2002. The role of a hurricane in the expansion of disturbances initiated by motor vessels on seagrass banks. *Journal of Coastal Research* 37: 86-99.

- Whitfield, P., Kenworthy, W., Durako, M., Hammerstrom, K., and Merello, M., 2004. Recruitment of *Thalassia testudinum* seedlings into physically disturbed seagrass beds. Marine Ecology Progress Series 267: 121-131.
- Whittaker, R., 1975. Communities and ecosystems. Macmillan.
- Williams, S., 1990. Experimental studies of Caribbean seagrass bed development. Ecological Monographs 60(4): 449-469.
- Wolfram, S., 1983. Statistical mechanics of cellular automata. Reviews of Modern Physics 55 (3): 601-644.
- Zieman, J., 1975. Seasonal variation of turtle grass, *Thalassia testudinum* konig, with reference to temperature and salinity effects. Aquatic Botany 1: 107-123.
- Zieman, J., 1976. The ecological effects of physical damage from motor boats on turtle grass beds in southern Florida. Aquatic Botany 2: 127-139.
- Zieman, J., Fourqurean, J., and Iverson, R., 1989. Distribution, abundance and productivity of seagrasses and macroalgae in Florida Bay. Bulletin Marine Science 44: 292-311.
- Zieman, J., Fourqurean, J., and Frankovich, T., 1999. Seagrass die-off in Florida Bay: Long-term trends in abundance and growth of turtle grass; *Thalassia testudinum*. Estuaries 22: 460-470.
- Zieman, J., and Wetzel, R., 1980. Handbook of Seagrass Biology: An Ecosystem Perspective. Garland Publishing, Inc., Ch. Productivity in Seagrasses: Methods and Rates.
- Zimmerman, R., Smith, R., and Alberte, R., 1987. Is growth of eelgrass nitrogen limited? A numerical simulation of the effects of light and nitrogen on the growth dynamics of *Zostera marina*. Marine Ecology Progress Series 41: 167-176.
- Zimmerman, R., Cabello-Pasini, A., and Alberte, R., 1994. Modeling daily production of aquatic macrophytes from irradiance measurements: a comparative analysis. Marine Ecology Progress Series 114: 185-196.

APPENDIX
MODEL PARAMETERS

Chapter 3: Sensitivity Analysis

Table A. Summary of parameters from the quantitative sensitivity analysis of the model to variations in the phosphorus half-saturation constant, K_m .

Parameter Value K_m (μM)	Phosphorus concentration (μM)	Sulfide Concentration (μM)
0.5	0.375	0
0.505	0.375	0
0.495	0.375	0
0.55	0.375	0
0.45	0.375	0
0.5	1.0	0
0.505	1.0	0
0.495	1.0	0

Table B. Summary of parameters from the quantitative sensitivity analysis of the model to variations in the proportion of production allocated to above and below-ground biomass.

Percentage of production allocated to below- ground	Phosphorus concentration (μM)	Sulfide Concentration (μM)
35	0.375	0
35.65	0.375	0
34.35	0.375	0
41.5	0.375	0
28.5	0.375	0

Chapter 4: Case Studies

Random Spatial Distribution

Table C. Simulation parameters for the model runs examining random spatial distributions.

Simulation	Phosphorus concentration (μM)	Sulfide Concentration (μM)
All runs	0.375	1000

Idealized Patterns

Table D. Simulation parameters for model runs examining the influence of the perimeter-to-area ratio on gap fill-in rates.

Number of Gaps	Gap Dimensions	Phosphorus concentration (μM)	Sulfide Concentration (μM)
1	40m x 40m	0.375	1000
1	30m x 30m	0.375	1000
2	45m x 10m	0.375	1000
9	10m x 10m	0.375	1000
22	10m x 4m	0.375	1000

Table E. Simulation parameters for model runs examining the effect of shape on the gap fill-in rate. All initial gaps are 100m^2 in area.

Model ID	Size/Shape	P concentration (μM)	Sulfide Concentration (μM)
A	Square (10m x 10m)	0.375	1000
B	Rectangle(25m x 4m)	0.375	1000
C	20-sided polygon	0.375	1000
D	12-sided polygon	0.375	1000

Table F. Simulation parameters for model runs examining the spread of rhizome and leaf biomass radiating from a central square patch of seagrass in the center of the grid.

Patch Size	Phosphorus concentration (μM)	Sulfide Concentration (μM)
30m x 30m	0.375	1000
9(10m x 10m)	0.375	1000
22(10m x 4m)	0.375	1000

Table G. Simulation parameters for model runs examining the spread of rhizome and leaf biomass radiating from various shapes of seagrass placed at the center of the grid.

Size/Shape	Phosphorus concentration (μM)	Sulfide Concentration (μM)
Square (10m x 10m)	0.375	1000
Rectangle (25m x 4m)	0.375	1000
20-sided polygon	0.375	1000
12-sided polygon	0.375	1000

Motor Vessel Injuries

Table H. Simulation parameters from model runs examining the effect of varying phosphorus concentrations (μM) on the recovery of *Thalassia* into a large-scale boat propeller blowout.

Model ID	Phosphorus concentration (μM)	Sulfide Concentration (μM)
A	0.35 ± 0.1	1000
B	0.35	1000
C	0.375	1000
D	0.25 ± 0.1	1000
E	0.3 ± 0.1	1000
F	0.325 ± 0.1	1000
G	0.3125 ± 0.1	1000

Table I. Simulation parameters for model runs examining the effect of varying phosphorus concentrations (μM) and sediment sulfide concentrations (μM) on the recovery into a gap in a seagrass bed.

Model Run ID	Phosphorus concentration (μM)	Sulfide Concentration (μM)
A	0.375	0
B	0.375 ± 0.1	0
C	0.3125 ± 0.1	0
D	0.4	0
E	0.4	1000
F	0.4	2000
G	0.4	4000
H	0.4	6000